Univerzita Karlova
Přírodovědecká fakulta

Studijní program: Biologie
Studijní obor: Fyziologie živočichů

Bc. Kateřina Remišová

DISTRIBUTION OF PHOTORECEPTOR TYPES IN RETINA OF FISHES FROM EXTREME ENVIRONMENTS

PROSTOROVÉ USPOŘÁDÁNÍ FOTORECEPTORŮ V SÍTNICI RYB Z EXTRÉMNÍCH PROSTŘEDÍ

Diplomová práce

Vedoucí práce: Mgr. Zuzana Musilová, Ph.D.

Praha 2019

Prohlášení

Prohlašuji, že jsem závěrečnou práci zpracovala samostatně a že jsem uvedla všechny použité informační zdroje a literaturu. Tato práce ani její podstatná část nebyla předložena k získání jiného nebo stejného akademického titulu.

V Praze 19. července 2019

Kateřina Remišová

Acknowledgements

I would like to express my gratitude to my supervisor Zuzana Musilová for her assistance, patience and guidance during my work on this thesis.

I thank all members of the Fish Evolution Research Group for their assistance and consultations. I would especially like to appreciate Monika Kłodawska, Gina Sommer and Dmytro Omelchenko for sample collections in the field.

I am also thankful to Sara M. Stieb and Fabio Cortesi for their help with protocol optimization, to Ondřej Šebesta for his help with microscopy imaging, and to Karen Carleton for her valuable advice on troubleshooting. I also thank Walter Salzburger and Adrian Indermaur for their support.

I am very grateful to my family and close friends for their unceasing encouragement, support and attention during my studies.

This work was supported by the Czech Science Foundation (GACR-16-09784Y), the Swiss National Science Foundation (PROMYS-IZ11Z0_166550), and Charles University Grant Agency (GAUK-1767618). Microscopy was performed in the Laboratory of Confocal and Fluorescence Microscopy co-financed by the European Regional Development Fund and the state budget of the Czech Republic (CZ.1.05/4.1.00/16.0347, CZ.2.16/3.1.00/21515) and supported by the Czech-BioImaging large RI (LM2015062).

Abstract

Cichlid visual system is highly adaptive to the environment. Fish visual abilities are determined by composition of opsin-based photosensitive pigments located in photoreceptor cells (rods and cones) as well as their distribution. In this thesis, four species of Lake Barombi Mbo cichlids were targeted: *Stomatepia mariae, Konia eisentrauti, Konia dikume* and *Myaka myaka*. Shallow-water cichlids *K. eisentrauti* and *S. mariae* express these types of cone opsin genes: *LWS*, *RH2A* (*RH2Aβ* more than *RH2Aα*), *SWS2A* and *SWS2B*. Contrarily, both seasonally deep-water *M. myaka* and deep-water *K. dikume* lack expression of *SWS2B* and *LWS* in their retinae, but they express *SWS2A* and *RH2Aα* more than *RH2Aβ,* which corresponds to modified light conditions in deep water – a dimmer habitat lacking marginal parts of the spectrum (i.e., ultraviolet and red wavelengths). The photoreceptor distribution of selected species was investigated by means of fluorescent *in situ* hybridization (FISH) in order to understand the performance and evolution of their visual perception with emphasis on the effect of depth. Distinctively, cichlid cones are arranged in a retinal mosaic consisting of short-wavelength sensitive single cones, each surrounded by four long-wavelength sensitive double cones. In this thesis, the same arrangement is described for all selected species beside *K. dikume*, whose retina appears less organized with dominant double cones and virtual lack of single cones. Such arrangement relates to vision in deep-water environment. In general, most of the cichlid double cones express different opsin genes in each of the double cone member, which is also the case for *S. mariae*. However, *K. eisentrauti* embodies additional *LWS*-only double cones – probably in order to enhance visual resolution. Additionally, all double cones of *M. myaka* express *RH2A* in both double cone members as this species lacks *LWS* expression. Findings of this work complement present knowledge of cichlid vision in particular and help to understand adaptability of fish visual system in general.

Key words

Vision, retina, photoreceptor, opsin, crater lakes, fish, cichlids, Africa, Cameroon.

Abstrakt

Zrakový systém cichlid je vysoce adaptibilní v závislosti na prostředí. Zrakové schopnosti ryb jsou dány jak skladbou opsinových fotopigmentů, které se nacházejí ve fotoreceptivních buňkách (tyčinkách a čípcích), tak jejich prostorovým rozložením. Tato práce se zabývala čtyřmi druhy cichlid z jezera Barombi Mbo, jmenovitě *Stomatepia mariae, Konia eisentrauti, Konia dikume* a *Myaka myaka*. Mělkovodní druhy *K. eisentrauti* a *S. mariae* exprimují tyto čípkové opsiny: *LWS, RH2A* (*RH2Aβ* více než *RH2Aα*), *SWS2A* a *SWS2B.* Narozdíl od toho sezóně hlubokovodní *M. myaka* i trvale hlubokovodní *K. dikume* v sítnici neexprimují *SWS2B* ani *LWS,* zato exprimují *SWS2A* a *RH2Aα* více než *RH2Aβ*. To odpovídá odlišným světelným podmínkám v hlubokých vodách, kam nepronikají okrajové části spektra (tzv. ultrafialové a červené záření). Struktura sítnice vybraných druhů byla zkoumána pomocí fluorescenční *in situ* hybridizace (FISH) za účelem pochopení vývoje a fungování jejich zrakového vnímání, především v závislosti na hloubce, kde žijí. Sítnice cichlid je typicky organizována do mozaiky skládající se z jednoduchých čípků citlivých na krátkovlnné světlo obklopených vždy čtveřicí dvojčípků, které jsou senzitivní v dlouhovlnné oblasti světelného spektra. Tato práce ukazuje stejné uspořádání sítnice u všech vybraných druhů s výjimkou *K. dikume*, jejíž sítnice je méně strukturovaná a dvojčípky převažují nad jednoduchými čípky, které téměř chybí. Taková skladba sítnice souvisí s viděním v hlubokých vodách. Dvojčípky většiny cichlid exprimují odlišné opsiny v každé z jejich částí, stejně tak je tomu u *S. mariae. K. eisentrauti* však navíc vykazuje i dvojčípky exprimující *LWS* v obou jejich částech, což by mohlo potenciálně vylepšovat zrakové rozlišení. Jelikož *M. myaka* neexprimuje *LWS,* v obou částech jejích dvojčípků se nachází *RH2A.* Zjištění uvedená v této práci rozšiřují současné znalosti zejména o zraku cichlid a pomáhají lépe pochopit adaptibilitu zrakového systému ryb obecně.

Klíčová slova

Zrak, sítnice, fotoreceptor, opsin, kráterová jezera, ryby, cichlidy, Afrika, Kamerun.

Contents

List of Abbreviations 9
Introduction 11
1. Literature Review 13
1.1. Fish Vision 13
1.1.1. Underwater Visual Environment 13
1.1.2. Optical System of Fish 14
1.1.3. Retinal Structure of Fish 15
1.1.4. Visual Pigments of Fish 20
1.1.5. Visual Adaptations of Fish 23
1.2. Cichlids of Lake Barombi Mbo 25
2. Aims of the Thesis 30
3. Materials and Methods 31
3.1. List of Reagents 31
3.1.1. Reagents for Probe Production 31
3.1.2. Reagents for Tissue Preparation 31
3.1.3. Reagents for Fluorescent *in situ* Hybridization 31
3.2. Probe Production 34
3.2.1. cDNA Synthesis 34
3.2.2. Primer Design 35
3.2.3. Template Production 35
3.2.4. Probe Preparation 36
3.3. Sample Collection 37
3.4. Tissue Preparation 37
3.5. Fluorescent *in situ* Hybridization 38
3.6. Microscopy Imaging and Image Processing 39
4. Results 40
4.1. Method Optimization 41
4.2. *Stomatepia mariae* 42
4.3. *Konia eisentrauti* 45
4.4. *Konia dikume* 50
4.5. *Myaka myaka* 50
4.6. Result Summary and Publication 53

5. Discussion 55
Conclusion 64
List of References 66
List of Graphs 73
List of Figures 73
List of Tables 74
Attachments 75
1. Poster Presented at Zoological Days 2017 75
2. Poster Presented at ESEB Congress 2017 76
3. Poster Presented at Cichlid Science Meeting 2017 77
4. Poster Presented at Zoological Days 2018 78
5. Poster Presented at ICN 2018 79

List of Abbreviations

agl	above ground level
anti-DIG-POD	Anti-Digoxigenin-Peroxidase, Fab Fragments
anti-DNP-POD	Anti-Dinitrophenylhydrazine-Peroxidase, Fab Fragments
anti-FL-POD	Anti-Fluorescein-Peroxidase, Fab Fragments
BF	bright field
cDNA	coding deoxyribonucleic acid
DIC	differential interference contrast = Nomarski interference contrast
DIG	digoxigenin
DNA	deoxyribonucleic acid
DNP	dinitrophenylhydrazine
dNTP	deoxynucleoside triphosphate
ds cDNA	double-strand coding deoxyribonucleic acid
DTT	dithiothreitol
E	irradiance – [$W.m^{-2}$]
E_d	downward irradiance – [$W.m^{-2}$]
EB	ethidium bromide
EDTA	ethylenediaminetetraacetic acid
ESEB	European Society for Evolutionary Biology
Fiji	Fiji Is Just ImageJ
FISH	fluorescent *in situ* hybridization
FL	fluorescein
fsn	fish sample number
ICN	International Congress of Neuroethology
IR	infrared
L (eye)	left eye
LR (fish)	laboratory-reared fish
LWS	long-wavelength sensitive opsin
LWS	long-wavelength sensitive opsin gene
MetOH	methanol
mRNA	messenger RNA
MWS	middle-wavelength sensitive opsin

MWS	middle-wavelength sensitive opsin gene
PBS	phosphate-buffered saline
PBST	phosphate-buffered saline with Tween-20 (0.1%)
PCR	polymerase chain reaction
PFA	paraformaldehyde
qPCR	quantitative polymerase chain reaction = real-time PCR
R (eye)	right eye
RH	rhodopsin-like opsin, including: RH2B, RH2Aβ, RH2Aα
RH	rhodopsin-like opsin gene, including: *RH2B, RH2Aβ, RH2Aα*
RH1	rhodopsin (rod opsin)
RH1	rhodopsin (rod opsin gene)
RIS	(photo)receptor inner segment
RMB	Roche Molecular Blocking Solution
RNA	ribonucleic acid
ROS	(photo)receptor outer segment
RPE	retinal pigment epithelium
RT	room temperature
ss cDNA	single-strand coding deoxyribonucleic acid
SSC	saline-sodium citrate
SSCT	saline-sodium citrate with Tween-20 (0,1%)
SWS	short-wavelength sensitive opsin, including: SWS1, SWS2B, SWS2A
SWS	short-wavelength sens. opsin gene, including: *SWS1, SWS2B, SWS2A*
TEN	solution consisting of Tris-HCl, EDTA and NaCl
Tris	tris(hydroxymethyl)aminomethane
TSA	Tyramide Signal Amplification Kit
TSA 488	Alexa Fluor 488 Tyramide Super Boost Kit
TSA 594	Alexa Fluor 594 Tyramide Super Boost Kit
TSA 647	Alexa Fluor 594 Tyramide Super Boost Kit
UTR	untranslated region
UV	ultraviolet
WC (fish)	wild-caught fish
λ	wavelength – [nm]
λ_{max}	maximum absorbance – [$W.m^{-2}$]

Introduction

Vision is one of the most important animal senses, as a vast number of behaviours is visually-guided, including predator and prey detection, mate evaluation, visual communication, recognition of individuals or habitat selection (Land & Nilsson, 2012). The visual information is carried by light, which is a great sensory stimulus by virtue of its high speed and direct spread (Abrahamson et al., 1972).

Light is electromagnetic radiation of wavelengths in an approximate range of 100 nm – 1 mm; however, only a small part of the range is visually utilisable. The spectrum of sunlight reaching the Earth surface lies between 300 and 900 nm. Elementary particles of light are photons that exhibit wave-particle duality properties. Thus, light behaves as a wave when it travels; however, it behaves as a package of particles when emitted or reaching. As the result of the particle-like behaviour, light can interact with matter in three ways – reflection, transmission and absorption. Light may be characterized on the basis of its wavelength λ (or frequency f) by virtue of its wave-like behaviour (Crowell, 2019; Björn, 2015; Wolken, 1995).

In the visual apparatus, light is focused by the eye on a photosensitive cell layer – a retina, where the image is formed. Retinal cells (cones and rods) contain opsin-based photosensitive pigments, which absorb light. Opsins vary in their absorption maxima λ_{max} – the wavelength at which the highest light absorption is observed. Such spectral tuning is relevant for colour vision; therefore, the photoreceptors are subject to adaptive evolution. Once photons are detected by photoreceptors, received information about the presence of light is transformed into neuronal impulses and further processed by the nervous system (Björn, 2015; Abrahamson et al., 1972).

Cichlids are fish from the diverse family Cichlidae in the order Cichliformes (formerly classified within Perciformes) found mainly in tropical freshwaters. They are mostly known for their adaptive radiation, ecological diversity and species richness (Turner, 2007). African lake cichlids are a classic example of a rapid adaptive ecological radiation (Kocher, 2004). In Cameroonian Lake Barombi Mbo, a small flock of eleven species including a specialised sponge-eater, herbivores, filter-feeders, predators, and a dwarf zooplanktivore sympatrically radiated. Barombi Mbo cichlids diversified thank to, among others, depth preference: nine species inhabit shallow waters while two species independently colonized deep waters (Trewavas et al., 1972).

Apart from various feeding strategies and different habitats, cichlids in general developed complex social behaviour, which is often visually guided. Consequently, evolution of cichlid visual system is driven by its key role in adaptation to different ecological niches, habitats and speciation facilitated by mate preference. As a result, cichlids possess well-developed colour vision supported by a great range of opsin genes (Turner, 2007).

To understand the performance and evolution of cichlid visual perception, I focused on the level of spatial photoreceptor distribution in the retina. In this thesis, I report on the investigation of the effect of depth on the retinal organization of cichlids from the Barombi Mbo crater lake by means of the fluorescent *in situ* hybridization (FISH) method.

1. Literature Review

Vision is a very important sensory system for many fish species. However, it is greatly challenged by specific light conditions that occur in, e.g., deep-water habitats. In the field of visual ecology, there are many well-established correlations between composition of the light environment and the visual system arrangement, including morphological attributes and spectral sensitivity adjustments (Björn, 2015). This part of the thesis presents current knowledge of aquatic environment light properties and fish vision followed by description of the target group of this thesis – cichlids from Lake Barombi Mbo.

1.1. Fish Vision

How do fish see? This puzzling question is hard to answer. Despite the fact fish eyes are in general similar to the eyes of terrestrial vertebrates, yet many species from extreme environments possess particular adaptations such as multibank retinae (Denton & Locket, 1989), mirror eyes (Partridge et al., 2014; Wagner et al., 2009) or multiple rod opsins (Musilova et al., 2019).

As the properties of water influence light conditions in a grand manner, the aquatic environment offers a great variety of visual habitats. Consequently, the fish visual systems may adapt to them, which subsequently impacts the fish vision (Levine & MacNichol, 1982). As the opsin-based pigments determine light wavelengths the fish can perceive, variations in the expression of opsin genes are the direct way fish adapt to their visual environment, as the opsin gene expression rate reflects the level of opsin protein production, i.e., the amount of the visual pigment (Douglas & Djamgoz, 1990; Loew & Lythgoe, 1978).

1.1.1. Underwater Visual Environment

In clear water, wavelengths around 460 nm (approximately blue) are transmitted the most. Both shorter (ultraviolet – UV) and longer (infrared – IR, and red) wavelengths are more affected by absorption and scattering (Warrant & Locket, 2004). Water molecules scatter light in all directions causing loss of brightness and decrease of contrast and directionality, which impairs two-dimensional image formation. Apart from natural water properties, contents such as phytoplankton, dissolved organic matter and inorganic compounds can affect optical characteristics of water to a great extent (Björn, 2015; Loew

& McFarland, 1990). As a result of the above mentioned, spectral irradiance *E* (power density at a particular wavelength) differs across depths, which is apparent from Graph 1. It provides various visual environments for aquatic organisms, consequently influencing the spectral location of their visual pigments (Loew & McFarland, 1990).

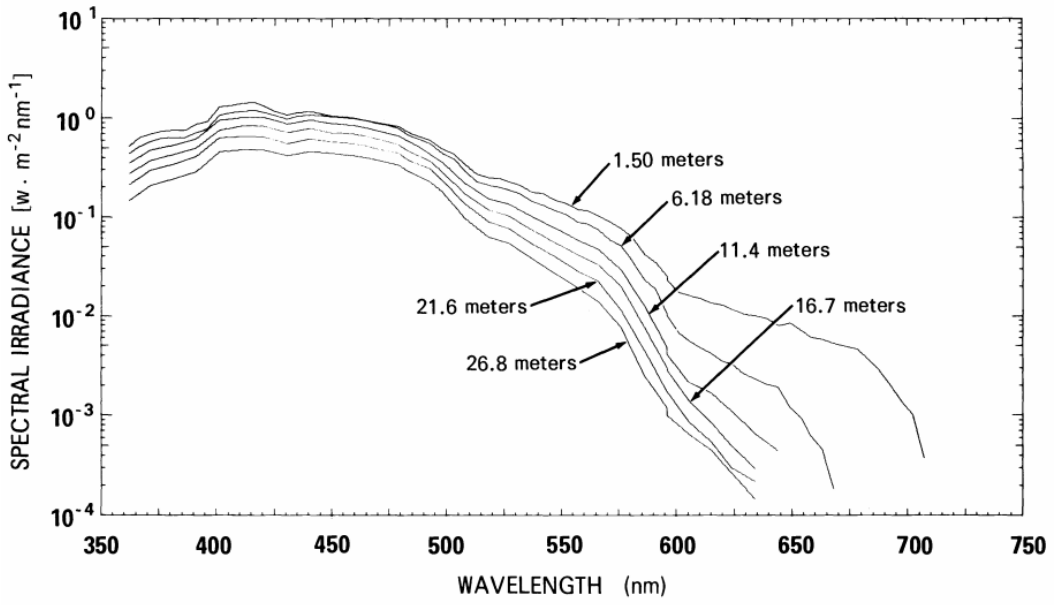

Graph 1 Downwelling Spectral Irradiance E_d for a Crater Lake (Gordon et al., 1980)

1.1.2. Optical System of Fish

Fish eyes are constructed in a common way, as shown in Figure 1, except for cases of specific adaptations. The structure of teleosts eyes resembles the construction of land vertebrates eyes. The main refractory element of the terrestrial eye is the interface between air and a cornea. However, the corneal refractive index is close to the refractive index of water. Therefore, underwater eyes do not optically benefit from the cornea, so the only real refractive power must be provided by a lens, which must, thus, be more curved. As the lens cannot be too large due minimalization of the eye size, fish possess spherical lenses of a great refractive power (Björn, 2015; Fernald, 1988). The spherical lens shape may suffer from spherical and chromatic aberrations; however, fish lenses often exhibit a refractive index gradient increasing from the periphery towards the centre as an effective solution (Jagger, 1992). Apart from that, such inhomogeneity also shortens the focal length, which is crucial for aquatic animals (Land, 1988). The accommodation is provided by the movement of the lens back and forth (in contrast to terrestrial vertebrates that accommodate by lens shape modification), which results in the fact that different parts of the eye are simultaneously focussed at different distances from the eye (Fernald, 1988; Beer, 1894).

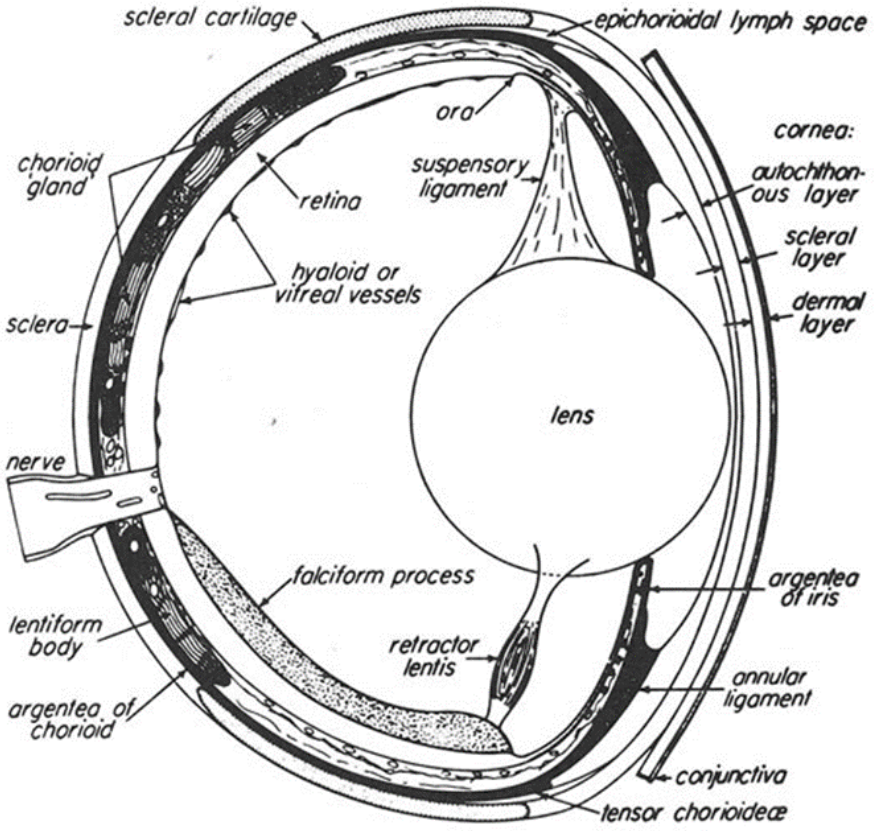

Figure 1 Diagrammatical Vertical Section of Generalized Teleost Eye (*Walls, 1942 in Fernald, 1988)
Some structures shown may not be present in some eyes, such as lentiform body or falciform process.

In summary, light enters the eye through the cornea with no relevant refraction and passes through the pupil controlled by the iris. Subsequently, light passes through the lens that focuses the rays onto the retina. Retinal photoreceptive cells transform the information of the light presence into neuronal impulses, which are transferred along the optic nerve to the brain, where the information is further processed, and signals are converted into images. Finally, these images are cognitively processed (Nilsson, 2013). Note the eye is composed of more than only above-mentioned structures important for image formation, as evident from Figure 1.

1.1.3. Retinal Structure of Fish

The crucial part of the eye is the retina – the extension of the brain that converts information of visual stimuli into neuronal impulses. Among fishes, the retina is a morphologically highly diversified tissue, depending upon the ecological and ethological demands rather than taxonomic classification (Zaunreiter et al., 1991; Wagner, 1990). However, light sensitivity, spatial resolution and wavelength discrimination are key factors for any retina (Wagner, 1990). Light sensitivity refers to a threshold-value of a stimulus

to be registered, spatial resolution characterises a capacity to detect details, and wavelength discrimination indicates a threshold-value to discriminate different wavelengths (van der Meer, 2013). All of them are dependent mainly on photoreceptors; however, they can be highly modified by other retinal cell types as well as receptive fields and other neural features (Wagner, 1990).

The vertebrate retina is organized in layers composed of various cell types: photoreceptor cells, horizontal cells, bipolar cells, amacrine cells, and ganglion cells (Cohen, 1963) as shown in Figure 2. Neighbouring cells of the same layer are linked through electrical synapses and gap junctions, while they bind by chemical synapses across the layers. Visual signals are transferred through an excitatory pathway: photoreceptor cells → bipolar cells → ganglion cells, and modified by inhibitory neurons – horizontal cells and amacrine cells. There are many subtypes of each cell type, varying in both physiological as well as morphological properties, associated into parallel pathways. Such organization allows first visual processing via organization of receptive fields and consecutive ON/OFF pathways. In general, retina is inhomogeneous both horizontally and vertically. Cells in regions adapted to specific visual tasks reflect such needs in their form, size and distribution (Stell, 1972).

Visual function of the eye is greatly dependent on retinal pigment epithelium (RPE) that is in a close structural interaction with photoreceptor cells. RPE has many complex functions such as metabolic support, immune reactions, preservation of homeostasis, light absorption, nourishment of photoreceptors and retinal re-isomerisation (in the process called the visual cycle of retinal) (Strauss, 2005).

Rods and cones are two groups of vertebrate photoreceptor cells that gain and transfer information of light presence. Rods are long and slender while cones appear shorter and bulkier (Cohen, 1972). In general, rods operate in dim light conditions while cones are used at higher light intensities (Baker & Kerov, 2013). As shown in Figure 3, a photoreceptor cell composes of a cell body with a nucleus (soma), an axon with a synaptic terminal heading towards second order neurons, and a ventricle consisting of inner (RIS; closer to soma) and outer (ROS; closer to RPE) segments. RIS and ROS are bonded by a connecting cilium. Outer segment contains double membrane discs where visual pigments are located. As the inner segment consists of many mitochondria, Golgi apparatus and endoplasmic reticulum, it is the main metabolic and house-keeping centre (Baker & Kerov, 2013; Cohen, 1972).

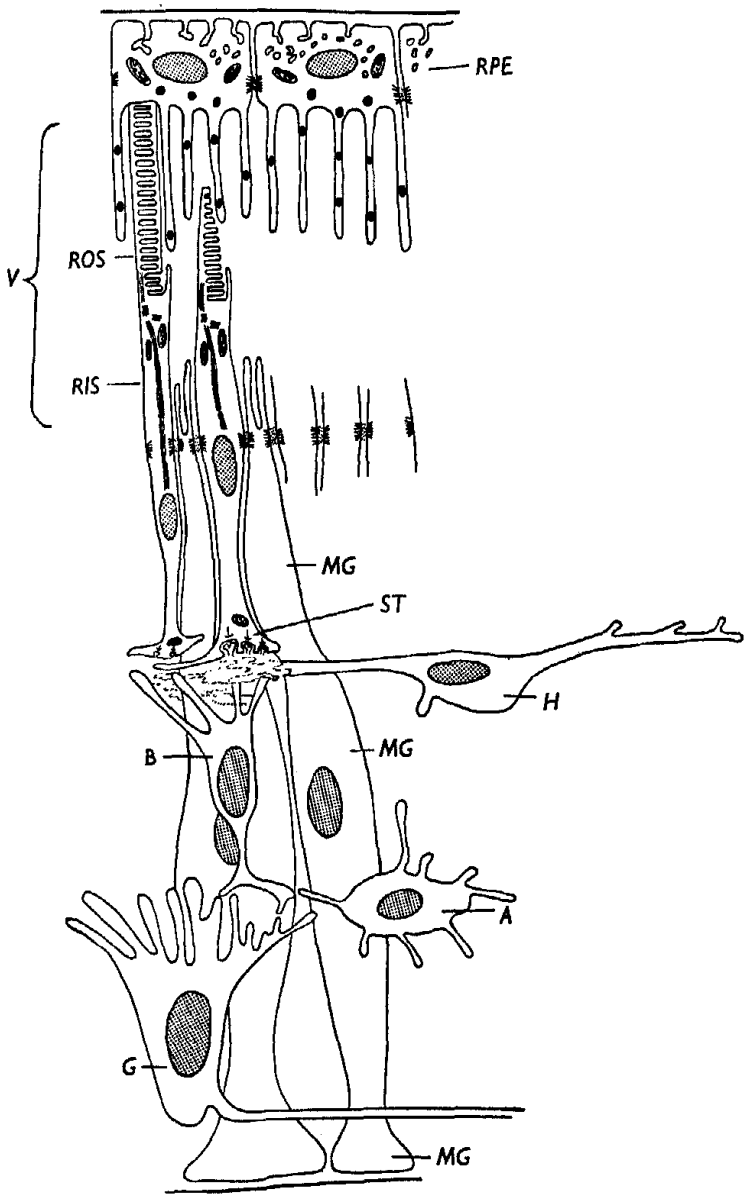

Figure 2 Diagram of a Vertebrate Retina (modified after Cohen, 1963)
Description from the back of the eye towards the lens: (RPE) retinal pigment epithelium, (ROS) receptor outer segment, (RIS) receptor inner segment, (V) ventricle, (ST) synaptic terminal, (B) bipolar cell, (G) ganglion cell, (H) horizontal cell, (A) amacrine cell, (MG) Müller glia

With photoreceptor cells, there are various types of bipolar cells associated. Generally, the rod bipolar cell has a larger body located closer to the receptor, a bigger dendritic tree and a stouter axon with a more proximal and enlarged terminal, than the cone bipolar cell (Stell, 1972). The bipolar cells interconnect the photoreceptor cells with the ganglion cells, which project axons through the optic nerve to the central nervous system. Therefore, the amount of visual information brought into the brain is also determined by the number and distribution of ganglion cells (Hughes, 1985). The whole retinal image processing is further modified by the horizontal and amacrine cells that promote lateral connections through numerous synapses within retinal cell layers (Dowling, 1970).

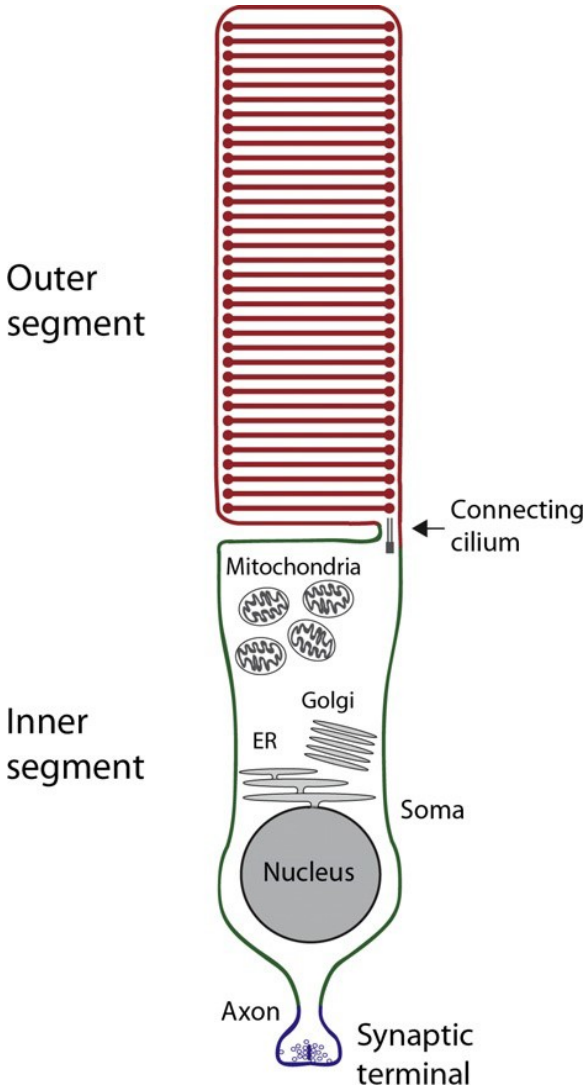

Figure 3 Structure of a Photoreceptor Cell (Baker & Kerov, 2013)

Most fishes exhibit duplex retina (consisting of both rods and cones) (Bowmaker, 1990). However, pure-rod retinae are present in some species living in great depths as their optical system is adapted for high sensitivity at low light intensity (Locket, 1977). Contrarily, diurnal fish living closer to the surface possess a high percentage of cones to allow colour vision (Bowmaker, 1990). Cones exhibit a great morphological diversity among fishes – across individual retina and both intraspecific and interspecific (Bowmaker, 1990). The same applies for their density and size (van der Meer, 1992).

In teleosts with colour vision, spectral cone type corresponds with the cone morphology. The longest cones are usually red-sensitive, middle-length cones are sensitive to green part of the spectrum, short cones are blue-sensitive, and the shortest ones are even sensitive to ultraviolet light (Wagner, 1990). Above-mentioned correlation of spectral sensitivity and cone length can be demonstrated by extremes such as miniature blue

cones in goldfish (Stell & Hárosi, 1976) and oblique cones in rudd (Scholes, 1975). The cone connectivity to other above-mentioned retinal cells correlates with the spectral cone type too – the number of synapsis increases with the wavelength of maximal absorption. Apart from that, several morphological cone types were described – single cones, double cones and twin cones (Wagner, 1990). Furthermore, triple and quadruple cones were also reported, e.g. in the minnow (Lyall, 1956). Single cones are standard "textbook" cones; however, the definition of double and twin cones of individual authors slightly differs and might be confusing. Bowmaker (1990) describes double cones as two closely associated but morphologically distinct cells while twin cones are morphologically indistinguishable. According to Wagner (1990), twin cones refer to double cones of identical partners, when majority of double cones are composed of a larger principal and a smaller accessory member. Also Loew & McFarland (1990) comment confusion on the double/twin cone terminology mentioning that in general, double cones possess structurally different members while twin cones have structurally indistinguishable members; however, a twin cone expressing different visual pigments by each member might not really be a twin cone, so they class twin and double cones to subgroups of identical and non-identical twin or double cones. For simplicity and clarity this thesis does not discern the difference between double and twin cones and uses the term "double cones" only further in the text.

Double cones maximise cone packing. High cone packing favours acuity and/or sensitivity; hence, double cones increase sensitivity in dim light (van der Meer, 1992). In some cone pairs, both members produce the same pigment; however, they can also differ. Moreover, various cone types may be differently distributed within the retina. They can be either apparently randomly arranged or precisely organized into square or row patterns as shown in Figure 4. In teleosts, the mosaics usually consist of a small central single cone sensitive to short wavelengths surrounded by larger four longer-wavelength-sensitive double cones (van der Meer, 1992; Bowmaker, 1990). Photopigments in the double cones forming a square around the single cone often show an alternating symmetry pattern (Fernald, 1981). Furthermore, these mosaics can even change according to light and dark adaptation (Kunz, 1980) or during ontogenetic development (Lyall, 1957b).

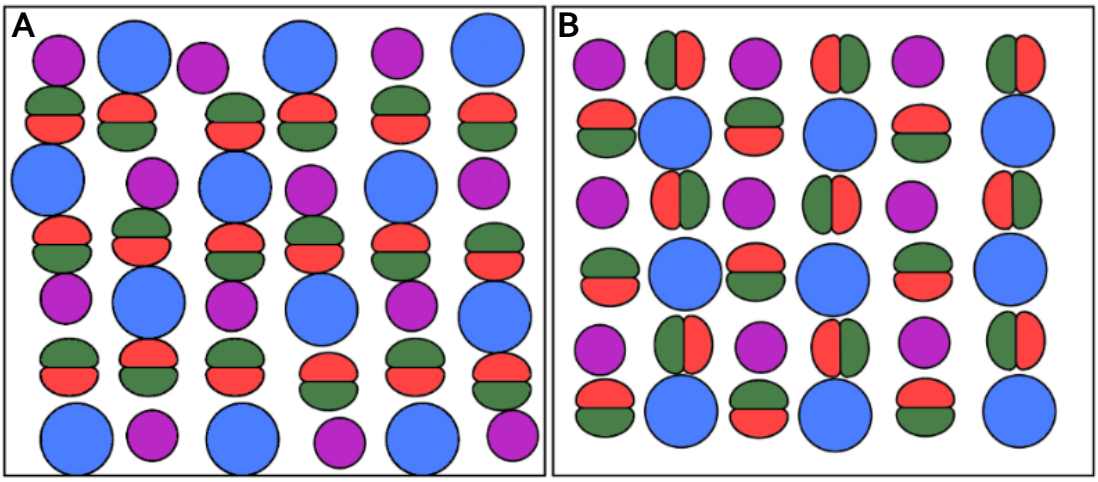

Figure 4 Cone Mosaics of Fish Retina, (A) Row Mosaic in Zebrafish and (B) Square Mosaic in Medaka
(modified after Tohya et al., 2003)
Four types of cones in each retina are indicated by corresponding colours: UV- and blue-sensitive single cones are surrounded by double cones consisting of red- and green-sensitive cones.

1.1.4. Visual Pigments of Fish

Vision depends on determination of the presence of light by photoreceptive molecules – visual pigments. All vertebrate visual pigments consist of a prosthetic group – retinal, which is an aldehyde of vitamin A, embedded in an apoprotein – opsin (Yokoyama, 2000; Bowmaker, 1990). Opsins are integral membrane proteins passing through membranes of the discs within the outer segments of photoreceptor cells, see Figure 5. They consist of a chain of amino acids whose sequence is given by opsin genes. Retinal is covalently linked to the specific lysine residue of the opsin by the Schiff linkage (Yokoyama, 2000; Bowmaker, 1990). The binding of retinal to opsin is schematically shown in Figure 5. Based on the origin of retinal, two families of visual pigments are recognised: the rhodopsins (11-*cis*-retinal from vitamin A1) and the porphyropsins (11-*cis*-3, 4-dehydroretinal from vitamin A2). Rhodopsins are common among vertebrates, whereas porphyropsins are found only in some teleosts, amphibians and aquatic reptiles (Bowmaker, 1990). It is important to note that whilst any opsin + 11-*cis*-retinal complex is correctly termed a rhodopsin (as used in this thesis), the term rhodopsin is most commonly applied to the rod opsin + 11-*cis*-retinal complex, i.e. visual pigment of rods (Lythgoe, 1979), which is denoted as rod opsin or Rh1 in this thesis. The name rhodopsin comes from the Greek words meaning rose and vision as rod opsins appear pink because they transmit red and blue light, whereas green part of the spectrum is absorbed (Levine & MacNichol, 1982).

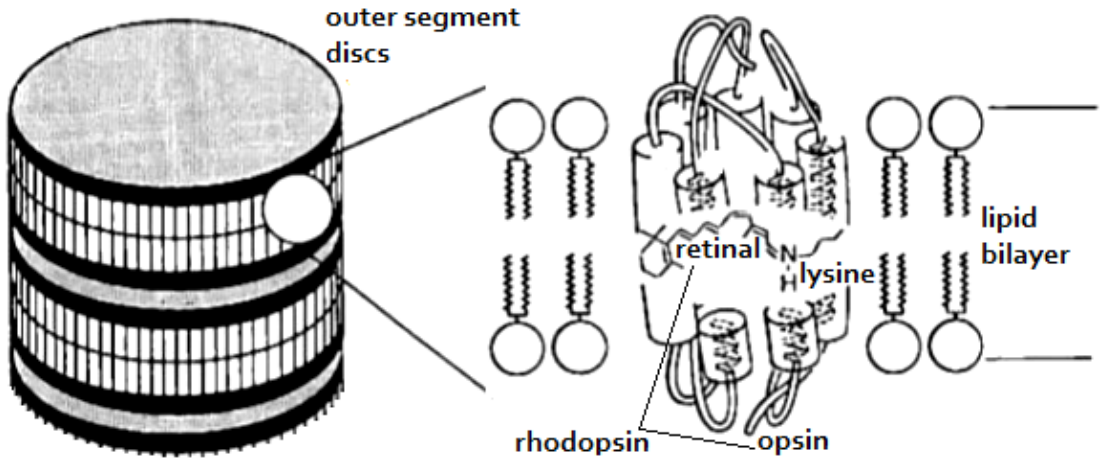

Figure 5 Schematic Model of the Molecular Structure of a Photoreceptor Cell (modified after Wolken, 1995)

The maximum absorbance (λ_{max}) of visual pigments is determined by both the amino acid sequence of the opsin and the type of retinal. Opsins absorb maximally below the wavelength of 300 nm, whereas retinal maximum absorbance is at 380 nm (400 nm for 3-dehydroretinal) (*Knowles and Dartnall, 1977 in Douglas & Djamgoz, 1990). Opsin-retinal binding leads to a broad absorbance band in the visible region of light spectrum as shown in Graph 2. The exact rhodopsin λ_{max} is determined by amino acid sequence of the specific opsin (given by the opsin gene) and its relationship with the retinal. Porphyropsins have additional double bond compared to rhodopsins, thus their λ_{max} is generally shifted into longer wavelengths (Bowmaker, 1990) as evident from Graph 2.

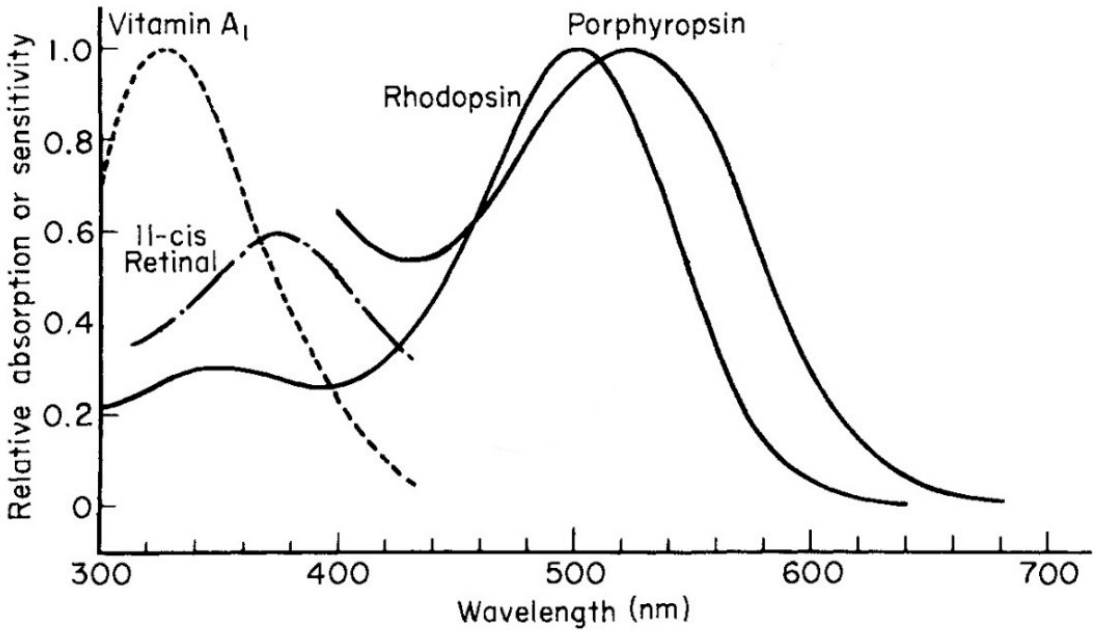

Graph 2 Relative Absorption Spectra of Vitamin A1, 11-cis Retinal, Rhodopsin and Porphyropsin
(modified after Wolken, 1995)

Visual pigments are further described by spectral sensitivity, which is relative efficiency of light detection by a photoreceptor as a function of wavelength (Sabbah et al., 2010). In vertebrates, five classes of spectrally distinct visual pigments were established. One of them is found in rods (RH1 – rhodopsins with λ_{max} of about 500 nm) and other four in cones (SWS1 – very short-wavelength sensitive group with λ_{max} of 360–430 nm; SWS2 – short-wavelength sensitive group with λ_{max} of 440–460 nm; RH2 – rhodopsin-like group with λ_{max} of 470–510 nm; MWS/LWS – middle/long-wavelength sensitive group with λ_{max} of 510–560 nm) (Yokoyama, 2000). Rods are responsible for scotopic vision while cones provide photopic vision (Bowmaker & Hunt, 2006).

Colour vision requires, apart from neural processing, at least two classes of differentially sensitive cone photoreceptors (Sabbah et al., 2010). The cone opsin genes arose through duplications of a single ancestral opsin gene. Additional mutations in duplicated genes have led to diversification of opsins even within the visual pigment classes. As a result, many teleost fishes embody a great variety of opsin genes (Sabbah et al., 2010; Yokoyama, 2000). In African cichlids, a set of eight spectrally distinct opsins can be found: one rod opsin RH1 and seven cone opsins SWS1, SWS2B, SWS2A, RH2B, RH2Aβ, RH2Aα and LWS (Spady et al., 2006) as shown in Figure 6. Interspecific variation in expression of corresponding opsin genes can generate different opsin subsets, which may potentially lead to variation in spectral sensitivity among cichlid species and consequently affect the fishes vision (Sabbah et al., 2010).

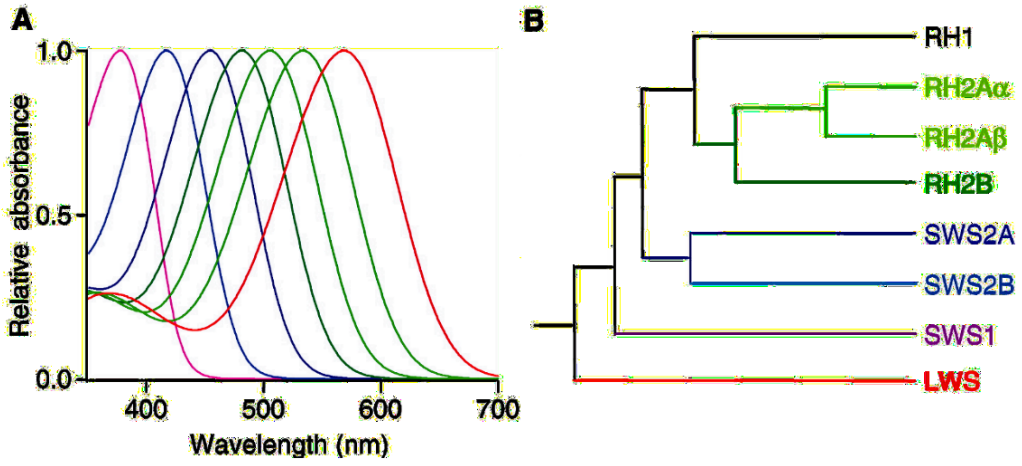

Figure 6 Opsins & Opsin Genes in African Cichlids (Bowmaker & Hunt, 2006)
(A) Absorbance of the 7 cone opsins colour-coded with opsin class. (B) Schematic of the phylogenetic arrangement of the opsins illustrating the gene duplications that have occurred within the SWS2 and RH2 opsin classes.

1.1.5. Visual Adaptations of Fish

Many fishes undergo great transitions during their development including changes in morphology, behaviour as well as in environment. Adults often live in drastically different visual conditions than juveniles, as the fish migrates to another habitat of a different depth or even water type during ontogeny (e.g., eels spend most of their lives in freshwater; however, once they undergo maturity metamorphosis, they migrate to the ocean to breed). Consequently, their visual system changes too (Bowmaker, 1995). In addition to other modifications such as morphological adjustments, lens pigmentation or chromophore switches; the relative opsin gene expression ratio (a percentage of total opsin gene expression) often shifts (Spady et al., 2005). As shown in Figure 7, such developmental opsin gene expression shifts are present, e.g., in Nile tilapia, *Oreochromis niloticus*, which is an ancestral outgroup to the cichlid radiations in the Great Lakes (Spady et al., 2006). Certain plasticity in opsin gene expression was reported also in adult fish when their rearing environment changes depending on developmental rearing conditions as proven on guppies by Ehlman et al. (2015). It is also important to point out that opsin gene expression profiles may differ between wild-caught and lab-reared fish even though such plasticity is species-dependent as demonstrated by Hofmann et al. (2010).

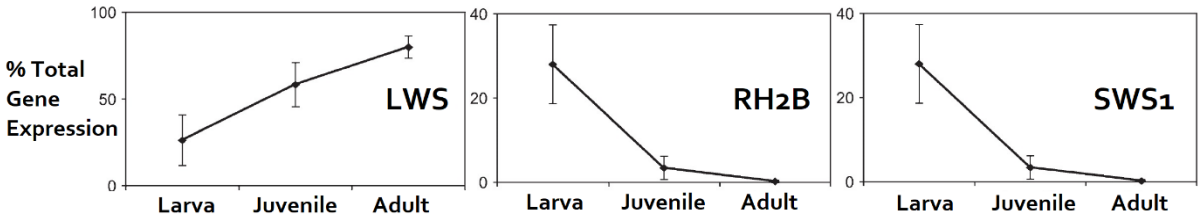

Figure 7 Relative Cone Opsin Gene Expression of Selected Opsins in Nile Tilapia – Larva, Juvenile and Adult
(modified after Spady et al., 2006)

Even though African cichlids possess seven classes of cone opsin genes, their expression varies among species resulting in significantly different spectral sensitivities dependent on the light conditions of the habitat. Opsin expression remarkably varies in-between sand and rock dwellers. Another main influencing factor is the mode of foraging. Species searching for prey in sand by vibrations are not visually specialized, though longer-wavelength sensitivity (LWS) can be of a great advantage in turbid water. Contrarily, ultraviolet vision (SWS1) increases the efficiency of fish feeding on zooplankton or algae in the water column. Opsin expression can be also influenced by fish colour patterns related to mate choice as well as communication in general. Based on expressed opsin

gene profiles African cichlids can be divided into three clusters corresponding with various life strategies including factors mentioned above, as demonstrated in Figure 8. All this proves a great adaptability of cichlids and high plasticity of their visual system (Terai et al., 2017; Hofmann et al., 2009; Parry et al., 2005; Carleton & Kocher, 2001).

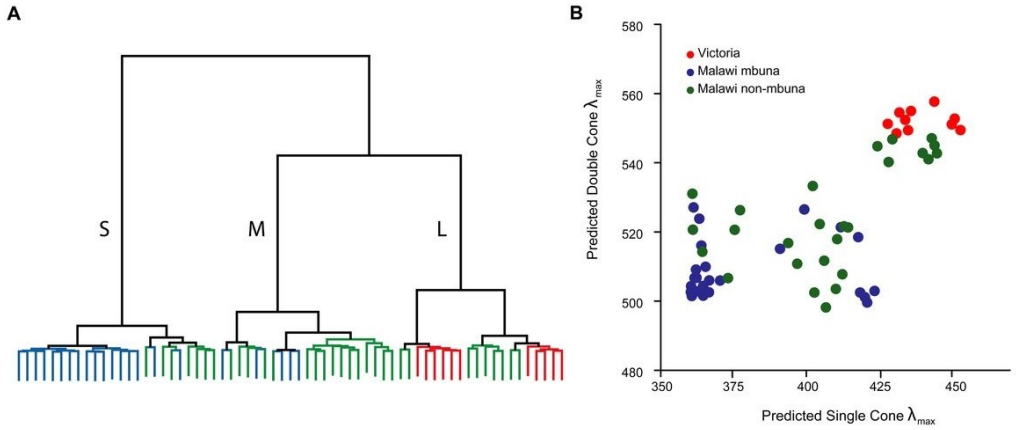

Figure 8 Opsin Gene Expression Profiles as Well as Single- and Double-Cone Sensitivities of Lake Malawi and Lake Victoria Cichlids Form Three Clusters (Hofmann et al., 2009)
(A) Three hierarchical clusters of species' opsin gene expression profiles: S – short-wavelength, M – medium-wavelength, L – long-wavelength. (B) Estimates of single- and double-cone sensitivities suggesting that these three clusters correspond to visual palettes sensitive to short-, medium-, and long-wavelength portions of the cichlid visible light spectrum. Single- and double-cone λ_{max} values were estimated by weighting the peak absorbance of each opsin by its relative expression level. ; Cichlids from Malawi mbuna clade (rock-dwelling species, in blue) predominantly express shorter-wavelength opsins – *SWS1* and *SWS2B* in their single cones, a few of them express *LWS* in their doubles cones. Non-mbuna Malawi cichlids (sand-dwelling or pelagic species, in green) collectively express six opsins, but the middle- and longer-wavelength classes are predominant – all three *SWS* opsins in their single cones, majority expresses *LWS* in their double cones. Lake Victoria cichlids (turbid waters, in red) collectively express four different opsin classes – all express *SWS2A* in their single cones, *RH2A* and *LWS* in their double cones, some also express *SWS2B* in their single cones.

Functional and environmental demands also greatly affect photoreceptor cell patterns in retina described in Chapter 1.1.3. Detail discrimination is determined by the resolution as a function of cone density and enhanced by colour discrimination (demanding presence of various visual pigments). Vision in dim light is determined by sensitivity, which is a function of both cone convergence and cone size. As cone density and cone size are features of space in receptor layer, they cannot be maximized simultaneously; and hence, they must be balanced. Apart from that, colour-specific cone types also compete for the space. As maximal cone packing improves photon catching ability, a purely double cone row mosaic is appropriate for vision in a dim homochromatic environment. High resolution can be obtained by minimizing the size of the pattern units, whereas movement detection can be improved by maximizing their symmetry; therefore, a triangular pattern is suitable for high resolution and accurate movement detection. Finally, a square mosaic has a high adaptive capacity for varying spectral distributions (van der Meer, 1992).

Variations in opsin gene expression may significantly manifest in retinal mosaics. Torres-Dowdall et al. (2017) performed *in situ* hybridization staining of opsin genes *RH2B, RH2Aβ* and *LWS* in laboratory reared fish of two Midas cichlids benthic species: *Amphilophus citrinellus* from turbid great lake Nicaragua and *Amphilophus astorquii* from clear crater lake Apoyo (shown in Figure 9) . Retina of *A. citrinellus* was dominated by double cones expressing mainly *LWS* in both members. The authors propose that such dominance of long-wavelength-sensitive cones could be an adaptation to the dim-light conditions of turbid waters as the long-wavelength-sensitive cones could be used for achromatic vision. Apart from *LWS*, double cones of *A. citrinellus* expressed also *RH2Aβ* and some even coexpressed *LWS* and *RH2Aβ* or *LWS* and *RH2B*. Retinae of *A. astorquii* embodied higher variability than those of *A. citrinellus.* Most *A. astorquii* double cones expressed *LWS* in one of the double cone members and *RH2Aβ* in the other. Some of the cones coexpressed *RH2Aβ* with *LWS* or *RH2B*. *RH2B* was sometimes expressed even by itself.

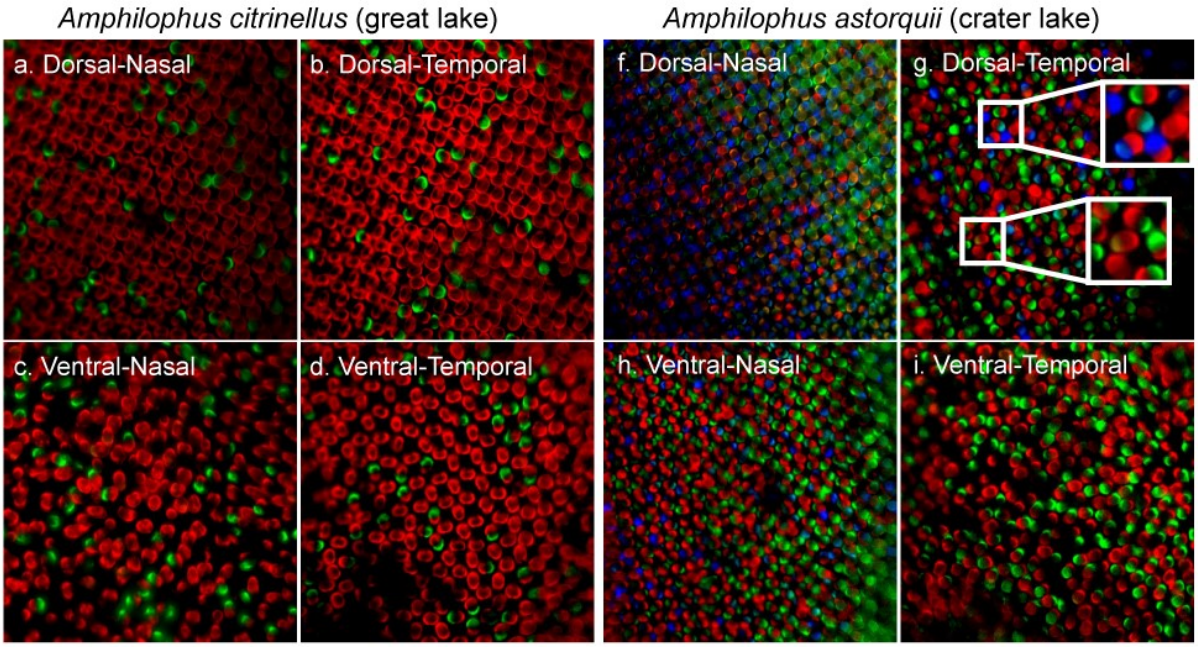

Figure 9 Fluorescent *in situ* Hybridization Staining of Two Midas Cichlid Species (Torres-Dowdall et al., 2017) *In situ* hybridization staining of (a-d) *Amphilophus citrinellus* and (f-i) *Amphilophus astorquii* across four quadrants of the retina. *LWS* in red, *RH2Aβ* in green and *RH2B* in blue. Details in (g) show examples of coexpression.

1.2. Cichlids of Lake Barombi Mbo

Barombi Mbo is a crater lake near town of Kumba in Cameroon (see Figure 10) laying at an altitude of around 300 m agl, 4°39'N/9°24'E (Hughes & Hughes, 1992). The open water area of 453 ha makes it the biggest of the western equatorial crater lakes that were

formed over thousands of years ago on what were once volcanoes. It has 2,5 km in diameter and average depth of 69 m (Steeves, 2004). The maximum depth is 111 m; however, only about top 25 m contain acceptable oxygen levels for life (Steeves, 2004; Hughes & Hughes, 1992; Green et al., 1973) as shown in Figure 10. Table 1 lists 17 fish species that have been reported in Barombi Mbo, of which 12, including radiation of 11 cichlids, appear to be endemic (Trewavas et al., 1972). Even though the Barombi Mbo cichlid flock is one of the most convincing examples of sympatric speciation, it probably carries more complex history (Martin et al., 2015; Turner, 2007; Schliewen & Klee, 2004; Schliewen et al., 1994).

Table 1 List of Fish Species from Barombi Mbo (modified after Trewavas et al., 1972)

Species	Barombi name
Cyprinidae	
Barbus batesii	suh, kimbundu
Clariidae	
Clarias walkeri	nyongo
Clarias maclareni	nyongo
Cyprinodontidae	
Aphyosemion oeseri	
Epiplatys sexfasciatus	longo katta
Procatopus similis	lenge
Cichlidae	
Sarotherodon lohbergeri	leka keppe
Sarotherodon steinbachi	kululu
Sarotherodon linnellii	kippé, unga
Sarotherodon caroli	fissi, unga
Myaka myaka	myaka
Konia eisentrauti	konye
Konia dikume	dikume
Pungu maclareni	pungu
Stomatepia mariae	nsess
Stomatepia pindu	pindu
Stomatepia mongo	mongo

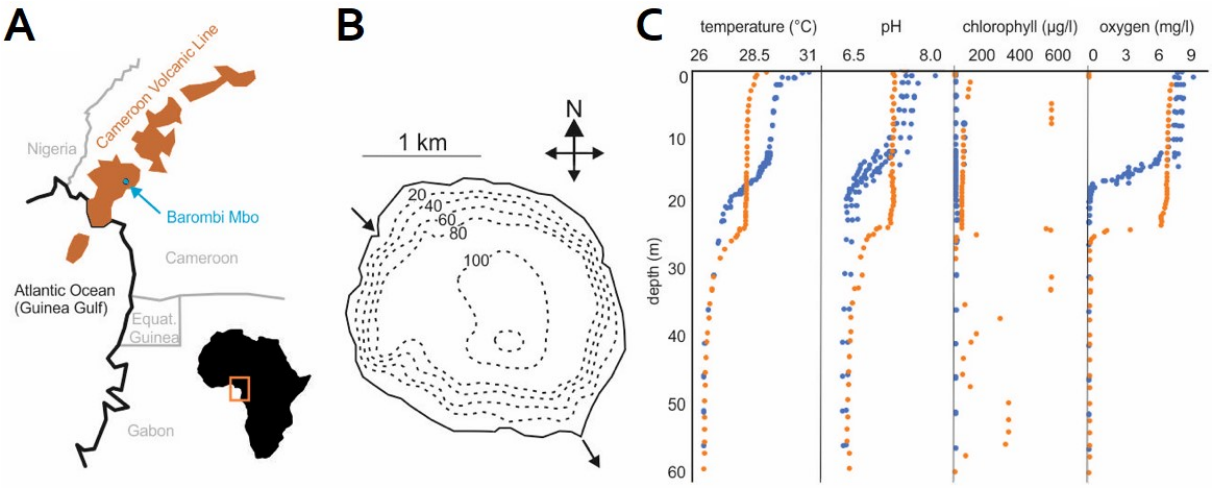

Figure 10 Description of Lake Barombi Mbo (Musilová et al., accepted)
(A) Location of the Barombi Mbo crater lake in South-West Cameroon in West Africa. (B) Simplified topographical map after Schliewen et al. (1994). (C) Limnological parameters in different depths of the crater lake measured in the dry (blue dots, 22nd February 2017, three measurements) and in the rainy season (orange; 27th of July 2017; one measurement) show the presence of an oxy- and thermocline around 15 - 25 m of depth.

The Barombi Mbo cichlid lineage has evolved from a *Sarotherodon* ancestor. Phylogenetic reconstruction revealed four lineages within the Barombi Mbo flock: one combining the fine-particle feeders of *Sarotherodon* with the highly specialized spongivore *Pungu*, one of *Myaka* dwarf zooplanctivore, another one containing macro-invertebrate feeding sister taxa to genus *Konia,* and last one of predatory genus *Stomatepia* (Schliewen & Klee, 2004).

Musilová et al. (accepted) investigated the cone opsin expression profiles of all 11 cichlid species from Lake Barombi Mbo (see Figure 11). Significant differences between the profiles of deep-water and shallow-water species were reported. A shift towards the middle-wavelength sensitive opsins (i.e., towards shorter wavelengths in double cones, and towards longer wavelengths in single cones) was observed in deep-water species *Konia dikume* and *Myaka myaka*. Specifically, they lack expression of red-sensitive opsin *LWS* and blue/violet-sensitive opsin *SWS2B*; furthermore, longer-wavelength-green-sensitive opsin *RH2Aα* is more abundant than shorter-wavelength-green-sensitive opsin *RH2Aβ*. Contrarily, remaining nine cichlid species inhabiting shallow waters of Barombi Mbo express *RH2Aβ* more than *RH2Aα* or express only one green-sensitive opsin. Single cones of the deep-water species express only *SWS2A*, while shallow-water palette is dominated by the expression of *SWS2A* together with *SWS2B* or *SWS1* in single cones. Expression of UV-sensitive *SWS1* was found only in one species, *Sarotherodon steinbachi.* In general, the cone opsin gene expression profiles of shallow-water species were richer and more diversified than the ones of deep-water species.

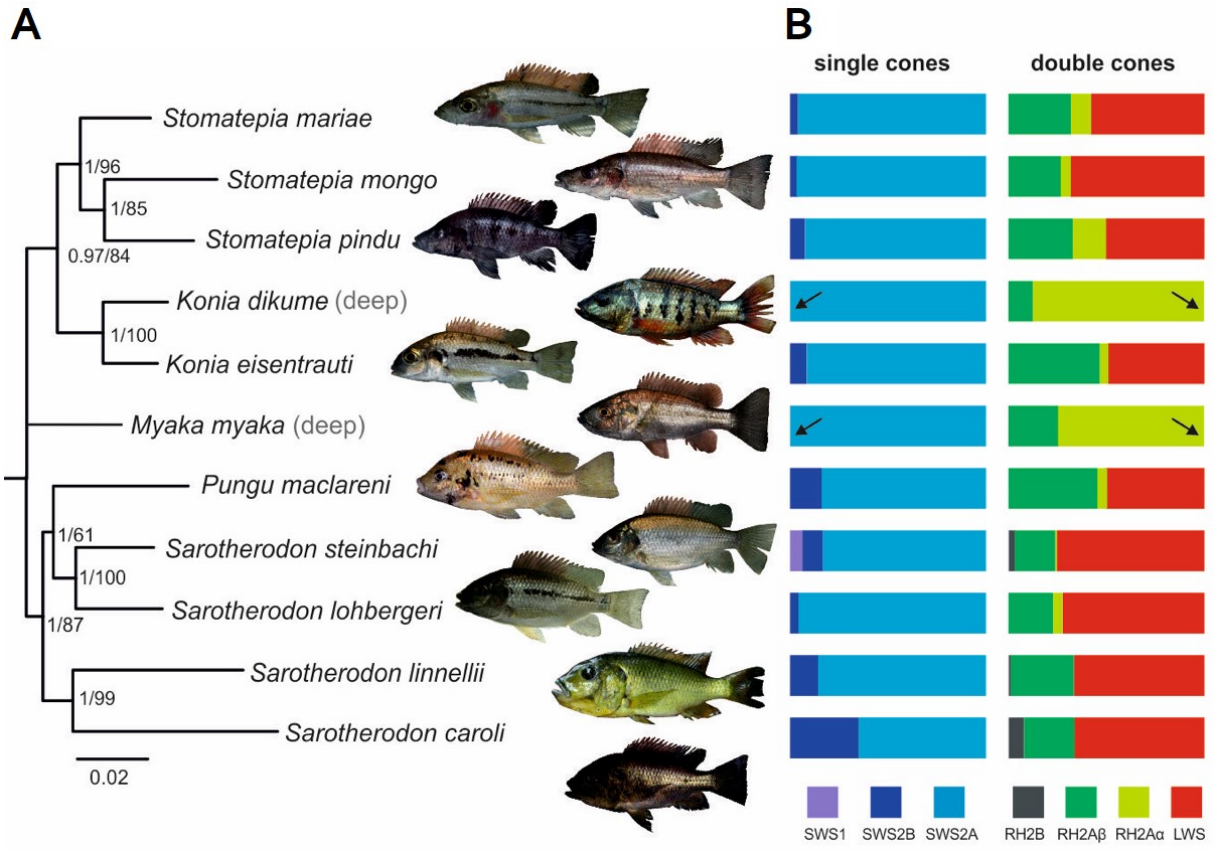

Figure 11 Cichlids of Barombi Mbo – Phylogenetic Tree Based on Retinal Transcriptome Sequences and Opsin Gene Expression Profiles (Musilová et al., accepted)
(A) Phylogenetic hypothesis based on retinal transcriptome sequences of all 11 cichlid species from Barombi Mbo using Nile tilapia as an outgroup. (B) Opsin gene expression profiles of all 11 cichlid species inhabiting the Barombi Mbo crater lake based on the retina transcriptomes and qPCR. For each species, the cone opsin expression levels are shown per gene and as proportions of the total cone opsin expression per species, separated into single and double cones. The deep-water species, *Konia dikume* and *Myaka myaka*, lack *SWS2B* expression (arrow-marked) and only show expression of *SWS2A* in the single cones. In the double cones of both deep-water species, *LWS* is virtually not expressed (arrow-marked) and *RH2Aα* is more abundant than *RH2Aβ*.

The key question is how the difference in the opsin gene expression profiles between shallow-water and deep-water species of Barombi Mbo manifests at retinal level, which is a subject matter of this thesis. Four species were chosen for this study: shallow-water species *Stomatepia mariae* and *Konia eisentrauti,* deep-water species *Konia dikume* and seasonally deep-water species *Myaka myaka*. All of them are pictured in Figure 12 (and also Figure 11 next to the phylogenetic tree), their description follows.

Stomatepia mariae is an about 12 cm big silvery grey fish with a dark horizontal band along the body and a long snout. It lives about 0.5–1 m deep, swims in groups and spawns in substrate and then picks, carries and incubates eggs in the mouth. Even though its diet includes plants and organic debris; in particular, it is a predator of aquatic arthropods, terrestrial insects and even fish (Steeves, 2004; Trewavas et al., 1972).

Konia eisentrauti is a grey species with a black band of uneven width, black blotches parallel to the dorsal outline and colourless fins. It is distinctive by its evenly decurved snout. It feeds mostly on invertebrates (especially mayfly larvae) in water about 1–2 m deep; however, plants and even cichlid eggs were found in its stomach. *K. eisentrauti* usually occurs in small groups and feeds by watching a particular object, snapping it up and spitting out some of the debris that was taken with it (Steeves, 2004; Trewavas et al., 1972).

Konia dikume has an acute snout in contrast to *K. eisentrauti*. When freshly caught, *K. dikume* does not embody any dark marking, but when preserved, couple of dark blotches appears between upper lateral line and dorsal fin. It is a silver colour 12cm mouth brooder with a dark snout and fins tinted in watery yellow (Steeves, 2004; Trewavas et al., 1972). *K. dikume* lives in deep water (around 20 m of depth) where it feeds on insect larvae. It feeds mostly on the larvae of the midge *Chaoborus*, which spend the daytime at depths bellow 20 m and ascend to upper layers at night, where they feed mainly on rotifers *Brachionus falcatus*. *K. dikume* can dive even into the deoxygenated depths thanks to its large blood volume and high haemoglobin concentration as well as erythrocyte count. Such adaptation extends the time available for feeding on *Chaoborus* larvae when it migrates during a short period of dusk and dawn, which is very important as the fish is a visual feeder (Green et al., 1973).

Myaka myaka is a small (8 cm) grey pelagic planktivore with small teeth, usually yellow pelvic fins and distinctive red orange eye socket (Steeves, 2004; Trewavas et al., 1972). It is less robust than other cichlids of Lake Barombi Mbo (Trewavas et al., 1972). *M. myaka* spends dry season in deep water and migrates into shallow littoral zone for spawning at the peak of the rainy season (June–August). It feeds on organic debris and phytoplankton probably close to the bottom (Green et al., 1973; Trewavas et al., 1972).

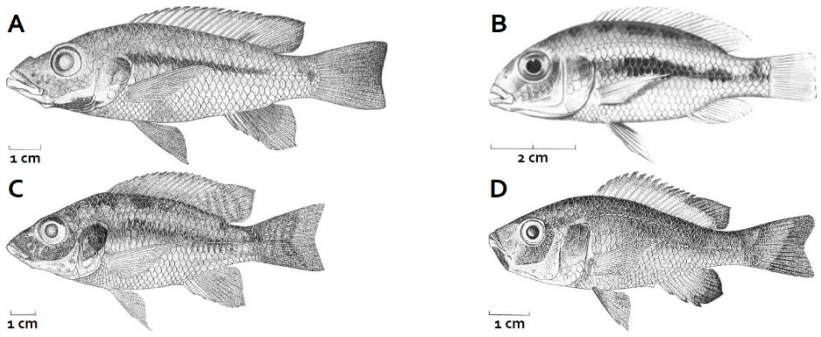

Figure 12 Four Selected Cichlid Species of Barombi Mbo (Trewavas et al., 1972)
Barombi Mbo cichlid species living in shallow water: (A) *Stomatepia mariae* and (B) *Konia eisentrauti*; and in deep water: (C) *Konia dikume* and (D) *Myaka myaka*.

2. Aims of the Thesis

Cichlids are one of the most adaptive fishes, well-known for their rapid diversification (Turner, 2007). Hence, cichlids have been lately investigated into a great extent by various researchers including vision scientists (Mameri et al., 2019; Escobar-Camacho et al., 2019; Härer et al., 2018; Terai et al., 2017; Hauser et al., 2017; Härer et al., 2017; Torres-Dowdall et al., 2017; Dalton et al., 2017). Fishes from the extreme environments such as deep water adapt to lower light intensity and different colour composition of the light spectrum. The adaptations include, among others, variations in opsin gene expression and alternations in retinal cell patterns (mosaics) (Levine & MacNichol, 1982; Engström, 1963). It was investigated that deep-water cichlid species of Cameroonian Lake Barombi Mbo exhibit significantly different cone opsin gene expression profiles than the ones living in shallow water (Musilová et al., accepted). However, the distribution of the opsins throughout retinae has remained unknown.

The main focus of this thesis is visualization of photoreceptor cells in retinae of selected Barombi Mbo cichlids by the modern method of fluorescent *in situ* hybridization (FISH) employing RNA probes on whole mounts. FISH is an excellent method for localizing position of target molecules (e.g., mRNA) within tissue (e.g., retina) through binding to fluorescent probes with high specificity and sensitivity. Hence, it provides an efficient way of mapping distribution of the expressed opsin genes in cichlid retinae. The aims of this thesis are:

1) reconstruction of retinal mosaics in selected cichlids of Lake Barombi Mbo (*Stomatepia mariae*, *Konia eisentrauti, Konia dikume* and *Myaka myaka*),

2) exploring the effect of depth on the function and organization of retinae in cichlids from shallow- (*S. mariae*, *K. eisentrauti*) and deep- (*K. dikume, M. myaka*) water environment,

3) testing hypothesis on possible coexpression of photoreceptor genes in cones.

Another important object of this thesis is development of the whole-mount retina FISH staining method for Barombi Mbo cichlid species including its optimization and standardization for further use.

3. Materials and Methods

For the purposes of this thesis, fluorescent *in situ* hybridization (FISH) employing RNA probes was performed on retinae whole mounts of cichlids from Lake Barombi Mbo. FISH is a time-demanding complex method employing a great number of reagents, materials, equipment and procedures. This chapter is introduced with a list of reagents which were used during the procedures, whose description follows.

3.1. List of Reagents

For better clarity, the reagents are divided into three lists: 1) reagents for probe production including coding DNA (cDNA) synthesis and polymerase chain reaction (PCR), 2) reagents for tissue preparation including dissection, fixation and storage, and 3) reagents for FISH together with solution recipes.

3.1.1. Reagents for Probe Production

Mint-2 cDNA Synthesis Kit (Evrogen)
PPP Master Mix (Top-Bio)
MinElute Gel Extraction Kit (Qiagen)
Digoxigenin (DIG) RNA Labelling Mix (Roche)
Fluorescein (FL) RNA Labelling Mix (Roche)
Protector RNase Inhibitor (Roche)
T3 RNA Polymerase with Transcription Buffer (Roche)

3.1.2. Reagents for Tissue Preparation

RNAlater
phosphate-buffered saline (PBS)
4% paraformaldehyde (PFA) in PBS
70% methanol (MetOH)
100% methanol

3.1.3. Reagents for Fluorescent *in situ* Hybridization

To prevent RNase contamination during the prehybridization procedures, prehybridization solutions were made with RNase free water, autoclaved (except solutions containing Tris) and stored at 5 °C. All labware and glass were cleaned and sterilised for both, reagent preparations and during the procedures.

Basic Reagents

water	sucrose
RNase-free water	maleic acid
phosphate-buffered saline (PBS)	1 M Tris-HCl pH 7.5
sodium citrate dihydrate	Roche Molecular Blocking Reagent (RMB)
NaH_2PO_4 (monohydrate)	ethylenediaminetetraacetic acid (EDTA) disodium salt
Na_2HPO_4 (heptahydrate)	100× Triton X-100
NaOH pellets	0.1% Tween-20 in PBS (PBST)
NaCl	30% H_2O_2 in water
deionized formamide	10% paraformaldehyde (PFA) in water
methanol	50% dextran sulfate in water
xylene	70% glycerol in PBST
Tween-20	50%, 70% and 90% MetOH in PBST
proteinase K	50:50 xylene:methanol

0.5M EDTA

18.6 g EDTA disodium salt dihydrate was dissolved in 85 ml RNase-free water. To adjust the solution to pH 8, NaOH pellets were added. The solution was then brought up to 100 ml with water and autoclaved.

5× Maleic Acid (0.5M Maleic Acid + 0.75M NaCl)

58 g maleic acid was dissolved in 850 ml RNase-free water. To adjust the solution to pH 7.5, NaOH pellets were added. After cooling down, the pH was finally adjusted. 43.8 g NaCl was added into the solution which was then brought up to 1 l with water.

1.67× phosphate buffer w/ sucrose

Mixture of 0.20 g NaH_2PO_4, 1.63 g Na_2HPO_4 and 3.75 g sucrose was brought up to 45 ml with RNase free water.

4% Paraformaldehyde in 100mM Phosphate Buffer w/ 5% Sucrose

4% PFA in phosphate buffer with sucrose was freshly made each time by adding 800 µl 10% PFA to 1 200 µl 1.67 phosphate buffer w/5% sucrose.

Proteinase K in PBST

10× stock (100 ug/ml) of proteinase K in PBST was made. It was stored at -20 °C in 1ml aliquots. 1× solution was made up freshly each time by diluting the stock 1:10 in PBST.

3% H_2O_2 in PBST

The hydrogen peroxide was diluted from 30% stock: 50 µl H_2O_2 and 450 µl PBST.

5M NaCl

87.66 g NaCl was dissolved in 250 ml RNase-free water. The solution was brought up to 300 ml and autoclaved.

Tris-HCl+EDTA+NaCl (TEN) Solution

5 ml 1M Tris-HCl pH 7.5, 30 ml 5M NaCl and 1 ml 0.5 M EDTA was brought together.

Roche Molecular Blocking Solution (RMB)

10× RMB was made by adding 10 g Roche Blocking Reagent powder into 100 ml 1× maleic acid buffer (20 ml 5× maleic acid and 80 ml water) and heated (65 °C) to dissolve. It was autoclaved and stored at -20 °C. For use, 1× RMB was made by diluting 10× RMB in 1× maleic acid, aliquoted and stored at -20 °C.

Saline-Sodium Citrate (SSC) Solutions

20× SSC was made by dissolving 87.6 g NaCl in 350 ml water; 44.12 g sodium citrate dihydrate was added to the solution which was then brought to final volume 500 ml. 2× 0.1% Tween-20 in SSC (SSCT) was made by mixing 50 ml water, 5 ml 20× SSC and 50 µl Tween. 0.2× SSCT was made by mixing 50 ml water, 500 µl 20× SSC and 50 µl Tween. 50% formamide in 2× SSC was made by mixing 20 ml water, 25 ml 100% formamide, 5 ml 20× SSC and 50 µl Tween.

1× Maleate buffer/ 0.1% Triton X-100

40 ml water, 10 ml 5× maleic acid and 50 µl 100× Triton X-100 were mixed together.

(Pre)Hybridization Solution without Water/Probes

3.6 ml TEN solution, 25 ml 100% formamide, 10 ml 50% dextran sulfate and 5 ml 10× Roche Blocking Solution were mixed and stored at -20 °C.

(Pre)Hybridization Solution

Prehybridization solution mix was made from 261.6 µl (pre)hybridization solution without water/probes and 38.4 µl RNase-free water.

Hybridization solution was made from 130.8 µl (pre)hybridization solution without water/probes, 1.5 µl each corresponding DIG and FL probe and 16.2 µl RNase-free water for smaller retinae, or double amount for bigger ones.

Antibodies

Anti-Digoxigenin-Peroxidase, Fab fragments (anti-DIG POD) (Roche)

Anti-Fluorescein-Peroxidase, Fab fragments (anti-FL POD) (Roche)

Tyramide Signal Amplification (TSA) Kits

Alexa Fluor™ 488 Tyramide Super Boost™ Kit (TSA 488) (Invitrogen)

Alexa Fluor™ 594 Tyramide Super Boost™ Kit (TSA 594) (Invitrogen)

3.2. Probe Production

In this case, the probe is a DIG- or FL-labelled complementary RNA strand to localize mRNA of expressed opsin genes. To produce the probes, custom primers were designed based on transcriptomes of Barombi Mbo cichlids (Musilová et al., accepted) and used cDNA obtained by transcription of RNA from *K. dikume* and K*. eisentrauti*. To optimize, cDNA was produced from 4 different RNA samples of each species and primers were designed to vary in amplicon length and product position. As a result, the annealing temperature of some PCRs was reduced by 2 degrees compared to the one indicated.

3.2.1. cDNA Synthesis

The cDNA was produced according to the cDNA preparation protocol with Mint-2 cDNA Synthesis Kit (Evrogen). Tubes were vortexed and spun prior to heating in all steps.

To make single-strand cDNA (ss cDNA), RNA samples of each species, *Konia eisentrauti* and *Konia dikume,* were preheated to 65 °C. 3 µl of each RNA sample were mixed with 1 µl CDS-Adapter and 1 µl PlugOligo-Adapter. The solutions were incubated at 70 °C for 2 min and then at 42 °C, while RT master mix (2 µl 5× first-strand buffer, 1 µl 20 mM DTT, 1 µl 10mM dNTP, 1 µl mint reverse transcriptase) was prepared. 5 µl RT master mix was added to each tube containing RNA sample. The tubes were incubated at 42 °C for 30 min. When 5 µl IP-solution was added to each reaction tube, the mixtures were incubated at 42 °C for 1.5 h and then placed on ice to terminate the reaction. Generated single-strand cDNA was either directly used to create double-strand cDNA or stored at 5 °C.

To make double-strand cDNA (ds cDNA), polymerase chain reaction (PCR) mixture (40 µl RNase-free water, 5 µl 10× encyclo buffer, 1 µl dNTP mix – 10mM each, 2 µl 10µM PCR primer-M1, 1 µl ss cDNA from previous procedure and 1 µl 50× encyclo polymerase mix) were amplified through the following programme: initial denaturation at 95 °C

for 1 min, 20 cycles of 95 °C for 15 s, 66 °C for 20 s and 72 °C for 3 min. Generated ds cDNA was either directly used for template production or stored at 5 °C.

3.2.2. Primer Design

For each opsin gene, primers carrying promoter sequence of T3 RNA Polymerase were designed so forward and reverse primers were approximately 500 bp apart. The accuracy of the design was tested at OligoCalc website. Designed primers are listed in Table 2.

Table 2 List of Designed Primers

Opsin	Primer	Sequence	Start	End
SWS2A	F1	**TAATACGACTCACTATAGGG**GAACTTGTCAGCAGCAAACCTTCTTG	250	
	F2	**TAATACGACTCACTATAGGG**TAACACTCGGTGGGATGGTAAGC	350	
	R1	**AATTAACCCTCACTAAAGGG**GCCTTGGCTGCCATTTTCAGTG		720
	R2	**AATTAACCCTCACTAAAGGG**GTCGCCAATCTCAGATCGAATGAC		880
LWS	F1	**TAATACGACTCACTATAGGG**TCTCAACTTGTGGTATTGCTGCTC	400	
	R1	**AATTAACCCTCACTAAAGGG**AAGGCATATCCAGGGTTGGCTG		890
RH2Aα	F1	**TAATACGACTCACTATAGGG**CTTTTGAGTACCCTCAATATTATATGGT	110	
	F2	**TAATACGACTCACTATAGGG**TTAGAAATCCTTTTGAGTACCCTCAA	100	
	R1	**AATTAACCCTCACTAAAGGG**CAGTGTGTAGTAGTCAGGACCA		600
	UTR	**TAATACGACTCACTATAGGG**CCACACAAGTAGACTCTTTACGC	5UTR	
	ex1	**AATTAACCCTCACTAAAGGG**AGGAAGAACATGTAGAAAGCTAGAAC		ex1 - 200
	ex3	**TAATACGACTCACTATAGGG**TCTTCATCATTTTCTTCACTTATGGAAGT	760	
	3UTR	**AATTAACCCTCACTAAAGGG**TGGCAAAAACTTTCTCTAATGGGATG		3UTR - 1200
RH2Aβ	F1	**TAATACGACTCACTATAGGG**AGTACTCCCAGTATTACCTGGC	110	
	F2	**TAATACGACTCACTATAGGG**CCTTTTGAGTACTCCCAGTATTAC	100	
	R1	**AATTAACCCTCACTAAAGGG**AGTGTGTAGTAGTCAGGACCG		600
	UTR	**TAATACGACTCACTATAGGG**TTCCATCAGCTGAAACTCAATCAAACTA	5UTR	
	ex1	**AATTAACCCTCACTAAAGGG**GAAGAACATGTAGAAAGCCAGGAG		ex1 - 200
	ex3	**TAATACGACTCACTATAGGG**TCTTCATCATTTTTTTCACATATGGAAGC	760	
	3UTR	**AATTAACCCTCACTAAAGGG**GCAAAAGATTTCTCTAATGGGAATTTTG		3UTR - 1200
RH2αβ	3UTR	**AATTAACCCTCACTAAAGGG**CATGATTAAGACACAGAGGACACC		3UTR
	ex1	**AATTAACCCTCACTAAAGGG**ATGTGAAGAGTACTCCAGCACC		exon2 - 480

3.2.3. Template Production

To make primers corresponding PCR mixtures (5 µl PPP Master Mix, 3.5 µl water, 0.25 µl forward primer, 0.25 µl reverse primer, 1 µl ds cDNA) were amplified through the following programme: 94 °C for 5 min and 35 times 94 °C for 40 s, 60 °C for 40 s, 72 °C for 1 min and to determine the reaction 72 °C for 5 min.

The PCR products were checked via electrophoresis (80 V, 70 mA, 40 min; 1% agarose gel with ethidium bromide – EB) and then passed through the 2% agarose gel with EB (electrophoresis: 80 V, 70 mA, 60 min), from which they were excised with a scalpel. The products were extracted and purified from the gel slices following Quick-Start Protocol using MinElute Gel Extraction Kit (Qiagen). The gel slices weighted about 0.25 g and all centrifugation steps were carried out at 13,000 rpm and the flow-through was discarded afterwards every time. 750 µl buffer QG was added to each gel slice in a tube. The tubes were incubated at 50 °C for 10 min and vortexed every 2.5 min to dissolve the gel slice. 250 µl isopropanol was added to the sample, which was then gently mixed by inverting. The samples were applied to the MinElute columns and centrifuged. 500 µl buffer QG was added into the columns which were spun, then twice 750 µl buffer PE was added. Subsequently, the columns were spun for 1 min to remove all residual ethanol. The columns were paced into fresh microcentrifuge tubes and 20 µl buffer EB was added twice. The tubes with templates stood for another minute; afterwards, they were centrifuged and then stored at -20 °C. The products were checked for their purity and concentration in NanoDrop. Product sequences were tested through sequencing in Macrogen.

3.2.4. Probe Preparation

To make probes 13 µl of 150 ng template were mixed with 2 µl 10× DIG labelling mixture and 2 µl 10× FL labelling mixture, 2 µl 10× transcription buffer, 1 µl RNase inhibitor and 1 µl polymerase T3, and boiled at 99 °C for 7 min, and then placed on ice to terminate the reaction. The probes were either directly used or stored at -20 °C.

Various probes were produced to optimize the procedure; however, only those listed in Table 3 were used for dying retinae showed in Results chapter.

Table 3 List of Used Probes

Opsin	cDNA	Primers
SWS2A	*k. eisentrauti*	F2 + R2
LWS	*k. eisentrauti*	F1 + R1
RH2Aαβ	*k. eisentrauti*	β ex3 + β 3UTR
	k. eisentrauti	α 5UTR + αβ ex12
	k. eisentrauti	αβ F2 + αβ R1
	k. eisentrauti	α F2 + α R1
	k. eisentrauti	β F1 + β R1
	k. dikume	β F1 + β R1
	k. dikume	β ex3 + β 3UTR

3.3. Sample Collection

Tissue samples were collected in the Barombi Mbo crater lake (4°39'N/9°24'E) in South-West Cameroon in February 2018, July 2017 and February 2017. Up to ten individuals of each of four selected species were collected using gill nets and selective capturing by snorkelling in the shallow-water zone, and with gill nets and minnow traps for the deeper zone. Only adult individuals were selected for the analyses. Retinae were dissected directly in the field from freshly euthanized specimens and fixed in RNAlater solution and stored at room temperature during the field work, then transferred to -80 °C upon arrival to the laboratory. Additionally, some of the wild-caught fish were reared in the laboratory.

I did not personally participate in the sampling in Cameroon. The sampling was performed by my colleagues as a part of sampling for further research purposes (permit numbers: 0000047,49/MINRESI/B00/C00/C10/nye, 0000116,117/MINRESI/B00/C00/C10/C14, 000002-3/MINRESI/B00/C00/C10/C11, 0000032,48-50/MINRESI/B00/C00/C10/C12).

3.4. Tissue Preparation

To prepare the whole mount tissue sample, the retinae were gently dissected and fixated according to the methods of Barthel & Raymond (2000). The tissue preparation in the field was performed by my colleagues; however, I dissected and fixated the retinae of the laboratory reared fish myself. The description of the procedure follows.

The adult fish eye was enucleated, the cornea cut out and the lens removed. Subsequently, the sclera was cut out and choroid was taken away with tweezers. The vitreous body was removed with tweezers and brushes. Later, the retina was detached from the retinal pigmented epithelium by introducing a stream of PBS into the subretinal space. When the retina was cleared of other tissues, the optic nerve was cut off. To aid in flattening the retina several radial cuts were made. If possible, dissecting microscope was used.

For the purpose of fixation dissected retina was spread with photoreceptors directed downwards on a small Petri dish with Sylgard elastomer. To keep the retina flat, minutien pins were used. In the field, the retina was fixed with 4% PFA in PBS for 20 minutes, then 3× washed in PBS for 5 minutes and transferred into RNAlater. In the lab conditions, the fixation with 4% PFA in PBS took place in the fridge overnight. Afterwards, the retina was washed twice in PBS for 5 minutes, then briefly put into 70% MetOH, into 100% MetOH for another 5 minutes and finally stored in fresh 100% MetOH at 5 °C.

3.5. Fluorescent *in situ* Hybridization

FISH was performed according to the methods of Barthel & Raymond (2000), optimized for present samples. The retinae were transferred to room temperature (RT) before the procedure. If the retina was stored in RNA later, it was rinsed three times in PBS for 5 minutes, then briefly washed in 70% methanol and 100% methanol for another 5 minutes. The prehybridization procedure followed these steps:

1) 5 min in 100% methanol at RT
2) 5 min in 50:50 methanol and xylene at RT
3) 30 min in 100% xylene at RT
4) 30 min in 100% methanol at RT
5) 5 min in 90% methanol in PBST at RT
6) 5 min in 70% methanol in PBST at RT
7) 5 min in 50% methanol in PBST at RT
8) 2×15 min in PBST at RT
9) 15 min in 1× proteinase K at 37 °C
10) 15 s in PBST at RT
11) 20 min in 4% PFA in 100mM phosphate buffer w/5% sucrose at RT
12) 3×20 min in PBST at RT
13) 2 hours in 300 µl prehybridization solution at 56 °C.

Probes were prepared and hybridization solutions made. Corresponding hybridization solutions were added to the reaction tubes (150/300 µl = 150 µl for smaller retinae, 300 µl for bigger retinae), when prehybridization solution was removed. The hybridization ran at 56 °C overnight.

Posthybridization the next day consisted of several steps held at 65 °C: 2×30 min in 50% formamide/2× SSC, 15 min in 2× SSCT and 2×30 min in 0.2× SSCT. The samples were blocked with about 300 µl 1× RMB for 2 hours at RT. Procedure of retinae dying followed this protocol:

1) overnight in 150 µl anti-FL-POD in 1× RMB in fridge
2) 3×30 min in 1× maleate buffer/0.1% Triton at RT
3) 15 min in PBST at RT
4) 2+ hours in 150/300 µl TSA 488 at RT
5) 3×10 min in PBST at RT
6) 45 min in 3% H_2O_2 in PBST at RT

7) 3×10 min in PBST at RT
8) overnight in 150 µl anti-DIG-POD in 1× RMB in fridge
9) 3×30 min in 1× maleate buffer/0.1% Triton at RT
10) 15 min in PBST at RT
11) 2+ hours in 150/300 µl TSA 594 at RT
12) 3×10 min in PBST at RT.

The dyed retinae were placed into 70% glycerol in PBST at RT for 10 min. Subsequently, 70% glycerol in PBST was replaced with a fresh one and the samples were either stored in the tubes or directly mounted on slides and stored at -20 °C.

3.6. Microscopy Imaging and Image Processing

The retinae were mounted in 70% glycerol in PBST on a Frost Plus slide with cone side facing coverslip and stored at -20 °C.

Each slide was examined under fluorescent microscopes Olympus BX51 with objective 40× and Olympus IX81 with objective UPLSAPO 60× Oil. Images of both fluorescent channels as well as bright field (BF) with differential interference contrast (DIC) were obtained using SPOT or xcellence software.

Samples well-stained by both probes were subsequently examined under laser scanning confocal microscope Zeiss LSM 800. Each sample was examined at several locations with objective Plan-Apochromat 63×/1.4 Oil using laser excitation: Argon 488 nm and DPSS 561 nm, and emission spectra: 499–553 nm for green (FL staining) and 596–695 nm for red (DIG staining). Multiple images were taken at different focal distances (Z-stacking) within three channels (red, green, transmission) using software ZEN Black.

The images were further processed in Fiji (Fiji Is Just ImageJ). Z-stack projection was created for each image from the confocal microscopy. Subsequently, both fluorescent channels (if available) were merged, and channel colours were adjusted so *LWS* appeared in red, *RH2A* in green and *SWS2A* in cyan. Furthermore, the brightness and contrast were balanced, and the scale bar added. A BF + DIC image for each sample location was created either by choosing a single transmission image from the stack or by merging several of them in case of fuzzy focal planes.

In addition, I tried to determine the approximate cones amount per area by manual counting in ZEN Blue from BF images from Zeiss Axioscan Z1; however, it turned out to be impossible due to several damages of the tissue and missing orientation of the samples.

4. Results

In my thesis, I optimized the FISH method and analysed retinae of four species including retinal mosaic description and photoreceptor distribution investigation.

The procedure of staining whole-mount cichlid retinae is very complex and had to be optimized throughout various approaches. The final optimized protocol is described in Chapter 3; however, some of the results of the optimization steps are introduced in this chapter, as the method development was also a great part of work on this thesis.

In total, about 30 opsin templates from cDNA were made, and from each of them probes were created and tested several times. 46 of samples from 26 eyes of 21 individuals underwent the FISH procedure, from which about a half stained at least by probe, as shown in Table 4. Confocal microscope images of retinae stained by both probes of each of the investigated species are introduced in this chapter (Tables 5, 7, 8, 11). A bright field with DIC retinal image for each species is implicated too (also in Table 9). Furthermore, Tables 6, 9, 12 contain fluorescent microscope images of all other samples stained by at least one probe (together with BF + DIC images). Findings are summarised in Table 13.

Table 4 List of All Samples

Sample indication is used also in Tables 5–11 : species with fish sample number (fsn – renamed from original label for better clarity; one number equals one fish), wild-caught (WC) or laboratory-reared (LR) fish, retina from left (L) or right (R) eye or a part of it marked by index a/b/c/d/e. DIG and FL probes used for successful (√) or unsuccessful (×) staining: *LWS, SWS2A* or *RH2Aαβ* (*RH2Aα* and *RH2Aβ* are marked separately for better clarity; however, they stained non-specifically and nonexclusively both *RH2Aα* and *RH2Aβ* as explained below).

Species with fsn	WC / LR	L / R	DIG Probe	DIG √ / ×	FL Probe	FL √ / ×
Stomatepia mariae 1	WC	R	*LWS*	√	*RH2Aβ*	×
Stomatepia mariae 2	LR	La	*LWS*	√	*SWS2A*	√
Stomatepia mariae 2	LR	Lb	*RH2Aβ*	×	*RH2Aα*	×
Stomatepia mariae 2	LR	Lc	*RH2Aβ*	×	*RH2Aα*	×
Stomatepia mariae 2	LR	Ld	*RH2Aβ*	×	*RH2Aα*	×
Stomatepia mariae 2	LR	Ra	*LWS*	√	*RH2Aβ*	√
Stomatepia mariae 2	LR	Rb	*RH2Aα*	√	*SWS2A*	√
Stomatepia mariae 2	LR	Rc	*RH2Aβ*	×	*SWS2A*	√
Stomatepia mariae 2	LR	Rd	*RH2Aβ*	×	*RH2Aα*	×
Stomatepia mariae 2	LR	Re	*RH2Aβ*	×	*RH2Aα*	×
Stomatepia mariae 3	LR	La	*RH2Aβ*	×	*RH2Aα*	×
Stomatepia mariae 3	LR	Lb	*RH2Aβ*	×	*RH2Aα*	×
Stomatepia mariae 3	LR	Lc	*RH2Aβ*	×	*RH2Aα*	×
Stomatepia mariae 3	LR	Ld	*RH2Aβ*	×	*RH2Aα*	×
Stomatepia mariae 3	LR	Ra	*LWS*	√	*RH2Aβ*	×
Stomatepia mariae 3	LR	Rb	*LWS*	√	*RH2Aβ*	×

Konia eisentrauti	1	WC	L	*RH2Aβ* ×	*RH2Aα* ×
Konia eisentrauti	2	WC	Ra	*RH2Aβ* ×	*SWS2A* √
Konia eisentrauti	2	WC	Rb	*LWS* √	*RH2Aβ* ×
Konia eisentrauti	3	WC	R	*LWS* √	*RH2Aβ* ×
Konia eisentrauti	4	WC	L	*LWS* √	*SWS2A* √
Konia eisentrauti	5	WC	L	*RH2Aα* √	*SWS2A* √
Konia eisentrauti	6	WC	L	*LWS* √	*RH2Aβ* √
Konia eisentrauti	7	WC	L	*RH2Aα* √	*RH2Aβ* √
Konia eisentrauti	8	WC	L	*LWS* √	*RH2Aβ* ×
Konia eisentrauti	9	LR	La	*LWS* √	*RH2Aβ* √
Konia eisentrauti	9	LR	Lb	*LWS* √	*RH2Aβ* √
Konia eisentrauti	9	LR	Lc	*LWS* √	*RH2Aβ* √
Konia eisentrauti	9	LR	Ld	*LWS* √	*RH2Aβ* √
Konia eisentrauti	10	LR	La	*RH2Aα* ×	*RH2Aβ* √
Konia eisentrauti	10	LR	Lb	*LWS* √	*SWS2A* √
Konia eisentrauti	10	LR	Lc	*RH2Aβ* ×	*RH2Aα* ×
Konia eisentrauti	10	LR	Ra	*SWS2A* √	*RH2Aβ* √
Konia eisentrauti	10	LR	Rb	*RH2Aβ* √	*RH2Aα* √
Konia eisentrauti	10	LR	Rc	*RH2Aβ* ×	*RH2Aα* ×
Konia eisentrauti	10	LR	Rd	- -	- -
Konia dikume	1	WC	R	*RH2Aα* ×	*RH2Aβ* ×
Konia dikume	2	WC	Ra	*RH2Aα* ×	*RH2Aβ* ×
Konia dikume	3	WC	L	*RH2Aα* ×	*RH2Aβ* ×
Konia dikume	4	WC	L	*RH2Aα* ×	*RH2Aβ* ×
Myaka myaka	1	WC	R	*SWS2A* √	*RH2Aβ* ×
Myaka myaka	2	WC	L	*SWS2A* ×	*RH2Aβ* ×
Myaka myaka	3	LR	L	*RH2Aα* √	*RH2Aβ* √
Myaka myaka	3	LR	R	*RH2Aα* ×	*SWS2A* ×
Myaka myaka	4	LR	L	*RH2Aα* ×	*RH2Aβ* ×
Myaka myaka	4	LR	R	*RH2Aα* √	*SWS2A* √

4.1. Method Optimization

Several approaches of the eye dissection were tested including usage of various tools as well as reagents, such as hyaluronidase and collagenase (used to dissolve and remove vitreous body) which were not finally employed. The dissection in the laboratory (especially when using dissecting microscope) was for practical reasons much finer and accurate than in the field, which is a cause of highly pigmented spots and impaired photoreceptors in defective retinae from the field. Apart from that, the retinal orientation in the samples from the field was not maintained.

The primers were designed into various locations as the probe length can greatly influence FISH procedure, which has also shown in practice. Even though probes for

SWS2B were designed, they were never tested. In contrast, the testing of probes for *RH2Aα* and *RH2Aβ* showed they do not stain mutually exclusively. As the aim was to stain both *RH2Aα* and *RH2Aβ* specifically and exclusively, many other variations of the probes were designed targeting among others also untranslated regions (UTR) of the genes. Over twenty various *RH2Aα/β* probes of several lengths based on numerous primers were tested, but none of them turned out to be specific. As a result, all *RH2Aα* or *RH2Aβ* probes labelled both *RH2Aα* and *β*; hence, a distinction is not made between particular probes in the text below and images in Tables 5–9, 11 and 12).

The FISH procedure itself underwent great optimization too, mostly reflected by different labware employed, temperatures and times applied. For example, various temperatures of prehybridization + hybridization and of posthybridizasion were tested; however, any temperature differing from the ones given in the Chapter 3.5 did not work.

Obtaining samples itself is quite challenging due to the difficulty of catching especially deep-water fish, seasonal fluctuations as well as the political situation in Cameroon. To reduce wastage of poorly available samples, retinae were often cut into 2–5 pieces prior to the procedure to test the probes and optimize the method.

4.2. *Stomatepia mariae*

Sixteen retinae samples coming from five eyes of three individuals of *Stomatepia mariae* underwent the whole procedure; but, only retinae from both eyes of a fish (fsn 2) reared in the laboratory stained by both probes (one piece for *LWS* + *RH2A*, another for *RH2A* + S*WS2A* and one for *LWS* + *SWS2A* – all shown in Table 5 together with an exemplary BF with DIC image of another sample). Another piece of *S. marie* 2 stained only for *SWS2A*. Apart from that, one retina of a wild-caught fish and one sample of a fish reared in the laboratory stained for *LWS* only. Both stained samples are shown in Table 6.

In *S. mariae, SWS2A* probes labelled single cones, and each of *RH2A* and *LWS* probes stained complementary one part of each double cone, i.e. revealing standard cichlid retinal mosaic of a short-wavelength sensitive single cone surrounded by four *RH2A/LWS* double cones.

Table 5 Retinae of *Stomatepia mariae* Stained by Both Probes (on the next page)
Sample indication follows Table 4 (species + fish sample number), all are laboratory-reared (LR) fish, retina from left (L) / right (R) eye or a part of it marked by index a or b. *LWS* is displayed in red, *SWS2A* in cyan and *RH2A* in green. B-F are samples of both retinae coming from a single fish. C and D come from an identical sample, E and F come from an identical sample. The scale is 20 µm.

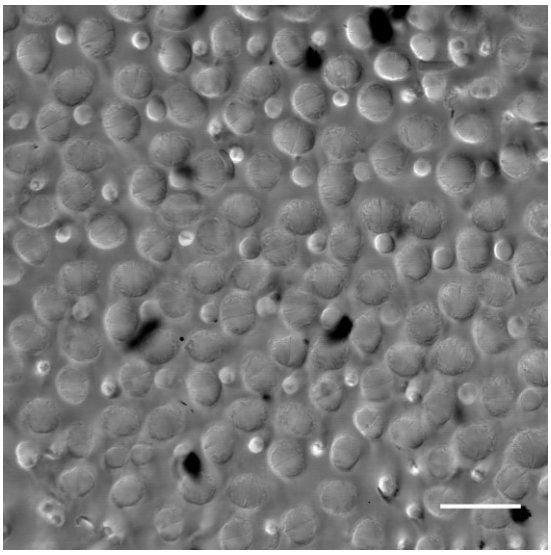

A) Bright field (*S. mariae* 3, LR, Rb)

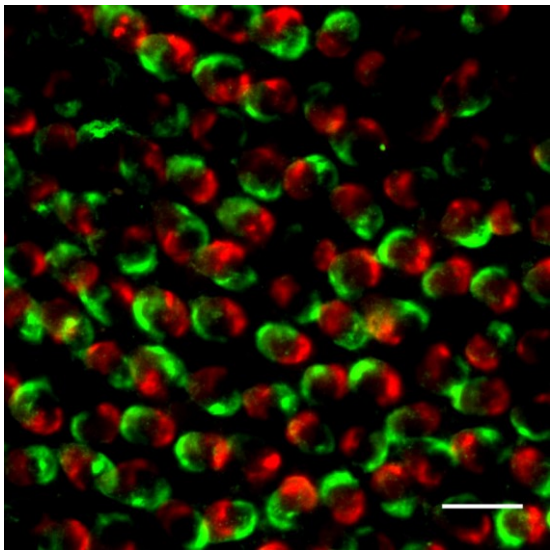

B) *LWS* + *RH2A* (*S. mariae* 2, LR, Ra)

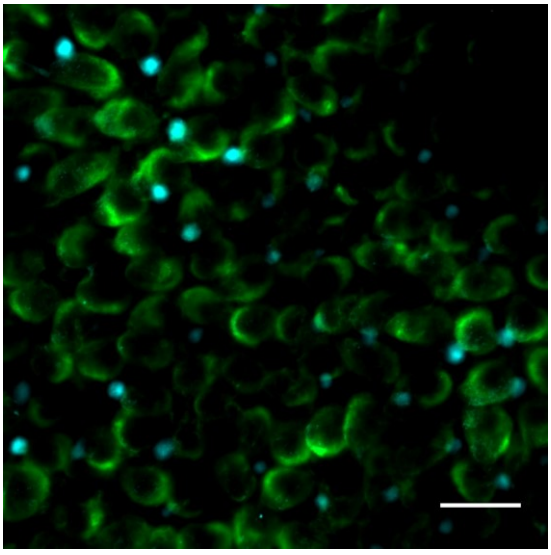

C) *RH2A* + S*WS2A* (*S. mariae* 2, LR, Rb)

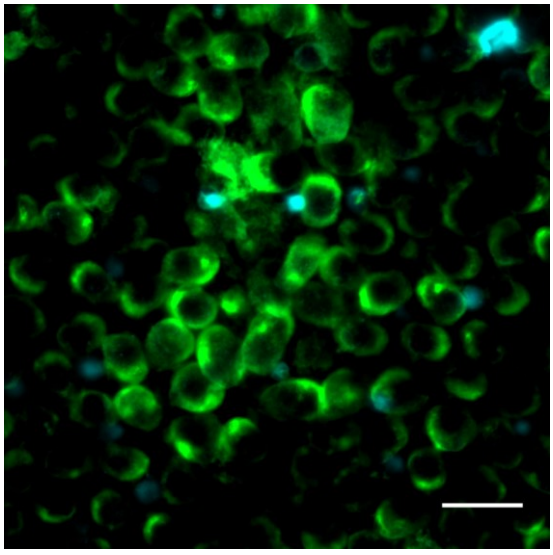

D) *RH2A* + S*WS2A* (*S. mariae* 2, LR, Rb)

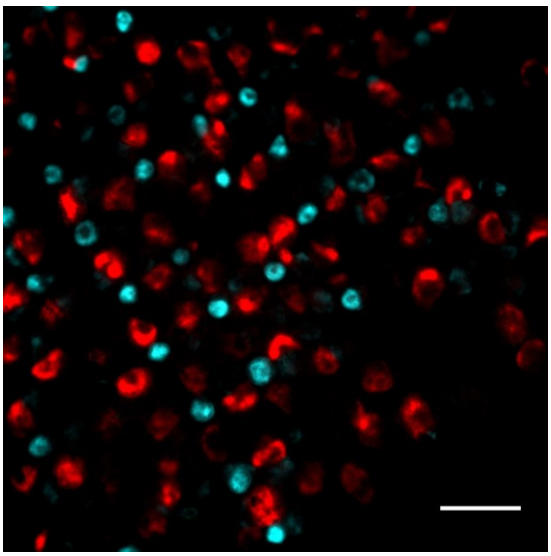

E) *LWS* + *SWS2A* (*S. mariae* 2, LR, La)

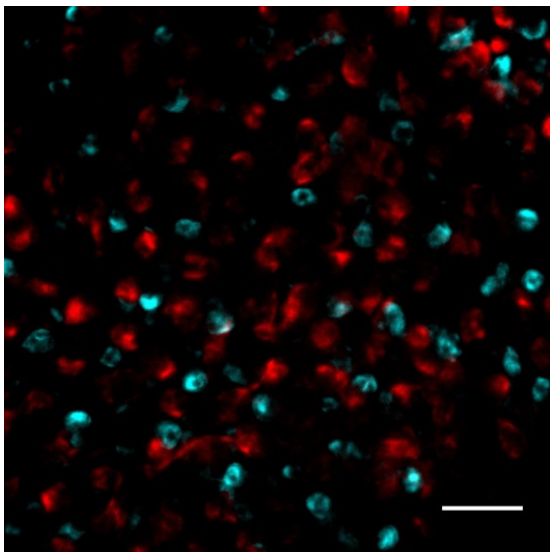

F) *LWS* + *SWS2A* (*S. mariae* 2, LR, La)

Table 6 Retinae of *Stomatepia mariae* Stained by One Probe

Sample indication follows Table 4 (species + fish sample number), wild-caught (WC) / laboratory-reared (LR) fish, retina from left (L) / right (R) eye or a part of it marked by index a or c. Images of identical sample location are displayed in rows – left in bright field with DIC and right in fluorescent channel.
LWS is displayed in red and *SWS2A* in cyan. The scale is 20 µm.

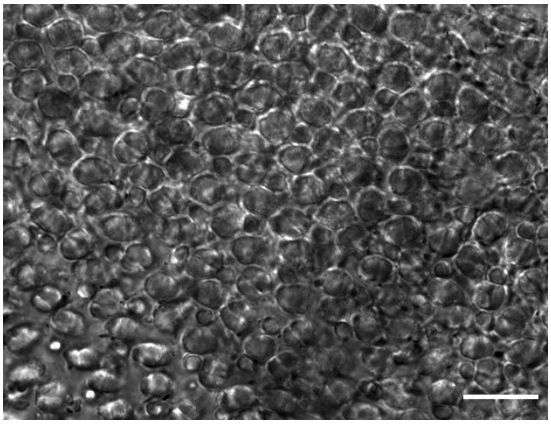

A) Bright field (*S. mariae* 1, WC, R)

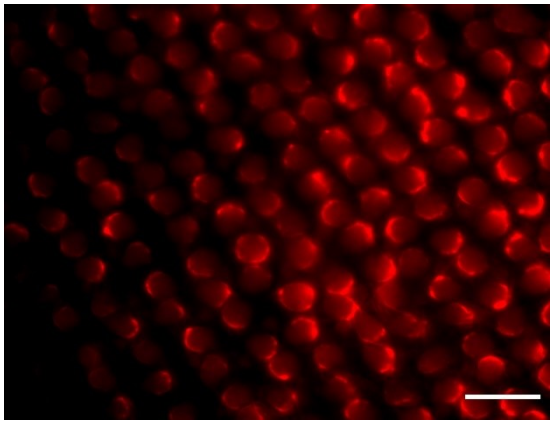

B) *LWS* (*S. mariae* 1, WC, R)

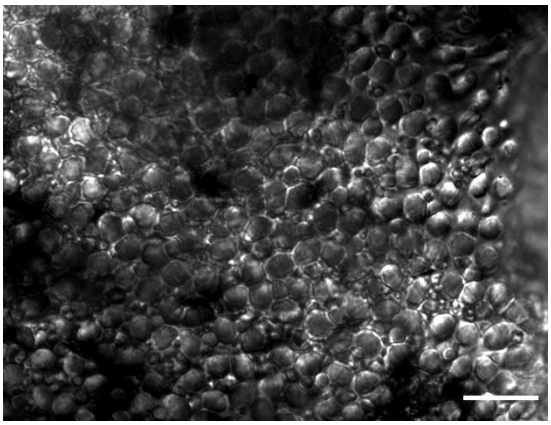

C) Bright field (*S. mariae* 2, LR, Rc)

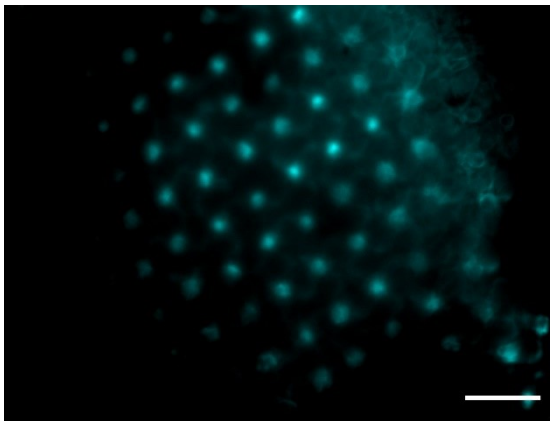

D) S*WS2A* (*S. mariae* 2, LR, Rc)

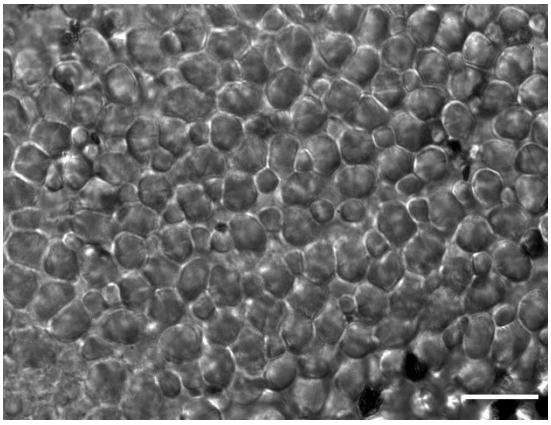

E) Bright field (*S. mariae* 3, LR, Ra)

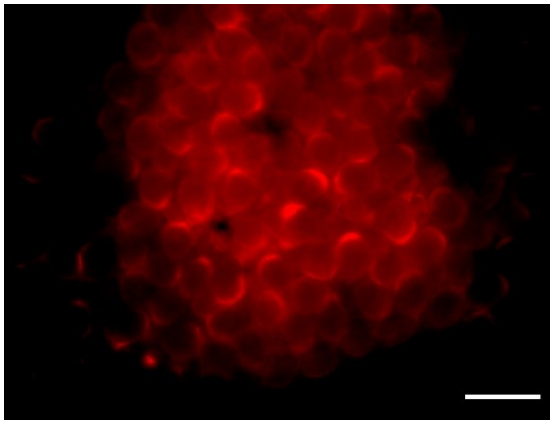

F) *LWS* (*S. mariae* 3, LR, Ra)

4.3. *Konia eisentrauti*

Twenty retinae samples coming from eleven eyes of ten individuals of *Konia eisentrauti* underwent the procedure. Sixteen of them stained for at least some of the probes. Moreover, one extra retina of laboratory-reared *K. eisentrauti* underwent the procedure with unlabelled probes to test the procedure and optimize confocal microscopy imaging. Four retinae of the wild-caught fish stained by both probes; however, one of them was stained for *RH2Aα* and *RH2Aβ*, which stained non-specifically. The others were labelled for *LWS* + *SWS2A*, *LWS* +*RH2A* and *RH2A* + *SWS2A*. Three more retinae of wild-caught fish stained only for *LWS*, and one only for *SWS2A.* The retinae of fish reared in the laboratory were used mainly for testing the procedure and probes; hence, only pieces of them were dyed. Four of them stained for *LWS* + *RH2A*, one for *LWS* + *SWS2A*, one for *SWS2A* + *RH2A* and one for both non-specific *RH2A* probes (originally targeted on *RH2Aα* and *RH2Aβ*). One of the pieces stained only for *RH2A* by a non-specific probe originally targeted on *RH2Aβ*.

The retinal mosaic of both *K. eisentrauti* and *S. mariae* had a general cichlid appearance. In contrast to *S. mariae, LWS* probes labelled not only one cell of the double cones but in some cases both double cone members (see Table 7). *RH2A* probes stained other part of the non-purely *LWS* double cones. Single cones were labelled by *SWS2A* probes.

Table 7 Comparism of the retinae of A) *Stomatepia mariae* and B) *Konia eisentrauti*
Sample indication follows Table 4 (species + fish sample number), wild-caught (WC) / laboratory-reared (LR) fish, retina from left (L) / right (R) eye or a part of it marked by index a. *LWS* is displayed in red, *RH2A* in green. The scale is 20 µm. White arrows point to double cones expressing *LWS* in both parts.

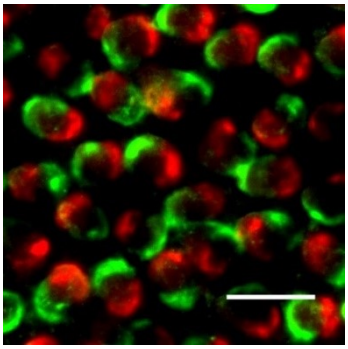

A) *LWS* + *RH2A* (*S. mariae* 2, LR, Ra)

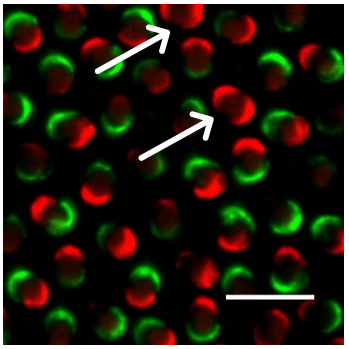

B) *LWS* + *RH2A* (*K. eisentrauti* 6, WC, L)

Table 8 shows images of retinae stained by both probes from confocal microscope and Table 9 shows images of retinae stained by just one of the probes or stained for *RH2A* by both probes (non-specifically) from fluorescent microscope. Samples of laboratory-reared *K. eisentrauti* 9 Lb and Lc are not shown as they are alike samples La and Ld of the same fish specimen – variations of *RH2A* probes were used; however, the staining came off the same as the probes were non-specific (demonstrated by C and D of Table 8).

Table 8 Retinae of *Konia eisentrauti* Stained by Both Probes

Sample indication follows Table 4 (species + fish sample number), wild-caught (WC) / laboratory-reared (LR) fish, retina from left (L) / right (R) eye or a part of it marked by index a/b/d. *LWS* is displayed in red, *SWS2A* in cyan and *RH2A* in green. A and B are identical images of the same sample location, only in different channels. C and D are samples from the same retina of a single fish; however, stained independently (with different *RH2A* probe). E and F come from an identical sample. I and J come from an identical sample. The scale is 20 µm. White arrows point to double cones expressing *LWS* in both parts.

** Cones of the sample displayed in G show a great degree of autofluorescence in green spectrum; however, the staining is still evident.*

° The SWS2A probe (cyan) in the sample K. eisentrauti 4, WC, L (I and J) was contaminated as evident from labelling double-cones. Only single cones should be stained as evident from other staining, e.g., E–H.

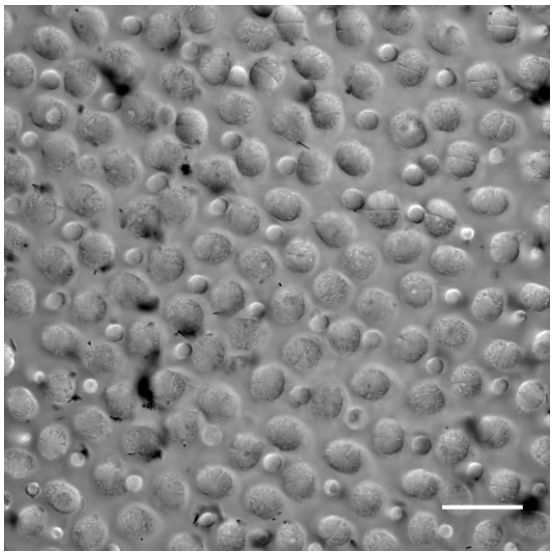

A) Bright field (*K. eisentrauti* 6, WC, L)

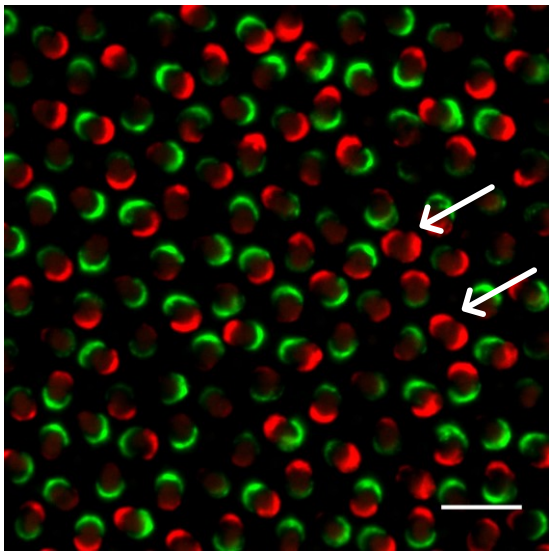

B) *LWS* + *RH2A* (*K. eisentrauti* 6, WC, L)

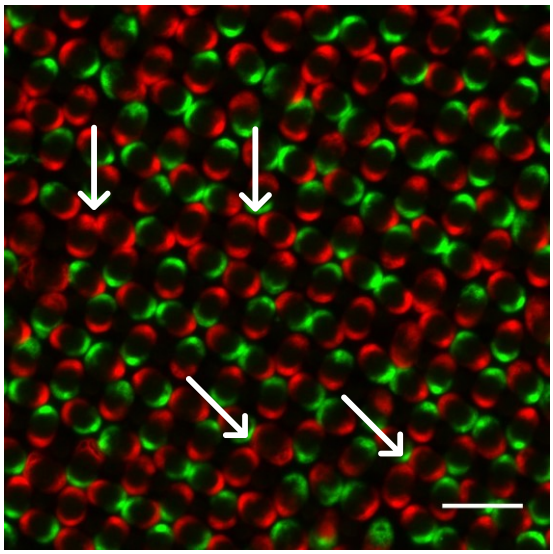

C) *LWS* + *RH2A* (*K. eisentrauti* 9, LR, La)

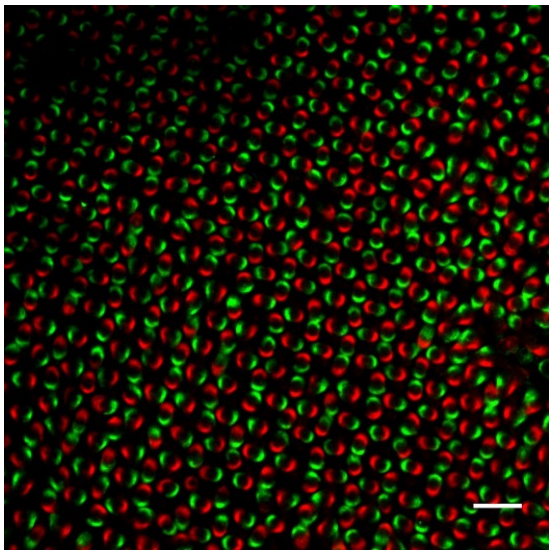

D) *LWS* + *RH2A* (*K. eisentrauti* 9, LR, Ld)

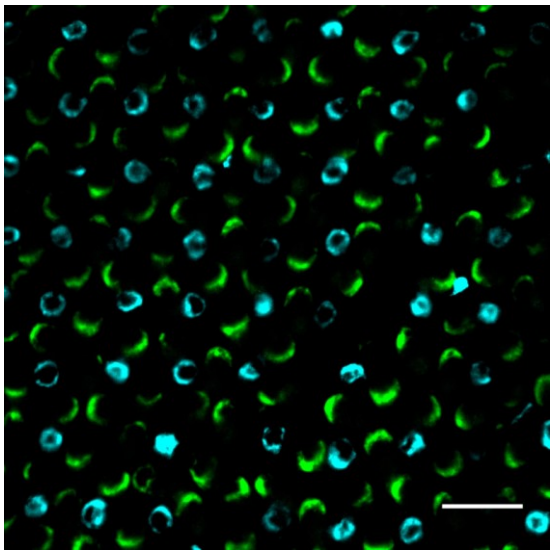

E) *RH2A* + S*WS2A* (*K. eisentrauti* 5, WC, L)

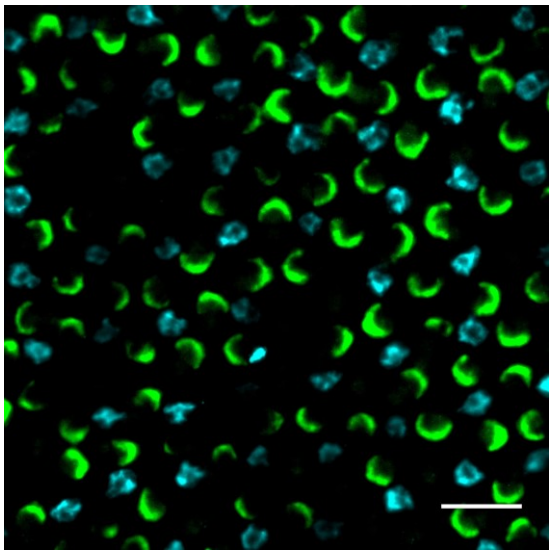

F) *RH2A* + S*WS2A* (*K. eisentrauti* 5, WC, L)

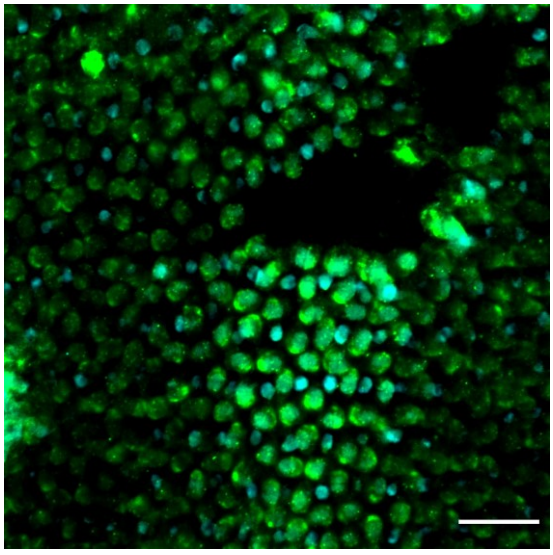

G) *RH2A* + S*WS2A* (*K. eisen.* 10, LR, Ra) *

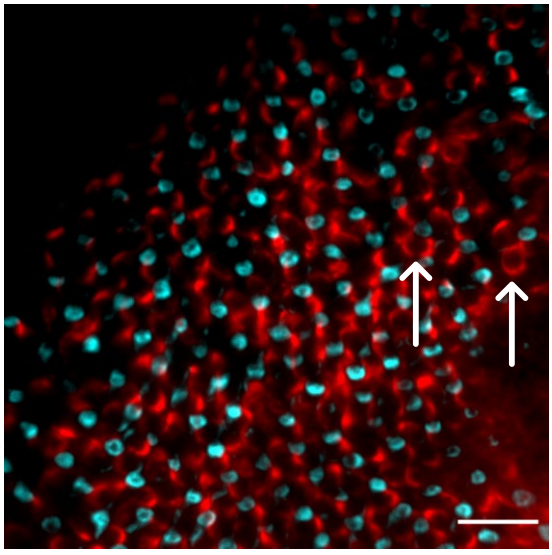

H) *LWS* + *SWS2A* (*K. eisen.* 10, LR, Lb)

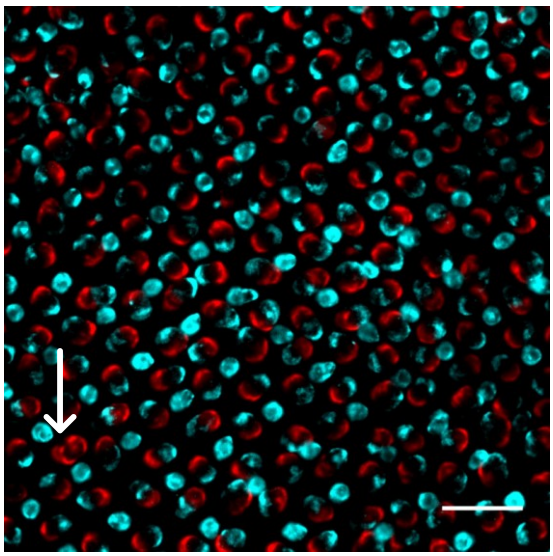

I) *LWS* + *SWS2A* (*K. eisentrauti* 4, WC, L) °

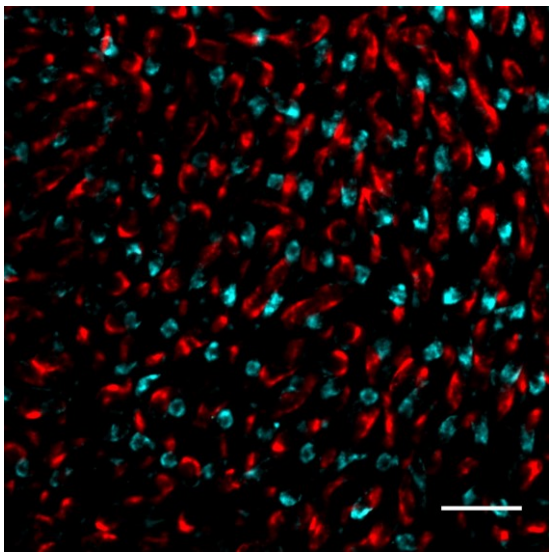

J) *LWS* + *SWS2A* (*K. eisentrauti* 4, WC, L) °

Table 9 Retinae of *Konia eisentrauti* Stained by One Probe

Sample indication follows Table 4 (species + fish sample number), wild-caught (WC) / laboratory-reared (LR) fish, retina from left (L) / right (R) eye or a part of it marked by index a or b. Images of identical sample location are displayed in rows – left in bright field with DIC, right in fluorescent channel. *LWS* is displayed in red, *SWS2A* in cyan and *RH2A* in green. Some samples show a high degree of cone autofluorescence. The scale is 20 µm.

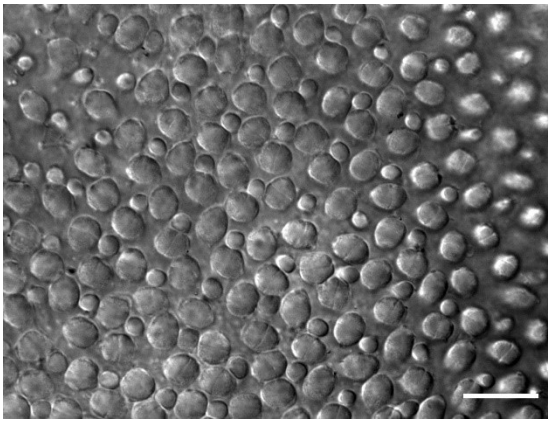

E) Bright field (*K. eisentrauti 2*, WC, Ra)

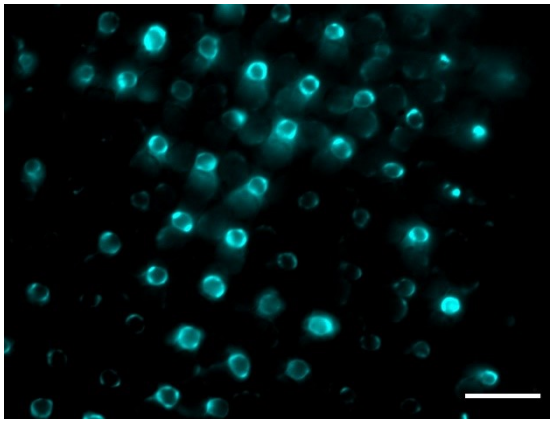

F) S*WS2A* (*K. eisentrauti* 2, WC, Ra)

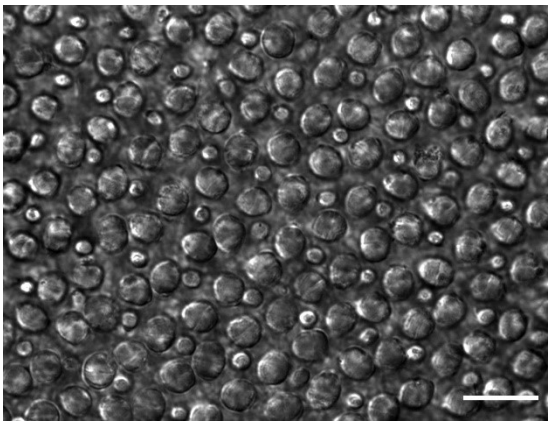

A) Bright field (*K. eisentrauti* 2, WC, Rb)

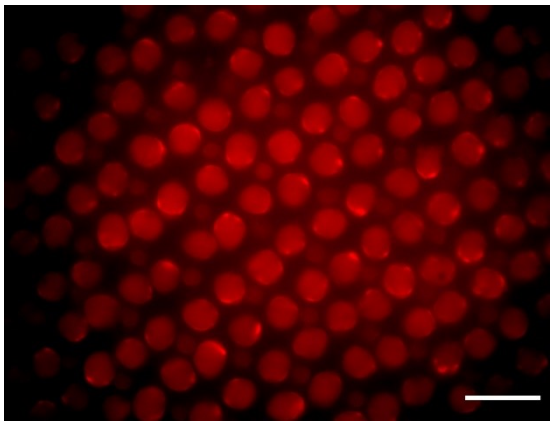

B) *LWS* (*K. eisentrauti* 2, WC, Rb)

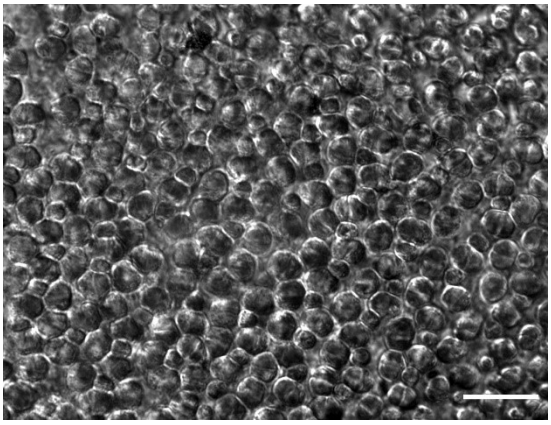

C) Bright field (*K. eisentrauti* 3, WC, R)

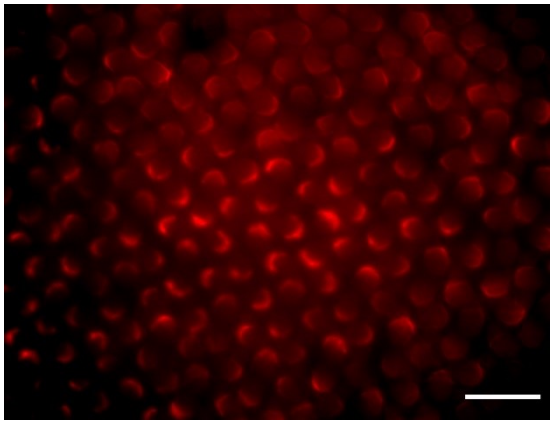

D) *LWS* (*K. eisentrauti 3*, WC, R)

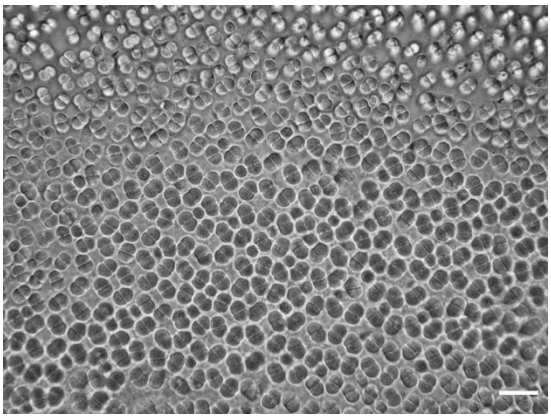

G) Bright field (*K. eisentrauti* 7, WC, L)

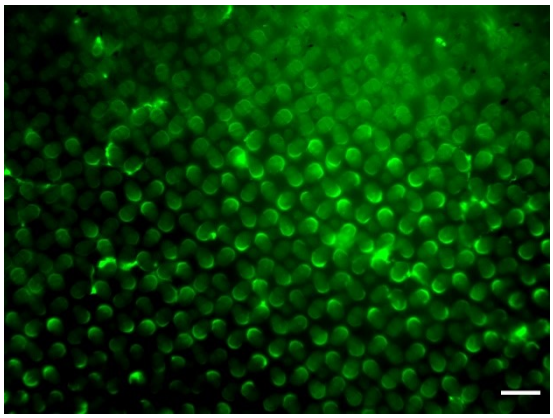

H) *RH2A* (*K. eisentrauti* 7, WC, L)

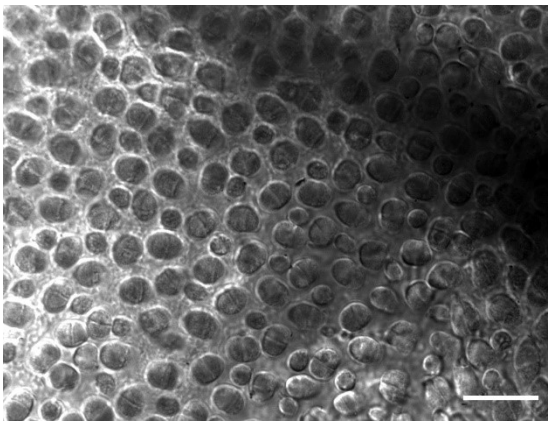

I) Bright field (*K. eisentrauti* 8, WC, L)

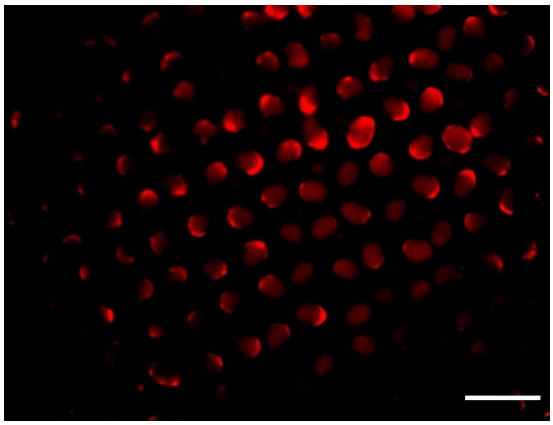

J) *LWS* (*K. eisentrauti* 8, WC, L)

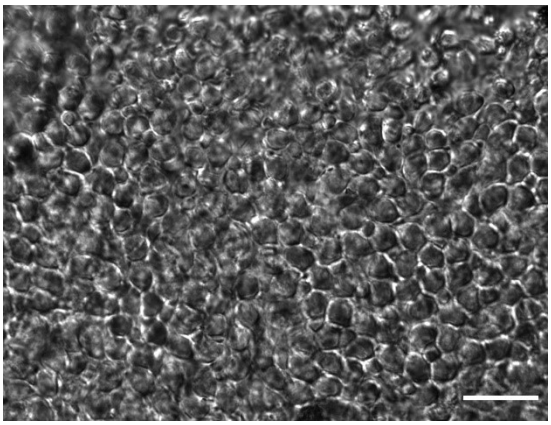

K) Bright field (*K. eisentrauti* 10, LR, La)

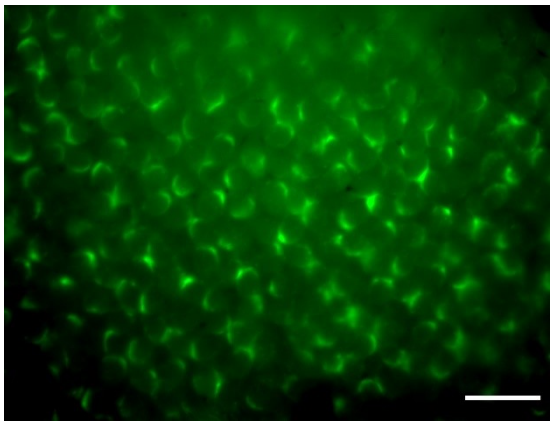

L) *RH2A* (*K. eisentrauti* 10, LR, La)

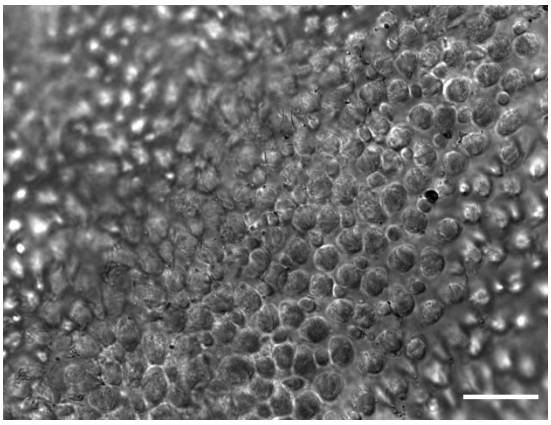

M) Bright field (*K. eisentrauti* 10, LR, Rb)

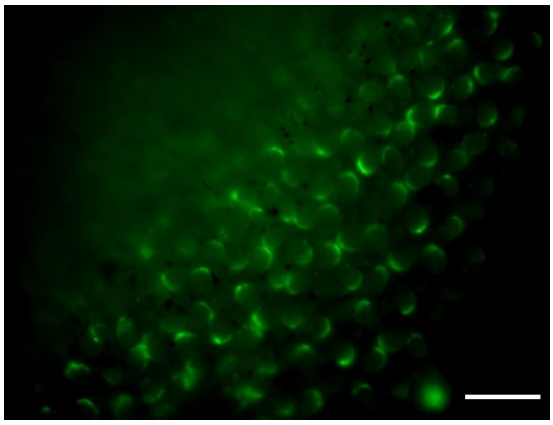

N) *RH2A* (*K. eisentrauti* 10, LR, Rb)

4.4. *Konia dikume*

Four individual retinae of *Konia dikume* underwent the procedure; however, none of them stained for any probe. Hence, Table 10 presents only BF +DIC images of them. The retinal mosaic of *K. dikume* consisted of mostly double cones with minimum of single cones.

Table 10 Retinae of *Konia dikume*

Sample indication follows Table 4 (species + fish sample number), both fish were wild-caught (WC). The scale is 20 µm. White arrows mark single cones.

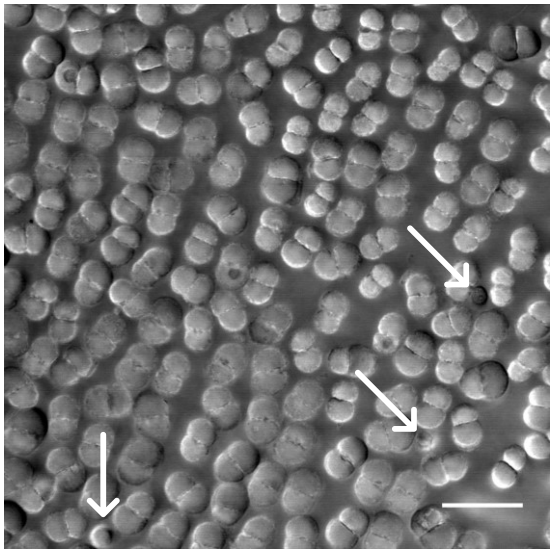

A) Bright field (*K. dikume* 3, WC, L)

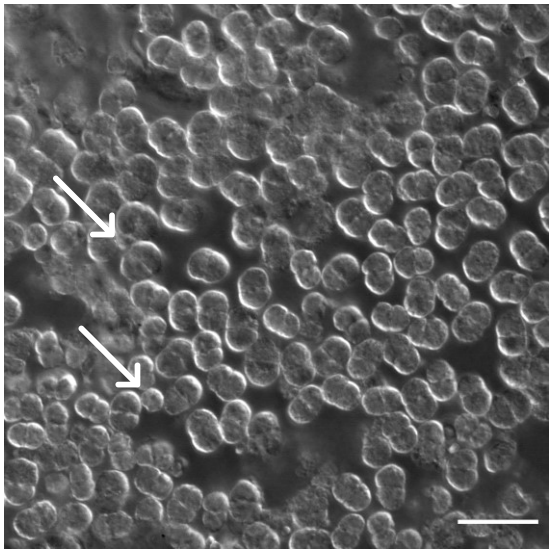

B) Bright field (*K. dikume* 1, WC, R)

4.5. *Myaka myaka*

Six retinae of five individuals of *Myaka myaka* underwent the procedure; but, only one whole-mount retina of a laboratory-reared fish stained for both *RH2A* and *SWS2A* as shown in Table 11. Another whole-mount retina of a laboratory-reared fish stained for both probes (*RH2Aα* and *RH2Aβ*); however, all *RH2A* probes stained non-specifically. Furthermore, one retina of a WC fish stained for *SWS2A*. Both are shown in Table 12.

The retinal mosaic of *M. myaka* consists of single cones each surrounded by four double cones. *SWS2A* probes labelled single cones, while *RH2A* probes labelled both parts of double cones.

Table 11 Retinae of *Myaka myaka* Stained by Both Probes

To demonstrate the variety of the cone distribution within retina, this table shows various locations throughout a single sample of the right eye of the laboratory-reared *Myakka myaka 4* (fish sample indication follows Table 4). In B, red DIG labels *RH2A* and green FL labels *SWS2A*. B displays an overview of the stained retina and the locations of individual images C–F, where *SWS2A* is displayed in cyan and *RH2A* in green. A (bright field) and C (fluorescent) are identical images of the same location, only in different channels. The scale is 20 µm.

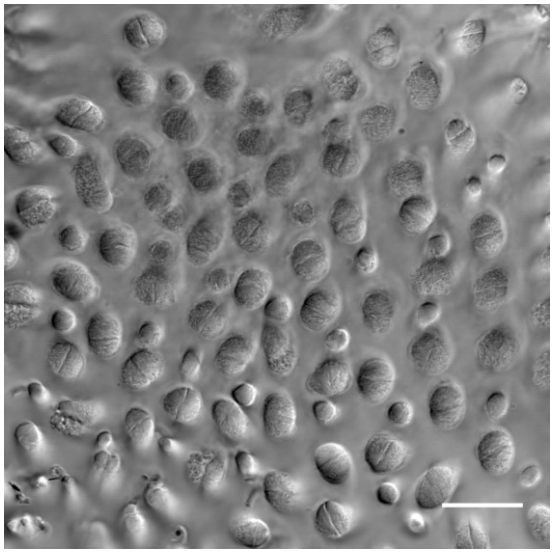

A) Bright field (*M. myaka* 4, LR, R)

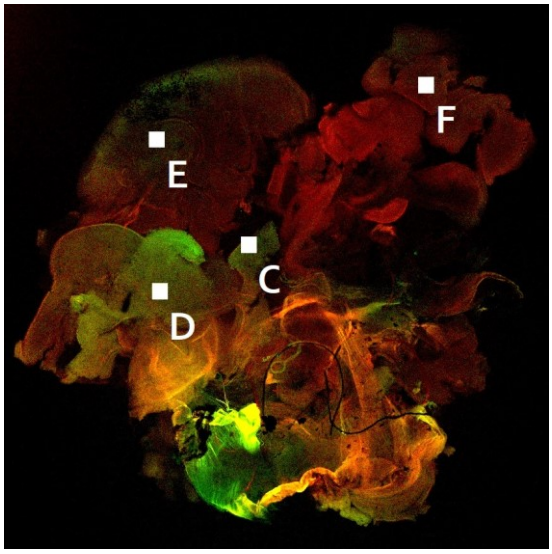

B) Position of C–F (*M. myaka* 4, LR, R)

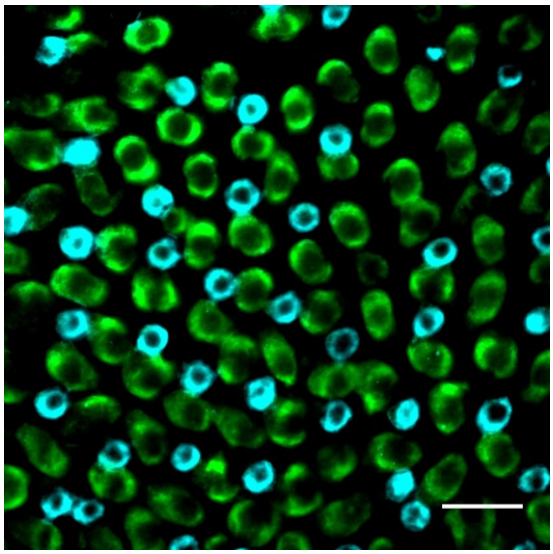

C) *RH2A* + S*WS2A* (*M. myaka* 4, LR, R)

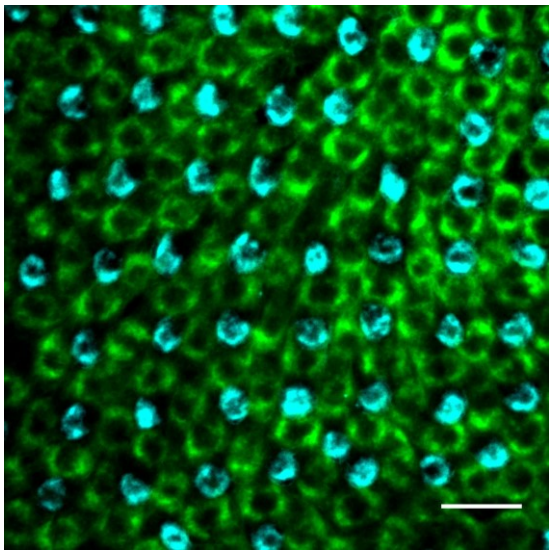

D) *RH2A* + S*WS2A* (*M. myaka* 4, LR, R)

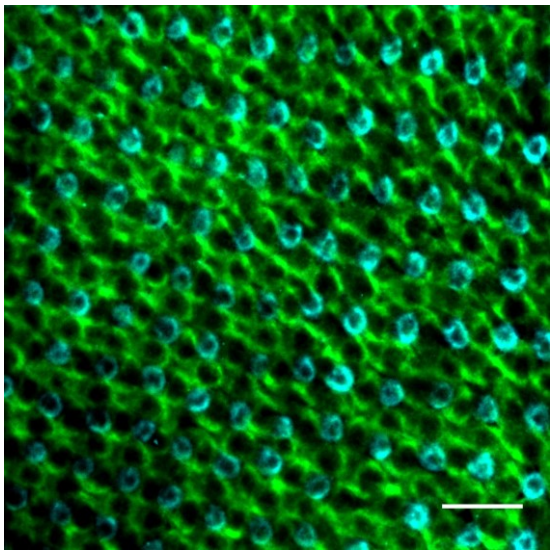

E) *RH2A* + S*WS2A* (*M. myaka* 4, LR, R)

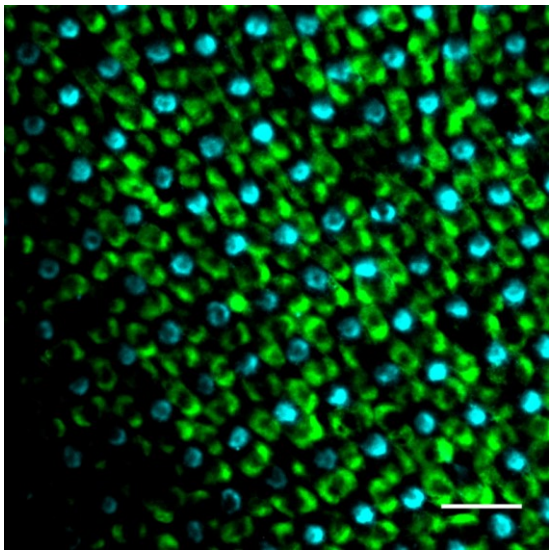

F) *RH2A* + S*WS2A* (*M. myaka* 4, LR, R)

Table 12 Retinae of *Myaka myaka* Stained by One Probe

Sample indication follows Table 4 (species + fish sample number), wild-caught (WC) / laboratory-reared (LR) fish, retina from left (L) / right (R) eye. Images of identical sample location are displayed in rows – left in bright field with DIC, right in fluorescent channel. *SWS2A* is displayed in cyan and *RH2A* in green. The scale is 20 µm.

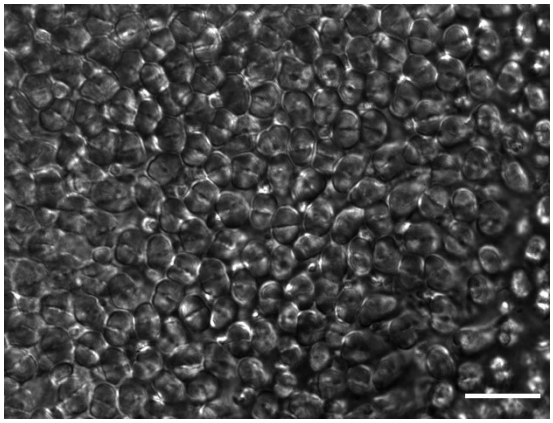

A) Bright field (*M. myaka* 1, WC, R)

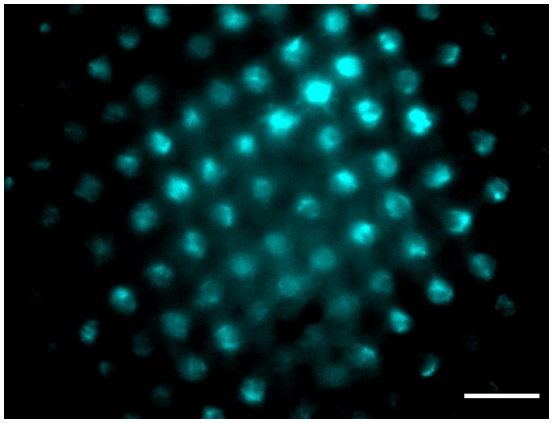

B) S*WS2A* (*M. myaka* 1, WC, R)

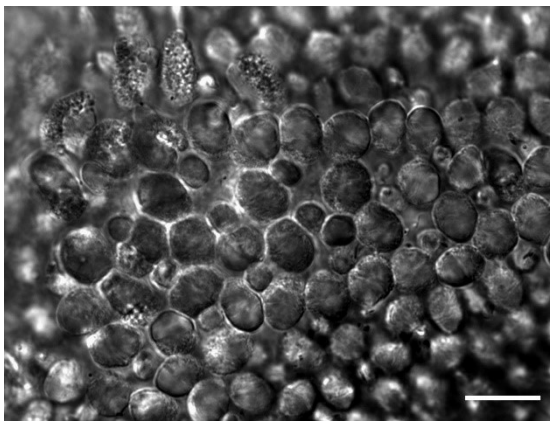

C) Bright field (*M. myaka* 3, LR, L)

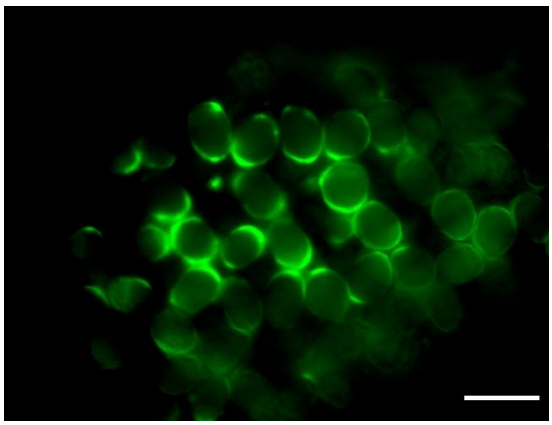

D) *RH2A* (*M. myaka* 3, LR, L)

4.6. Result Summary and Publication

To summarise the findings presented in previous chapters (4.2.–4.5.): *S. mariae* expressed *SWS2A* in single cones surrounded by four double cones with *LWS* in one and *RH2A* in second part. *K. eisentrauti* followed a similar pattern; however, some double cones expressed *LWS* in both parts. *M. myaka* embodied a standard square mosaic where *RH2A* was expressed in both parts of double cones, while single cones expressed *SWS2A*. The retinal mosaic of *K. dikume* was less organized with dominance of double cones and virtual lack of single cones; however, the spatial distribution of opsin genes was not determined. Table 13 displays schemes of retinal mosaics of all investigated species.

Table 13 Retinal Mosaics of Selected Barombi Mbo Cichlid Species

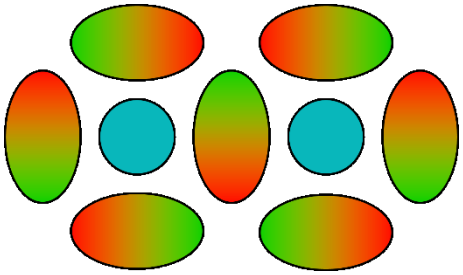

Stomatepia mariae

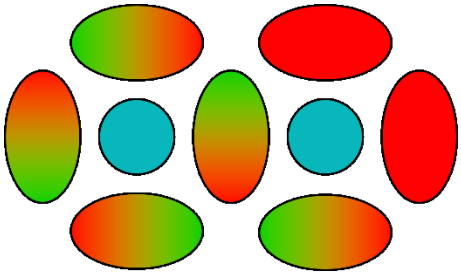

Konia eisentrauti

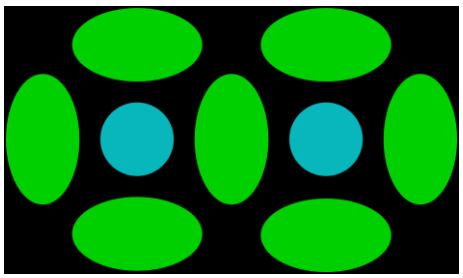

Myaka myaka

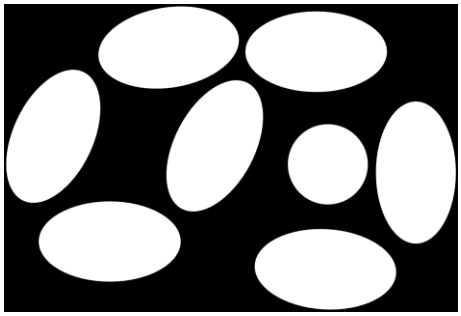

Konia dikume

The results of this thesis became a part of a scientific article (see Figure 13) accepted in the journal Molecular Ecology: Musilová, Z., Indermaur, A., Bitja-Nyom, A.R., Omelchenko, D., Kłodawska, M., Albergati, L., **Remišová, K.** & Salzburger, W. Accepted. Evolution of Visual Sensory System in Cichlid Fishes from Crater Lake Barombi Mbo in Cameroon. *Molecular Ecology*. Apart from that, the ongoing research was frequently presented at various conferences (see Attachments 1–5), namely European Society for Evolutionary Biology (ESEB) 16th Congress in 2017, Cichlid Science Meeting 2017, Zoological Days 2017 and 2018, and International Congress of Neuroethology (ICN) 2018.

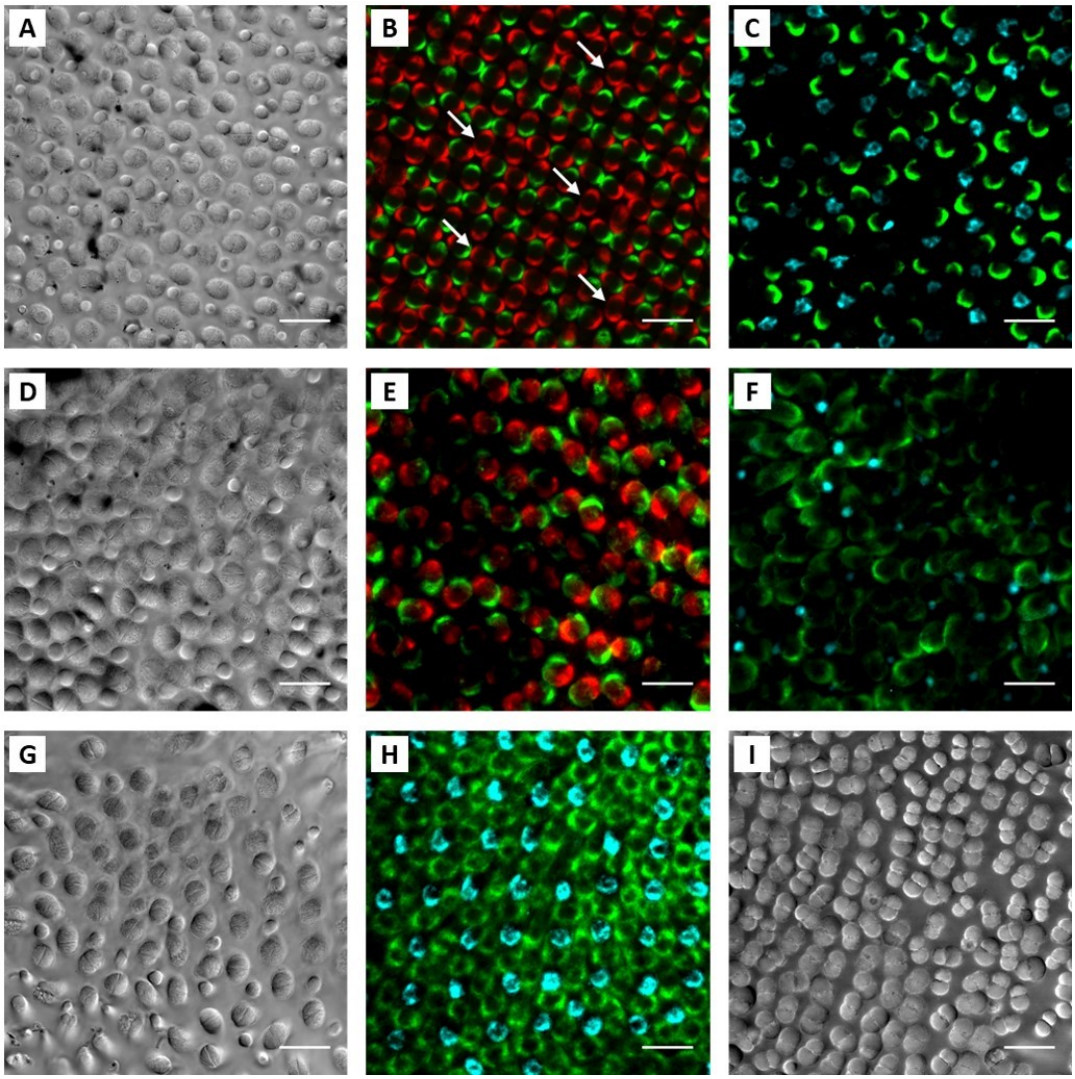

Figure 13 Table of Figures from the Article Musilová et al. (accepted)

Legend from the article: Cone cells in retina of the Barombi Mbo cichlid fishes. A, D, G, I – Double and single cones in the bright field light. B, C, E, F, H – Fluorescent in-situ hybridization (FISH) using RNA probes of opsin genes expressed in the cone cells. A – shallow-water species *Konia eisentrauti*; B – *K. eisentrauti* – red-sensitive opsin gene (*LWS*) in red, and green-sensitive opsin gene (*RH2Aα/β*) in green. Note that most of the double cone cells express *LWS* in one cell and *RH2A* in the other cell; however, more rare are the double cones expressing *LWS* in both cells (some marked by the white arrow); C – *K. eisentrauti* – green-sensitive opsin gene (*RH2Aα/β*) in green and blue-sensitive opsin gene (*SWS2A*) in cyan; D – shallow-water species *Stomatepia mariae*; E – *S. mariae* – red-sensitive opsin gene (*LWS*) in red and green-sensitive opsin gene *RH2A* (*α/β*) in green; F – *S. mariae* – green-sensitive opsin gene (*RH2Aα/β*) in green and blue-sensitive opsin gene (*SWS2A*) in cyan; G – seasonally deep-water species *Myaka myaka*; H – *M. myaka* – green-sensitive opsin gene (*RH2Aα/β*) in green and blue-sensitive opsin gene (*SWS2A*) in cyan. Note that *RH2A* is expressed in both cells of the double cones; I – deep-water species *Konia dikume*. Scale = 20 µm.

5. Discussion

Vision is a greatly important sense to cichlids considering their complex visually guided social behaviour (Escobar-Camacho & Carleton, 2015). It is thought to have played an important role in the explosive cichlid radiations (Hofmann et al., 2009). Fish visual abilities are determined by the composition of opsin-based photosensitive pigments located in photoreceptor cells as well as their distribution. Distinctively, cichlid cones are arranged in a retinal mosaic consisting of short-wavelength sensitive single cones, each surrounded by four long-wavelength sensitive double cones (Loew & Lythgoe, 1978).

Cichlids are well known for their rapid diversification and high adaptability to various habitats including extreme environments such as deep waters (Turner, 2007; Trewavas et al., 1972). Colour composition of the deep-water light spectrum differs from the shallow-water light conditions. The habitat is dimmer and lacking marginal parts of the spectrum (UV, IR and red wavelengths). As a result, deep-water fishes exhibit variations in opsin gene expression profiles and alternations in retinal cell patterns as compared to their shallow-water relatives (Levine & MacNichol, 1982).

In this thesis, I targeted cichlids of Lake Barombi Mbo as a great example of a small-scale adaptive radiation (Turner, 2007; Schliewen & Klee, 2004). From eleven Barombi Mbo cichlids, four species were selected for this study: shallow-water species *Stomatepia mariae* and *Konia eisentrauti,* deep-water species *Konia dikume* and seasonally deep-water species *Myaka myaka*. I investigated their retinal organization by means of fluorescent *in situ* hybridization (FISH) to understand the performance and evolution of their visual perception with emphasis on the effect of depth.

Research on this African endemic flock is challenging in many ways. Lake Barombi Mbo lays in a geopolitically unstable region in Cameroon (The Global Economy, 2018), which complicates sampling. Apart from that, inter- and intra-seasonal changes significantly affect sampling; it was virtually impossible to catch deep-water species in some of the sampling periods. Cooperation with local fishermen can also be tricky because of the uncertain time of the fish death. The time between death and processing of a specimen is crucial for the sample quality as RNA degrades with time. For the above-mentioned reasons, only 21 individuals were examined. To extend the research possibilities, some of the retinae were cut into pieces, especially for reasons of testing new probes plus method optimization and standardization.

Sample quality was greatly influenced by both specimen state before dissection and dissection precision. I personally dissected all laboratory-reared fish; however, I was not present in the field sampling, so the field dissections were performed by my colleagues. It is important to note that each person dissects in a slightly different way. Apart from that, dissection in the field cannot be as fine as the one in the laboratory for practical reasons (e.g. availability of devices such as a dissecting microscope, time constraints, etc.). Missing orientation information, major damages, RPE leftovers and even missing parts of the field dissected retinae forbid me to investigate morphological variations of photoreceptor cells – their size, position and orientation, as well as performing reliable cone cells counts to gain additional information on the retinal organization as mentioned in Chapter 3.6. The importance of these variables for retinal description related to the habitat is discussed below. For future, specific methodology should be applied if cell count and morphological description are desired, as they demand a great quality sample preparation including tissue clearance for better examination. For example, methodology of Lisney & Hawryshyn (2010) for cone photoreceptor topography investigation appears appropriate. Furthermore, Dalton et al. (2017) stereologically analysed cones in retina of cichlid *Metriaclima zebra.* Creation of such comprehensive topographic maps of ganglion cell densities, cone cell densities or even opsin coexpression levels requires especially fine dissection as well as specific treatment of the samples and instrumentation as apparent from the protocols described in de Busserolles et al. (2014a; 2014b). Apart from utilisation of these methods, greater number of specimens in general would allow more robust work; however, this is not an easily solvable issue as explained earlier.

It is not entirely possible to use only laboratory-reared fish in the research for two reasons 1) their poor accessibility and 2) research interpretation as Hofmann et al. (2010) demonstrated that the opsin gene expression may differ between wild-caught and lab-reared animals. Moreover, lab-reared fish retinae dissected in the laboratory generally exhibited better sample quality, so it was possible to cut them into pieces for extending the sample amount for staining. For all these reasons, samples of laboratory-reared fish were used primarily for probe testing, and wild-caught fish samples for final staining.

Two-colour FISH employing RNA probes was performed on 46 samples of retinae whole mounts. Unfortunately, only about half of them stained successfully in at least one probe. Torres-Dowdall et al. (2017) successfully applied three-colour FISH on retinae of Midas cichlids. Triple FISH using DNP was also tested as the labelling probe, anti-DNP

POD as the antibody and TSA 647 for signal enhancement following methodology of Torres-Dowdall et al. (2017) several times; however, it was not successful.

In general, FISH is a very complex and widely used method for sample staining. However, even subtle nuances (or very little contamination) can evoke a great difference. A great number of various FISH protocols exists and both troubleshooting and protocol improvement are lively discussed at social networks for scientists as well as described in scientific papers (Mülhardt & Beese, 2007; Welten et al., 2006). The method demands fine optimization even to various species investigated. Despite all efforts, putting the method into operation failed for one of four researched species – *K. dikume*. Possible reason of the failure is its eventually different membrane permeability as I am sure of accuracy of RNA and gene sequences used for primer design.

The FISH method optimization and standardization are very challenging and time-consuming as the whole process takes several days or even weeks if probe, sample and protocol preparation is counted. The aspects of the method optimization are described in Chapter 4.1. I personally consider the whole-mount double FISH method standardization for further use in the Fish Evolution Research Group as an important accomplishment of my work on this thesis and as one of the aims met despite arisen troubles and failures.

In teleosts, retinal mosaics usually consist of a small central single cone sensitive to short wavelengths surrounded by larger four longer-wavelength-sensitive double cones (van der Meer, 1992; Bowmaker, 1990; Fernald, 1981). Three of the investigated species (*S. mariae, K. eisentrauti, M. myaka*) embodied the standard square mosaic of single cones surrounded by double cones (see BF + DIC images in Tables 5, 8 and 11). However, retinae of deep-water *K. dikume* consisted of uneven rows of double cones with minimal numbers of single cones that were embedded among disordered double cones or rarely even surrounded by them similarly to a common cichlid retina. This finding corresponds with the fact that double cones maximize cone packing and therefore increase visual sensitivity in dim light (van der Meer, 1992), which is exactly what deep-water species such as *K. dikume* require (Lyall, 1957a).

Lyall (1957a) investigated retinal mosaics of teleost species and found among others an impressive range of retinal cone patterns in trout and minnow. He shows that double cones are associated with vision in deep water and reports that cod *Gadus morhua* and whiting *Gadus merlangus*, both living in considerable depths, exhibit almost exclusively double cones in their retinae. Lyall (1957a) suggests that the association of double cones

with vision in deep water might be a consequence of the fact that different parts of the light spectrum penetrate to different depths, which corresponds with my hypothesis.

In contrast, Wunder (1925) found double cones are most numerous in shallow-water fish as he did not find any in the deep-water ones; however, Engström (1963) declines this affirmation and attributes such error to an inaccurate technique and systematic mistake in Wunder's research.

Boehlert (1978) demonstrates the loss of single cones occurs in association with a migration from surface to deep water during ontogeny of rockfish *Sebastes diploproa*. This fish spends first year of its life at the sea surface and then migrates to depths averaging several hundred meters where it spends the rest of the life near the bottom. Small prejuveniles exhibited a complex retinal mosaic similar to medaka square mosaic shown in B of Figure 4. Peripheral regions of the surface prejuveniles retinae lack the additional single cones in the pattern. The entire retina of larger benthic juveniles exhibited a pattern of double cone rows, where cone density decreased but cone diameter increased. This finding of retinal mosaic transformation corresponding to changing environment in water depths supports the hypothesis of double cone retina being an adaptation to deep-water habitat. Interestingly, Boehlert (1978) also investigated fish reared in laboratory which were held in surface light conditions even beyond the time when migration normally occurs. The ratio of single : double cones was intermediate between values of surface prejuvenile and benthic adult rockfish. Therefore, Boehlert (1978) suggests that the complete loss of single cones is accelerated only after migration, presumably by the changes in intensity or spectral composition of light. This research shows a great adaptivity of fish visual system in general even during the lifetime of an individual fish. As a consequence, it is important to be careful about retinal mosaic interpretation; however, it is clear that adaptation to the deep-water habitat exists even on the retinal pattern level. I prove this by the great difference in retinal mosaic pattern in-between sister species *K. eisentrauti* and *K. dikume* – close relatives living in different depths. Unfortunately, size nor number of the photoreceptor cells in their retina for better comparison has not been quantified.

Engström (1963) proves on a great number of teleost fishes studied that variation of the cone mosaic greatly depends on the degree to which the fish relies upon vision. Regular mosaics are typical for eyes adapted to acute vision, while eyes or their parts with lower need for sharp vision are organized loosely or not at all. Engström (1963) shows

that the mosaic is phylogenetically determined with respect to the fish ecology and visual demands.

Despite the fact Green et al. (1973) refer to *K. dikume* as a visual feeder, no particular pattern was observed in the cones arrangement; however, some locations appeared little more organized than others. Moreover, slightly more single cones were present in certain locations, while other parts even completely lack them. I believe this finding corresponds with the theory of different parts of retina linked and adapted to certain behaviour patterns (Levine & MacNichol, 1982); however, I cannot verify this hypothesis because of the missing sample orientation. The same holds for the fact that retinae of other three species also showed minor differences among various locations in one retina. This can be demonstrated by Table 11, where four different locations of a single fully stained retina of *M. myaka* are displayed. It is evident that some retinal locations exhibit significantly higher cone density than others, where cones appear significantly smaller. In Nile Tilapia (ancestral cichlid lineage), the same effect was observed by Lisney & Hawryshyn (2010) – cell density was higher in the temporal retina, even though the picture evidence is not as distinctive as the images of *M. myaka* retina in this thesis. A similar phenomenon was reported also for, e.g., bream *Nemipterus japonicus* (Raveendran & Mohideen, 1986) or coral fish *Microcanthus strigatus* (Yamanouchi, 1956). Raveendran & Mohideen (1986) divide the bream eye into two functional areas: first consisting of temporal, dorso-temporal and ventro-temporal acuity, and the rest as a second area. The area 1 comprises twice as many cones than the area 2. They correlate such division with the fish bottom dwelling habitat as the feeding on the bottom requires more acute vision because of the dim conditions. I believe a similar pattern is likely for *M. myaka* as it feeds on organic debris and phytoplankton close to the bottom (Green et al., 1973; Trewavas et al., 1972).

The aforementioned findings correspond with behavioural measurements of visual acuity in African cichlids of Dobberfuhl et al. (2005), who associated differences in visual acuity with habitat complexity, feeding strategies and social organization – specifically mating system. They hypothesize that rock-dwelling species favour adaptation for enhanced spatial resolution necessitating higher visual acuity; while sand-dwelling species favour adaptation for enhanced temporal resolution as they are more exposed and need to avoid predators. Dobberfuhl et al. (2005) also mentioned cone density inverse relation to fish length, dampening the effect of lens size on visual acuity.

Teleost retinal cone arrangements in general were studied into a great detail by Engström (1963). He describes different behaviour of various cone type while dark adaptation, which can make some of them hard to identify or even impossible to see in certain samples. This applies especially to individual central single cones that may disappear from the arrangement for this reason. Engström (1963) notes that fish killed directly after being taken up from their natural habitat tend to be semi-adapted and that such cone disappearance should be further studied in light-adapted fishes in the early stages of development. In my samples, missing single cones also appeared as noticeable in bright field with DIC images of retinae of *K. eisentrauti*, e.g., figure A in Table 8. Importantly, this can be also the reason for varying number of single cones in between samples of *K. dikume* retinae.

Moreover, the level of dark/light adaptation greatly influences the appearance of rods (Burnside et al., 1982) as can be seen in figure C of Table 6. As a result, some of the retinae were hard to investigate as the obtained images were unclear. In addition, retinal samples tend to be crinkly on the slides, which is a reason why not the whole optical field of images from general fluorescent microscopes (Olympus IX81 and BX51) is "filled", noticeable especially in Tables 6 and 12. However, almost all cones of these locations were stained, they only occurred in different focal planes. The best solution to display all stained cones in one image is through confocal microscopy imaging as Z-stack projection allows to merge images from multiple focal planes. Only samples stained by both probes underwent confocal microscopy imaging by virtue of its demandingness.

Dalton et al. (2015) showed that rearing environment effects the opsin gene expression including its distribution in cichlid retina. With awareness of the possible difference in expression and distribution in between laboratory-reared and wild-caught fish, I report both in the Chapter 4 for possible comparison; however, as the orientation of the retinae was unknown, I discuss a general appearance of the opsin distribution in both LR and WC fish samples together as I have not registered any significant difference and cannot comment on the distribution throughout retina for same reasons.

In general, cichlids maintain seven cone opsins SWS1, SWS2B, SWS2A, RH2B, RH2Aβ, RH2Aα and LWS (Spady et al., 2006). Musilová et al. (accepted) discovered that Barombi Mbo cichlids express only some of them in distinct profiles (Figure 11), similarly to cichlids from Lake Malawi (Parry et al., 2005). Opsin gene expression profiles of Barombi Mbo shallow-water species are richer and more diversified than the ones

of deep-water species. Both for this thesis selected shallow-water species (*S. mariae* and *K. eisentrauti*) express primarily *SWS2A*, *RH2Aβ* and *LWS*, but also *SWS2B* and *RH2Aα*. In contrast, both for this thesis selected deep-water species (*K. dikume* and *M. myaka*) lack *LWS* and *SWS2B* expression, i.e., shift towards the middle-wavelength sensitive opsins. Furthermore, longer-wavelength-green-sensitive opsin RH2Aα is more abundant than shorter-wavelength-green-sensitive opsin RH2Aβ. Levine & MacNichol (1982) prove that cone opsins expression generally corresponds to the illumination available in the fish environment, which confirms these findings.

Despite the troubleshooting, I successfully stained retinae of three of four selected cichlid species (*S. mariae, K. eisentrauti, M. myaka*) in all four mostly expressed opsin genes: *LWS, SWS2A*, *RH2Aα* and *RH2Aβ*. As already explained in Chapter 4.1, I originally targeted *RH2Aα* and *RH2Aβ* separately; however, all over twenty produced probes stained both of them nonexclusively indicated as *RH2A* throughout the thesis.

According to Dalton et al. (2015), cichlids express *SWS1* and *SWS2B* in single cones, *RH2B* and *RH2Aβ* in one member of a double cone, and *RH2Aα* and *LWS* in the opposite member. However, all my *RH2A* probes stained *RH2A* always in the double cone member opposite the one expressing *LWS*. Therefore, it is questionable if my *RH2A* probes really stained both *RH2Aα* and *RH2Aβ*, or *RH2Aβ* only. Interestingly, Torres-Dowdall et al. (2015) reported coexpression of *RH2Aβ* with both *LWS* and *RH2B* in Midas cichlid *Amphilophus astorquii*, i.e., *RH2Aβ* was expressed in both members of the double cones (see Figure 9) in contrast to what Dalton et al. (2015) stated. This finding that various opsins can actually be found in various retinal cells, together with the fact I originally targeted *RH2Aα* and *RH2Aβ* separately, as well as the results from Macrogen sequencing support the presumption that my *RH2A* probes really stained both α and β copies rather than only one of them.

Stomatepia mariae exhibited standard cichlid retinal mosaic (Fernald, 1981) as *SWS2A* was found exclusively in single cones, while *RH2A* and *LWS* were expressed complementary by one part of each double cone (Tables 5 and 6). In contrast, *LWS* probes labelled not only one cell of the double cones but in some cases both double cone members in the retinae of *K. eisentrauti* (Table 7), while *RH2A* was found in the other part of the non-purely LWS double cones and *SWS2A* labelled single cones (Tables 8 and 9). Torres-Dowdall et al., (2015) report that retinae of Midas cichlid *Amphilophus citrinellus* from turbid lake Nicaragua are dominated by double cones expressing *LWS* in both members

(see Figure 9), which they explain as a possible adaptation to dim-light conditions experienced in turbid water as long sensitive cones can be used for achromatic vision. I doubt the same reason goes for *K. eisentrauti* as its retina is not that widely LWS-only double cones dominated as the retina of *A. citrinellus;* moreover, Barombi Mbo is an oligotrophic lake with high water transparency; hence not as turbid as Lake Nikaragua. Dalton et al. (2015) reports on various opsin coexpression patterns in double cones of Malawi cichlid *Metriaclima zebra*; however, none of the samples exhibited *LWS* expression in both double cone members. However, they rarely detected *RH2Aα* in both members of double cones. Unfortunately, they do not comment on this occurrence. It is interesting that LWS-only double cones appearance in *K. eisentrauti* is neither rare as RH2Aα-only double cones in *M. zebra* nor frequent as LWS-only double cones in *A. citrinellus.* I consider such LWS-only double cones occurrence typical for *K. eisentrauti* species as they were present in all *K. eisentrauti* investigated individuals (if stained for) including both wild-caught and laboratory-reared fish. The variations in combination of LWS with RH2 opsins in double cones cause differences in the double cone spectral sensitivity by which the fish visual abilities are tuned (Parry et al., 2005). Therefore, I suggest that purely LWS double cones could create an additional channel to LWS-RH2A cones.

As already described, opsin expression of *M. myaka* is shifted towards the middle-wavelength sensitive opsins – it expresses *SWS2A* but lacks both *SWS2B* (sensitive in violet) and *LWS* (red); however, it expresses *RH2Aα* more than *RH2Aβ*. *K. dikume* follows the same pattern. I have not managed to stain retinae of *K. dikume*; however, *M. myaka* expresses *SWS2A* in single cones and *RH2A* in both parts of double cones as expected. Interestingly, some saltwater fishes that live near the surface, such as *Cyphaena hippurus*, express also only two different cone opsins, one sensitive to blue and the other to green wavelengths (Levine & MacNichol, 1982), i.e., similarly to *M. myaka* and *K. dikume*. McFarland & Munz (1975) explain that such blue-and-green-sensitive systems allow both dark and bright objects to be discriminated against the background space light. When the fish looks upward, green-sensitive opsin allows to differentiate dark objects and blue-sensitive opsin allows to distinguish bright objects against the predominantly green background. While when the fish looks downward, the pigments work the other way around with the effect of object determination against the background.

To summarise, the shallow-water cichlids *Konia eisentrauti* and *Stomatepia mariae* express mainly three types of cone opsin genes: *LWS*, *RH2A* (*RH2Aβ* more than *RH2Aα*)

and *SWS2A*. Contrarily, both seasonally deep-water *Myaka myaka* and deep-water *Konia dikume* lack expression *SWS2B* and *LWS* in their retinae, they express *SWS2A* and *RH2Aα* more than *RH2Aβ,* which corresponds to the light conditions in deep water, where only green/blue part of the light spectrum is present. These two unrelated deep-water species probably developed such adaptation to the environment independently. The adaptation to the environment is also evident from the retinal mosaics. *S. mariae* embodies common cichlid retinal mosaic: single cones expressing *SWS2A* surrounded by four double cones with *LWS* in one and *RH2A* in second part. *K. eisentrauti* follows a similar pattern; however, some double cones express *LWS* in both parts, the reason is generally unknown. In morphologically standard retina of *M. myaka*, *RH2A* is found in both parts of double cones, i.e., replacing missing *LWS*, while single cones express *SWS2A*. The retinal mosaic of *K. dikume* is less organized with dominance of double cones and virtual lack of single cones; however, the spatial distribution of opsin genes remains unclear. I did not recover any opsins coexpressing. Table 13 summarises these findings in all four selected species.

The effect of depth on the retinal organization of selected cichlid species from Lake Barombi Mbo was apparent in several ways:

1) the overall cone mosaic of permanently deep-water *K. dikume* greatly differed from the mosaics of other three species in a way corresponding to the literature;

2) cone opsin gene expression profiles of shallow-water and deep-water species are unlike, deep-water species shift towards the middle-wavelength sensitive opsins lacking the sensitivity in red and violet part of the light spectrum;

3) *LWS* is replaced by *RH2A* in double cones of seasonally deep-water *M. myaka*. Additionally, differences in cone density possibly related to fish behaviour and habitat were recovered.

Finally, two-colour fluorescent in situ hybridization method employing RNA probes on whole mounts of cichlid retinae was developed and optimized for the purposes of the Fish Evolution Research Group as a part of this thesis.

Conclusion

This thesis was devoted to the topic of adaptations of fish visual system to extreme environments, i.e., distribution of photoreceptor types in retina of four selected cichlid species of Lake Barombi Mbo: shallow-water species *Stomatepia mariae* and *Konia eisentrauti,* deep-water species *Konia dikume* and seasonally deep-water species *Myaka myaka.* Retinal mosaic of all species was described, including general morphological appearance as well as opsin gene expression distribution in different cell types (except for *K. dikume*). No opsin genes coexpression was observed. Moreover, the effect of depth on the function and organization of cichlid retina was discussed into a detail.

To sum up, all major goals set were met except description of opsin gene distribution in *K. dikume*. Additionally, method of double FISH on whole mounts was developed, optimized and standardized for further use despite a great number of difficulties and troubleshooting, wherefor only half of the samples dyed. The retinae were stained for only four opsin genes: *SWS2A, LWS,* and *RH2Aα* plus *RH2Aβ* nonexclusively together as *RH2A* despite my great effort to develop specific probes targeting each *RH2A* copy alone.

Two most interesting findings of this thesis are double cone dominant arrangement of *K. dikume* retina and regular *LWS*-only double cones occurrence in retina of *K. eisentrauti.* Differences of cell densities throughout retina of *M. myaka* probably corresponding to its natural habitat are also worth mentioning. After all, retina of *S. mariae* appearing as a "standard" cichlid retina in all matters is actually exceptional, as there was no such "standard" retina described by FISH method – cichlid retinae either feature an unusual pattern or a specific coexpression.

This study is one of the few works applying FISH on cichlid retina, thus adding knowledge on Barombi Mbo cichlids to the research of photoreceptor distribution in Midas (Torres-Dowdall et al., 2017) and Malawi (Dalton et al., 2017; Dalton et al., 2015) cichlids. The results of this thesis greatly contribute to the understanding of the evolution of cichlid visual system and complement yet insufficient knowledge on the visual performance of cichlids from Lake Barombi Mbo. They are an important extension of opsin expression research for which they became a part of a scientific article (Musilová et al., accepted – Figure 13) and were frequently presented at various conferences (Attachments 1–5).

For future reference, there is a great potential for further work on the topic of cichlid vision. Current knowledge on the gene expression, opsin profiles and photoreceptor distribution is a solid inception to understanding how cichlids see. However, to get a bigger picture, it would be great to support already available information with data on retinal organization at higher levels than just opsin proteins and photoreceptor cells, i.e., to explore receptive fields of bipolar and ganglion cells; and ideally even investigate visual centres of the cichlid brain. Apart from histological methods, it would also require physiological and neurobiological approach.

List of References

Abrahamson, E.W., Baumann, C., Bridges, C.D.B., Crescitelli, F., Dartnall, H. J. A., Eakin, R.M., Falk, G., Fatt, P., Goldsmith, T.H., Hara, R., Hara, T., Japar, S.M., Liebman, P.A., Lythgoe, J.N., Morton, R.A., Muntz, W.R.A., Rushton, W.A.H., Shaw, T.I., Wiesenfeld, J.R. & Yoshizawa, T. 1972. *Photochemistry of Vision*. Herbert J. A. Dartnall, ed. Berlin, Heidelberg: Springer Berlin Heidelberg.

Baker, S.A. & Kerov, V. 2013. Photoreceptor Inner and Outer Segments. In V. Bennett, ed. *Current Topics in Membranes*. Academic Press: 231–265.

Barthel, L.K. & Raymond, P.A. 2000. In situ hybridization studies of retinal neurons. In M. I. Simon & J. N. Abelson, eds. *Methods*. Academic Press: 579–590.

Beer, T. 1894. Die Accommodation des Fischauges. *Pflüger, Archiv für die Gesammte Physiologie des Menschen und der Thiere*, 58(11–12): 523–650.

Björn, L.O. 2015. *Photobiology : the science of light and life*. 3rd ed. L. O. Björn, ed. Springer-Verlag New York Inc.

Boehlert, G.W. 1978. Intraspecific evidence for the function of single and double cones in the teleost retina. *Science*, 202(4365): 309–11.

Bowmaker, J.K. 1995. The visual pigments of fish. *Progress in Retinal and Eye Research*, 15(1): 1–31.

Bowmaker, J.K. 1990. Visual pigments of fishes. In R. Douglas & M. Djamgoz, eds. *The Visual System of Fish*. Dordrecht: Springer Netherlands: 81–108.

Bowmaker, J.K. & Hunt, D.M. 2006. Evolution of vertebrate visual pigments. *Current Biology*, 16(13): R484–R489.

Burnside, B., Evans, M., Fletcher, R.T. & Chader, G.J. 1982. Induction of dark-adaptive retinomotor movement (cell elongation) in teleost retinal cones by cyclic adenosine 3','5-monophosphate. *The Journal of General Physiology*, 79(5): 759–774.

de Busserolles, F., Fitzpatrick, J.L., Marshall, N.J. & Collin, S.P. 2014a. The Influence of Photoreceptor Size and Distribution on Optical Sensitivity in the Eyes of Lanternfishes (Myctophidae) E. J. Warrant, ed. *PLoS ONE*, 9(6).

de Busserolles, F., Marshall, N.J. & Collin, S.P. 2014b. Retinal Ganglion Cell Distribution and Spatial Resolving Power in Deep-Sea Lanternfishes (Myctophidae). *Brain, Behavior and Evolution*, 84(4): 262–276.

Carleton, K.L. & Kocher, T.D. 2001. Cone Opsin Genes of African Cichlid Fishes: Tuning Spectral Sensitivity by Differential Gene Expression. *Molecular Biology and Evolution*, 18(8): 1540–1550.

Cohen, A.I. 1972. Rods and Cones. In M. G. F. Fuortes, ed. *Physiology of Photoreceptor Organs. Handbook of Sensory Physiology*. Springer Berlin Heidelberg: 63–110.

Cohen, A.I. 1963. Vertebrate Retinal Cells and Their Organization. *Biological Reviews*, 38(4): 427–459.

Crowell, B. 2019. *Light and Matter*. Fullerton, California: Open Source Physics Textbooks. www.lightandmatter.com.

Dalton, B.E., de Busserolles, F., Marshall, N.J. & Carleton, K.L. 2017. Retinal specialization through spatially varying cell densities and opsin coexpression in cichlid fish. *The Journal of experimental biology*, 220(Pt 2): 266–277.

Dalton, B.E., Lu, J., Leips, J., Cronin, T.W. & Carleton, K.L. 2015. Variable light environments induce plastic spectral tuning by regional opsin coexpression in the African cichlid fish, Metriaclima zebra. *Molecular Ecology*, 24(16): 4193–4204.

Denton, E.J. & Locket, N.A. 1989. Possible Wavelength Discrimination by Multibank Retinae in Deep-Sea Fishes. *Journal of the Marine Biological Association of the United Kingdom*, 69(2): 409–435.

Dobberfuhl, A.P., Ullmann, J.F.P. & Shumway, C.A. 2005. Visual acuity, environmental complexity, and social organization in african cichlid fishes. *Behavioral Neuroscience*, 119(6): 1648–1655.

Douglas, R.H. & Djamgoz, M.B.A. eds. 1990. *The Visual System of Fish*. 1st ed. Dordrecht: Springer Netherlands.

Dowling, J.E. 1970. Organization of vertebrate retinas. *Investigative ophthalmology*, 9(9): 655–680.

Ehlman, S.M., Sandkam, B.A., Breden, F. & Sih, A. 2015. Developmental plasticity in vision and behavior may help guppies overcome increased turbidity. *Journal of Comparative Physiology A*, 201(12): 1125–1135.

Engström, K. 1963. Cone Types and Cone Arrangements in Teleost Retinae. *Acta Zoologica*, 44(1–2): 179–243.

Escobar-Camacho, D. & Carleton, K.L. 2015. Sensory modalities in cichlid fish behavior. *Current Opinion in Behavioral Sciences*, 6: 115–124.

Escobar-Camacho, D., Pierotti, M.E.R., Ferenc, V., Sharpe, D.M.T., Ramos, E., Martins, C. & Carleton, K.L. 2019. Variable vision in variable environments: the visual system of an invasive cichlid (Cichla monoculus) in Lake Gatun, Panama. *The Journal of experimental biology*, 222(Pt 6): jeb188300.

Fernald, R.D. 1988. Aquatic Adaptations in Fish Eyes. In J. Atema, R. R. Fay, A. N. Popper, & W. N. Tavolga, eds. *Sensory Biology of Aquatic Animals*. New York, NY: Springer: 435–466.

Fernald, R.D. 1981. Chromatic organization of a cichlid fish retina. *Vision Research*, 21(12): 1749–1753.

Gordon, H.R., Smith, R.C., Ronald, J. & Zaneveld, V. 1980. Introduction to ocean optics. In S. Q. Duntley, ed. *Proc. SPIE 0208, Ocean Optics VI*. 14–55.

Green, J., Corbet, S.A. & Betney, E. 1973. Ecological studies on crater lakes in West Cameroon - The blood of endemic cichlids in Barombi Mbo in relation to stratification and their feeding habits. *Journal of Zoology*, 170: 299–308.

Härer, A., Meyer, A. & Torres-Dowdall, J. 2018. Convergent phenotypic evolution of the visual system via different molecular routes: How Neotropical cichlid fishes adapt to novel light environments. *Evolution Letters*, 2(4): 341–354.

Härer, A., Torres-Dowdall, J. & Meyer, A. 2017. Rapid adaptation to a novel light environment: The importance of ontogeny and phenotypic plasticity in shaping the visual system of Nicaraguan Midas cichlid fish (Amphilophus citrinellus spp.). *Molecular Ecology*, 26(20): 5582–5593.

Hauser, F.E., Ilves, K.L., Schott, R.K., Castiglione, G.M., López-Fernández, H. & Chang, B.S.W. 2017. Accelerated Evolution and Functional Divergence of the DimLight Visual Pigment Accompanies Cichlid Colonization of Central America. *Molecular Biology and Evolution*, 34(10): 2650–2664.

Hofmann, C.M., O'Quin, K.E., Marshall, N.J., Cronin, T.W., Seehausen, O. & Carleton, K.L. 2009. The Eyes Have It: Regulatory and Structural Changes Both Underlie Cichlid Visual Pigment Diversity M. A. F. Noor, ed. *PLoS Biology*, 7(12): e1000266.

Hofmann, C.M., O'Quin, K.E., Smith, A.R. & Carleton, K.L. 2010. Plasticity of opsin gene expression in cichlids from Lake Malawi. *Molecular Ecology*, 19(10): 2064–2074.

Hughes, A. 1985. New perspectives in retinal organisation. *Progress in Retinal Research*, 4: 243–313.

Hughes, R.H. & Hughes, J.S. 1992. *A Directory of African Wetlands*. Nairobi: IUCN, UNEP, WCMC.

Jagger, W.S. 1992. The optics of the spherical fish lens. *Vision Research*, 32(7): 1271–1284.

Kocher, T.D. 2004. Adaptive evolution and explosive speciation: the cichlid fish model. *Nature Reviews Genetics*, 5(4): 288–298.

Kunz, Y.W. 1980. Cone mosaics in a teleost retina: Changes during light and dark adaptation. *Cellular and Molecular Life Sciences*, 36(12): 1371–1374.

Land, M.F. 1988. The optics of animal eyes. *Contemporary Physics*, 29(5): 435–455.

Land, M.F. & Nilsson, D.-E. 2012. *Animal Eyes*. 2nd ed. New York: OUP Oxford.

Levine, J.S. & MacNichol, E.F.J. 1982. Color Vision in Fishes. *Scientific American*, 246: 140–149.

Lisney, T.J. & Hawryshyn, C.W. 2010. Ocular dimensions and cone photoreceptor topography in adult Nile Tilapia Oreochromis niloticus. *Environmental Biology of Fishes*, 88(4): 369–376.

Locket, N.A. 1977. Adaptations to the Deep-Sea Environment. In F. Crescitelli, ed. *The Visual System in Vertebrates. Handbook of Sensory Physiology, vol 7/5*. Berlin, Heidelberg: Springer: 67–192.

Loew, E.R. & Lythgoe, J.N. 1978. The ecology of cone pigments in teleost fishes. *Vision Research*, 18(6): 715–722.

Loew, E.R. & McFarland, W.N. 1990. The underwater visual environment. In R. Douglas & M. Djamgoz, eds. *The Visual System of Fish*. Dordrecht: Springer Netherlands: 1–44.

Lyall, A.H. 1957a. Cone Arrangements in Teleost Retinae. *Journal of Cell Science*, s3-98(42): 189–201.

Lyall, A.H. 1956. Occurrence of Triple and Quadruple Cones in the Retina of the Minnow (Phoxinus laevis). *Nature*, 177(4519): 1086–1087.

Lyall, A.H. 1957b. The growth of the trout retina. *Quarterly Journal of Microscopical Science*, 98(1): 101–110.

Lythgoe, J.N. 1979. *The ecology of vision*. Oxford: Clarendon Press.

Mameri, D., van Kammen, C., Groothuis, T.G.G., Seehausen, O. & Maan, M.E. 2019. Visual adaptation and microhabitat choice in Lake Victoria cichlid fish. *Royal Society Open Science*, 6(3): 181876.

Martin, C.H., Cutler, J.S., Friel, J.P., Dening Touokong, C., Coop, G. & Wainwright, P.C. 2015. Complex histories of repeated gene flow in Cameroon crater lake cichlids cast doubt on one of the clearest examples of sympatric speciation. *Evolution*, 69(6): 1406–1422.

McFarland, W.N. & Munz, F.W. 1975. Part III: The evolution of photopic visual pigments in fishes. *Vision Research*, 15(10): 1071–1080.

van der Meer, H.J. 1992. Constructional morphology of photoreceptor patterns in percomorph fish. *Acta Biotheoretica*, 40(1): 51–85.

van der Meer, H.J. 2013. Vision in Cichlids. http://www.vision-in-cichlids.com 8 April 2018.

Mülhardt, C. & Beese, E.W. 2007. Investigating the Function of DNA Sequences. *Molecular Biology and Genomics*: 169–221.

Musilova, Z., Cortesi, F., Matschiner, M., Davies, W.I.L., Patel, J.S., Stieb, S.M., de Busserolles, F., Malmstrøm, M., Tørresen, O.K., Brown, C.J., Mountford, J.K., Hanel, R., Stenkamp, D.L., Jakobsen, K.S., Carleton, K.L., Jentoft, S., Marshall, J. & Salzburger, W. 2019. Vision using multiple distinct rod opsins in deep-sea fishes. *Science*, 364(6440): 588–592.

Musilová, Z., Indermaur, A., Bitja-Nyom, A.R., Omelchenko, D., Kłodawska, M., Albergati, L., Remišová, K. & Salzburger, W. Evolution of Visual Sensory System in Cichlid Fishes from Crater Lake Barombi Mbo in Cameroon. Accepted. *Molecular Ecology*.

Nilsson, D.-E. 2013. Eye evolution and its functional basis. *Visual Neuroscience*, 30(1–2): 5–20.

Parry, J.W.L., Carleton, K.L., Spady, T., Carboo, A., Hunt, D.M. & Bowmaker, J.K. 2005. Mix and Match Color Vision: Tuning Spectral Sensitivity by Differential Opsin Gene Expression in Lake Malawi Cichlids. *Current Biology*, 15(19): 1734–1739.

Partridge, J.C., Douglas, R.H., Marshall, N.J., Chung, W.-S., Jordan, T.M. & Wagner, H.-J. 2014. Reflecting optics in the diverticular eye of a deep-sea barreleye fish (Rhynchohyalus natalensis). *Proceedings. Biological sciences / The Royal Society*, 281(1782).

Raveendran, S. & Mohideen, H.M. 1986. Visual capacity of marine teleost Nemipterus japonicus (Bloch). *Proceedings: Animal Sciences*, 95(5): 567–577.

Sabbah, S., Laria, R., Gray, S.M. & Hawryshyn, C.W. 2010. Functional diversity in the color vision of cichlid fishes. *BMC Biology*, 8(1): 133.

Schliewen, U.K. & Klee, B. 2004. Reticulate sympatric speciation in Cameroonian crater lake cichlids. *Frontiers in Zoology*, 1(5): 9–14.

Schliewen, U.K., Tautz, D. & Pääbo, S. 1994. Sympatric speciation suggested by monophyly of crater lake cichlids. *Nature*, 368: 629.

Scholes, J.H. 1975. Colour Receptors, and their Synaptic Connexions, in the Retina of a Cyprinid Fish. *Philosophical Transactions of the Royal Society B: Biological Sciences*, 270(902): 61–118.

Spady, T.C., Parry, J.W.L., Robinson, P.R., Hunt, D.M., Bowmaker, J.K. & Carleton, K.L. 2006. Evolution of the Cichlid Visual Palette through Ontogenetic Subfunctionalization of the Opsin Gene Arrays. *Molecular Biology and Evolution*, 23(8): 1538–1547.

Spady, T.C., Seehausen, O., Loew, E.R., Jordan, R.C., Kocher, T.D. & Carleton, K.L. 2005. Adaptive molecular evolution in the opsin genes of rapidly speciating cichlid species. *Molecular Biology and Evolution*, 22(6): 1412–1422.

Steeves, G. 2004. A Little Insight on Barombi Mbo, Cameroon. *The Lateral Line*, 1(2): 3.

Stell, W.K. 1972. The Morphological Organization of the Vertebrate Retina. In M. G. F. Fuortes, ed. *Physiology of Photoreceptor Organs. Handbook of Sensory Physiology, vol 7/2*. Berlin, Heidelberg: Springer: 111–213.

Stell, W.K. & Hárosi, F.I. 1976. Cone structure and visual pigment content in the retina of the goldfish. *Vision Research*, 16(6): 647-IN4.

Strauss, O. 2005. The Retinal Pigment Epithelium in Visual Function. *Physiological Reviews*, 85(3): 845–881.

Terai, Y., Miyagi, R., Aibara, M., Mizoiri, S., Imai, H., Okitsu, T., Wada, A., Takahashi-Kariyazono, S., Sato, A., Tichy, H., Mrosso, H.D.J., Mzighani, S.I. & Okada, N. 2017. Visual adaptation in Lake Victoria cichlid fishes: Depth-related variation of color and scotopic opsins in species from sand/mud bottoms. *BMC Evolutionary Biology*, 17(1): 1–12.

The Global Economy. 2018. Cameroon Political stability. https://www.theglobaleconomy.com/Cameroon/wb_political_stability/ 15 July 2019.

Tohya, S., Mochizuki, A. & Iwasa, Y. 2003. Difference in the retinal cone mosaic pattern between zebrafish and medaka: Cell-rearrangement model. *Journal of Theoretical Biology*, 221(2): 289–300.

Torres-Dowdall, J., Henning, F., Elmer, K.R. & Meyer, A. 2015. Ecological and lineage-specific factors drive the molecular evolution of rhodopsin in cichlid fishes. *Molecular Biology and Evolution*, 32(11): 2876–2882.

Torres-Dowdall, J., Pierotti, M.E.R., Härer, A., Karagic, N., Woltering, J.M., Henning, F., Elmer, K.R. & Meyer, A. 2017. Rapid and Parallel Adaptive Evolution of the Visual System of Neotropical Midas Cichlid Fishes. *Molecular Biology and Evolution*, 34(10): 2469–2485.

Trewavas, E., Green, J. & Corbet, S.A. 1972. Ecological studies on crater lakes in West Cameroon Fishes of Barombi Mbo. *Journal of Zoology*, 167(1): 41–95.

Turner, G.F. 2007. Adaptive radiation of cichlid fish. *Current Biology*, 17(19): 827–831.

Wagner, H.-J. 1990. Retinal structure of fishes. In R. Douglas & M. Djamgoz, eds. *The Visual System of Fish*. Dordrecht: Springer Netherlands: 109–158.

Wagner, H.J., Douglas, R.H., Frank, T.M., Roberts, N.W. & Partridge, J.C. 2009. A Novel Vertebrate Eye Using Both Refractive and Reflective Optics. *Current Biology*, 19(2): 108–114.

Warrant, E.J. & Locket, N.A. 2004. Vision in the deep sea. *Biological Reviews*, 79(3): 671–712.

Welten, M.C.M., de Haan, S.B., van den Boogert, N., Noordermeer, J.N., Lamers, G.E.M., Spaink, H.P., Meijer, A.H. & Verbeek, F.J. 2006. ZebraFISH: Fluorescent In Situ Hybridization Protocol and Three-Dimensional Imaging of Gene Expression Patterns. *Zebrafish*, 3(4): 465–476.

Wolken, J.J. 1995. *Light Detectors, Photoreceptors, and Imaging Systems in Nature*. New York: Oxford University Press.

Wunder, W. 1925. Physiologische und vergleichend-anatomische Untersuchungen an der Knochenfischnetzhaut. *Zeitschrift für Vergleichende Physiologie*, 3(1): 1–61.

Yamanouchi, T. 1956. The visual acuity of the coral fish Microcanthus strigatus (Cuvier and Valenciennes). *Publications of the Seto Marine Biological Laboratory*, 5(2): 133–156.

Yokoyama, S. 2000. Molecular evolution of vertebrate visual pigments. *Progress in Retinal and Eye Research*, 19(4): 385–419.

Zaunreiter, M., Junger, H. & Kotrschal, K. 1991. Retinal Structure; Physiology and Pharmacology - Retinal Morphology of Cyprinid Fishes: a Quantitative Study of Changes and Interspecific Variation. *Vision Research*, 31(3): 383–394.

Secondary References

*Walls, G.L. 1942. The vertebrate eye and its adaptive radiation. Oxford, England: Cranbrook Institute of Science. In Fernald, R.D. 1988. Aquatic Adaptations in Fish Eyes. In J. Atema, R. R. Fay, A. N. Popper, & W. N. Tavolga, eds. *Sensory Biology of Aquatic Animals*. New York, NY: Springer: 435–466.

* Knowles, A. & Dartnall, H.J.A. 1977. The photobiology of vision. In Davson, H., eds. *The Eye*. London: Academic Press. In Bowmaker, J.K. 1990. Visual pigments of fishes. In R. Douglas & M. Djamgoz, eds. *The Visual System of Fish*. Dordrecht: Springer Netherlands: 81–108.

List of Graphs

Graph 1 Downwelling Spectral Irradiance E_d for a Crater Lake 14
Graph 2 Relative Absorption Spectra of Vitamin A1, 11-cis Retinal, Rhodopsin and Porphyropsin 21

List of Figures

Figure 1 Diagrammatical Vertical Section of Generalized Teleost Eye 15
Figure 2 Diagram of a Vertebrate Retina 17
Figure 3 Structure of a Photoreceptor Cell 18
Figure 4 Cone Mosaics of Fish Retina, (A) Row Mosaic in Zebrafish and (B) Square Mosaic in Medaka 20
Figure 5 Schematic Model of the Molecular Structure of a Photoreceptor Cell 21
Figure 6 Opsins & Opsin Genes in African Cichlids 22
Figure 7 Relative Cone Opsin Gene Expression of Selected Opsins in Nile Tilapia – Larva, Juvenile and Adult 23
Figure 8 Opsin Gene Expression Profiles as Well as Single- and Double-Cone Sensitivities of Lake Malawi and Lake Victoria Cichlids Form Three Clusters 24
Figure 9 Fluorescent *in situ* Hybridization Staining of Two Midas Cichlid Species 25
Figure 10 Description of Lake Barombi Mbo 27
Figure 11 Cichlids of Barombi Mbo – Phylogenetic Tree Based on Retinal Transcriptome Sequences and Opsin Gene Expression Profiles 28

Figure 12 Four Selected Cichlid Species of Barombi Mbo....29
Figure 13 Table of Figures from the Article Musilová et al. (accepted)....54

List of Tables

Table 1 List of Fish Species from Barombi Mbo....26
Table 2 List of Designed Primers....35
Table 3 List of Used Probes....36
Table 4 List of All Samples....40
Table 5 Retinae of *Stomatepia mariae* Stained by Both Probes....42
Table 6 Retinae of *Stomatepia mariae* Stained by One Probe....44
Table 7 Comparism of the retinae of A) *Stomatepia mariae* and B) *Konia eisentrauti*.... 45
Table 8 Retinae of *Konia eisentrauti* Stained by Both Probes....46
Table 9 Retinae of *Konia eisentrauti* Stained by One Probe....48
Table 10 Retinae of *Konia dikume*.... 50
Table 11 Retinae of *Myaka myaka* Stained by Both Probes....51
Table 12 Retinae of *Myaka myaka* Stained by One Probe....52
Table 13 Retinal Mosaics of Selected Barombi Mbo Cichlid Species....53

Attachments

1. Poster Presented at Zoological Days 2017, Brno, Czech Republic

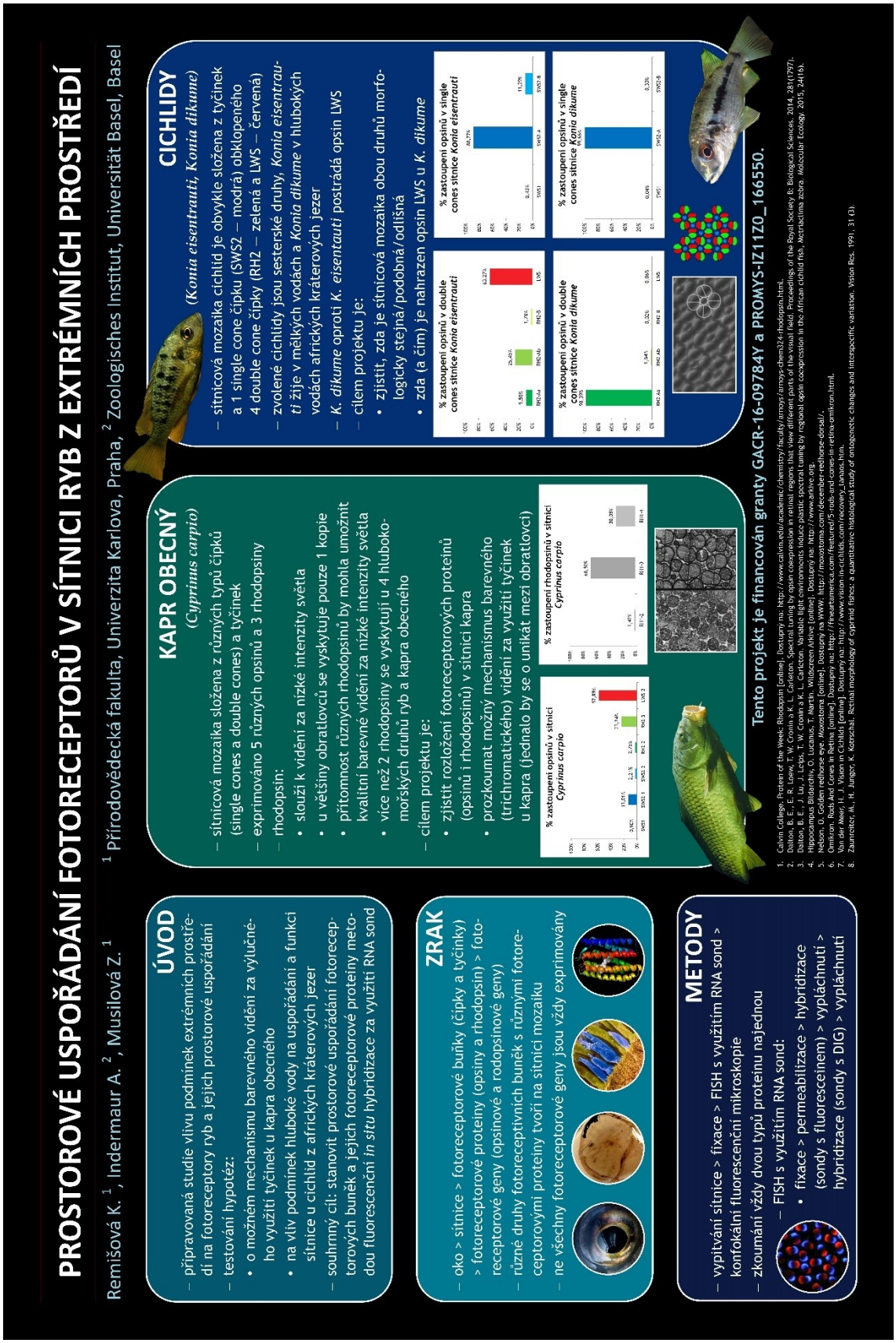

2. Poster Presented at European Society for Evolutionary Biology (ESEB) 16th Congress in 2017, Groningen, Netherlands

Photoreceptor Adaptations in Fishes from Extreme Environments

Remišová Kateřina [1], Indermaur Adrian [2], Musilová Zuzana [1]

[1] Faculty of Science, Charles University, Prague, Czech Republic, [2] Zoological Institute, University of Basel , Basel, Switzerland

INTRODUCTION

- **Vision** is a crucial sense for an organism's survival. The visual information is carried by **light**, hence vision depends on, among others, light detection. Specific light wavelengths are detected by various photoreceptor proteins (**opsins**) located in photoreceptor cells (**cones and rods**). Vertebrates typically possess three types of cone opsins used in light vision, **long-wave sensitive** (LWS), **short-wave sensitive** (SWS) and **rhodopsin** (RH) **opsins**. The majority of vertebrates express only one type of **rod opsin** usually used in night vision.
- Fish are generally able of very good colour vision thanks to the presence of several photoreceptor proteins in the retina. Moreover, various types of cones and rods are organized in the **retinal mosaics**. Distribution and representation of various photoreceptor proteins can be often influenced by different **optical properties of the aquatic environment** as there is basically entire light spectrum covered in the shallow waters, while blue and green wavelengths dominate in the deep water.
- **In this study, we investigated the opsin spatial distribution in retina of two cichlid sister species from the Barombi Mbo crater lake (*Konia eisentrauti* and *Konia dikume*) and the opsin and rod opsin distribution of the common carp (*Cyprinus carpio*) by the method of fluorescent in-situ hybridization (FISH) employing the RNA probes .**

CONCLUSIONS

- The overall retinal mosaic of ***Konia eisentrauti*** appears regularly organised, consisting of a central single cone surrounded by four double cones. We found a common cichlid pattern with the red (LWS) and green (RH2A) opsin genes expressed in the double cones, while the blue opsin gene (SWS2) is expressed in the single cones. Moreover, some of the double cones express only the red (LWS) opsin gene in both parts.
- The retinal mosaic of ***Konia dikume*** is less organised with dominance of double cones and virtual lack of single cones; the spatial distribution of opsin genes remains still unclear.
- We have not found any particular pattern of photoreceptor cells in the retina of ***Cyprinus carpio***. The red opsin gene (LWS2) is expressed in one side of double cones. However, the spatial distribution of the other opsin genes as well as rod opsin genes remains unclear.

KONIA EISENTRAUTI

- shallow water species
  - › entire light spectrum
    - › wide range of opsins
- picture A shows the overall view of the retina
- picture B shows the overall retinal mosaic
- picture C shows expression of the RH2A (green) and LWS (red) opsin genes in double cones
- picture D shows expression of the RH2A (green) and SWS2A (magenta) opsin genes
- graph shows relative representation of the opsin genes in the retina

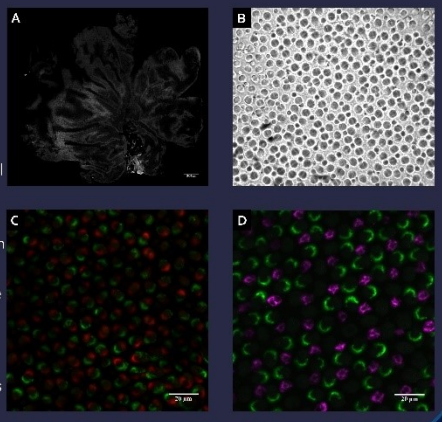

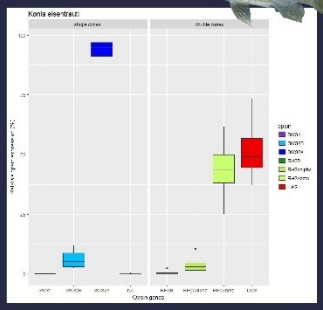

COMMON CARP

- lives in turbid water
- graphs show relative representation of the opsin (left) and rod opsin (right) genes in the retina
- left picture shows the overall pattern of photoreceptor cells in the retina
- right picture shows distribution of the LWS-2 opsin gene

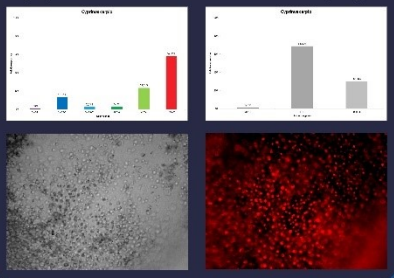

KONIA DIKUME

- deep water species
  - › blue and green wavelengths
    - › lacking LWS opsin
- graph shows relative representation of the opsin genes in the retina
- picture shows the overall retinal mosaic

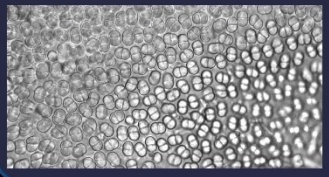

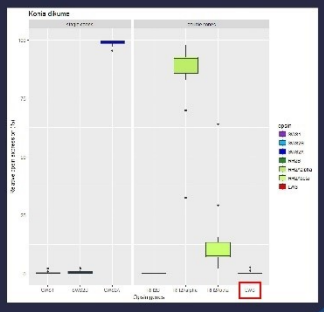

This study has been funded by GACR-16-09784Y and PROMYS-IZ11Z0_166550.

3. Poster Presented at Cichlid Science Meeting 2017, Prague, Czech Republic

DISTRIBUTION OF PHOTORECEPTOR TYPES IN RETINA OF CAMEROONIAN CRATER LAKE CICHLIDS

Kateřina Remišová [1X], Adrian Indermaur [2], Zuzana Musilová [1]

[1] Faculty of Science, Charles University, Prague, Czech Republic, [2] Zoological Institute, University of Basel , Basel, Switzerland

[X] k.remisova@gmail.com

INTRODUCTION

- **Vision** is a crucial sense for an organism's survival. The visual information is carried by **light**, hence vision depends on, among others, light detection. Specific light wavelengths are detected by various photoreceptor proteins (**opsins**) located in photoreceptor cells (**cones and rods**). Vertebrates typically possess three types of cone opsins used in light vision, **long-wave sensitive (LWS), short-wave sensitive (SWS)** and **rhodopsin (RH) opsins.** The majority of vertebrates express only one type of **rod opsin** usually used in night vision.
- Fish are generally able of very good colour vision thanks to the presence of several photoreceptor proteins in the retina. Moreover, various types of cones and rods are organized in the **retinal mosaics**. Distribution and representation of various photoreceptor proteins can be often influenced by different **optical properties of the aquatic environment** as there is basically entire light spectrum covered in the shallow waters, while blue and green wavelengths dominate in the deep water.
- **In this study, we investigated the opsin spatial distribution in retina of two cichlid sister species from the Barombi Mbo crater lake (*Konia eisentrauti* and *Konia dikume*) by the method of fluorescent in-situ hybridization (FISH) employing the RNA probes (following Dalton et al, 2014).**

CONCLUSIONS

- The overall retinal mosaic of ***Konia eisentrauti*** appears regularly organised, consisting of a central single cone surrounded by four double cones. We found a common cichlid pattern with the red (LWS) and green (RH2A) opsin genes expressed in the double cones, while the blue opsin gene (SWS2) is expressed in the single cones. Moreover, some of the double cones express only the red (LWS) opsin gene in both parts.
- The retinal mosaic of ***Konia dikume*** is less organised with dominance of double cones and virtual lack of single cones; the spatial distribution of opsin genes remains still unclear.

Acknowledgements:
We thank Sara M. Stieb and Fabio Cortesi for their help with the protocol optimization. We thank Monika Kłodawska and Dmytro Omelchenko for their help with collecting retina samples in the field. We thank Walter Salzburger for his kind and constant support. This study has been funded by the Czech Science Foundation (16-09784Y) and Swiss National Science Foundation (PROMYS-IZ1120_166550).

KONIA EISENTRAUTI

- A shallow water species expressing wide range of opsins due to the presence of the entire light spectrum in its environment.

The Overall Retinal Mosaic

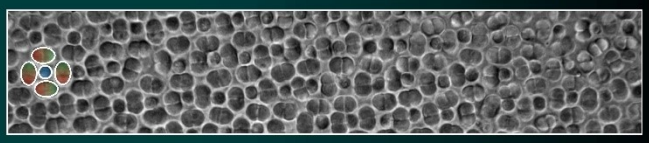

Expression of the RH2A* (in Green Colour) and LWS (in Red Colour) Opsin Genes

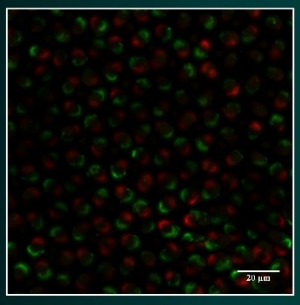

Expression of the RH2A* (in Green Colour) and SWS2A (in Magenta Colour) Opsin Genes

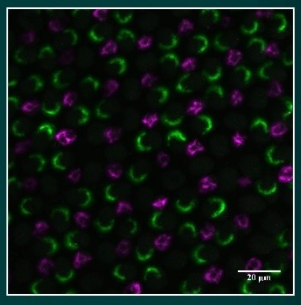

Representation of the Opsin Genes in the Retina

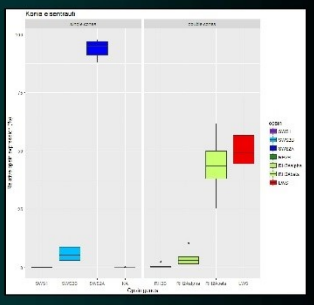

* We used the RH2A probe for staining both RH2Aalpha and RH2Abeta.

KONIA DIKUME

- A deep water species lacking LWS opsin as blue and green wavelengths dominate in its environment.

The Overall Retinal Mosaic

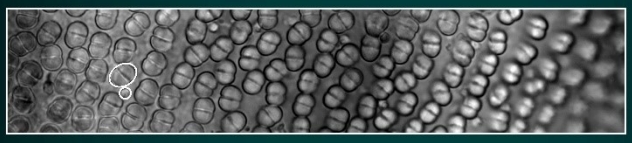

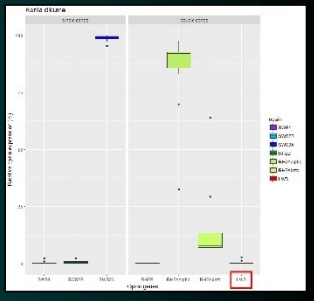

References: Dalton, B. E., Loew, E. R., Cronin, T. W. & Carleton, K. L. (2014). Spectral tuning by opsin coexpression in retinal regions that view different parts of the visual field.

4. Poster Presented at Zoological Days 2018, Prague, Czech Republic

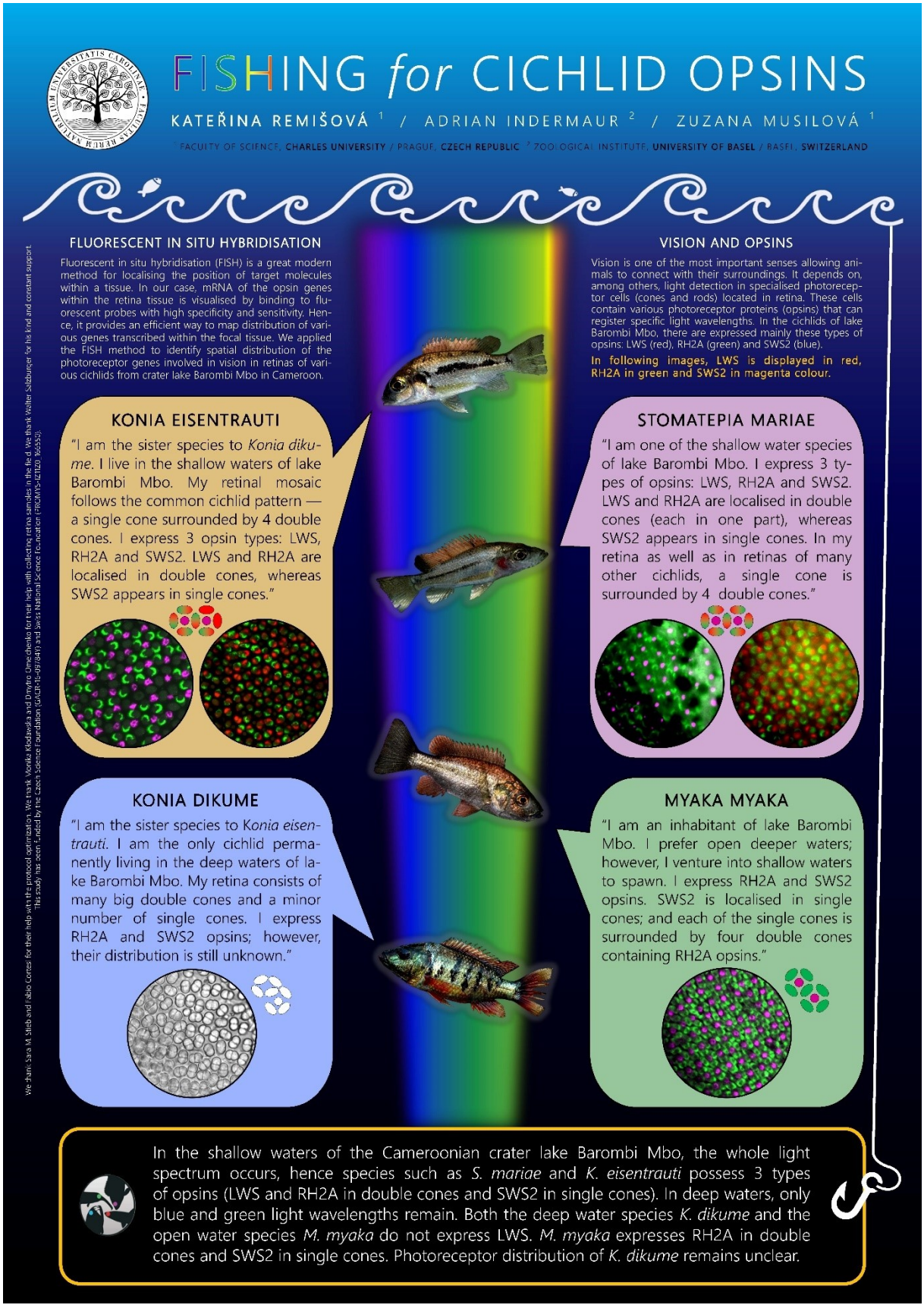

5. Poster Presented at International Congress of Neuroethology (ICN) 2018, Brisbane, Australia